Studies on Thermodynamics and Kinetics of Protein Folding for Interpretation of Some Basic Assumptions

A Thesis
Submitted for the Degree of
DOCTOR OF PHILOSOPHY

by

RAMAKRISHNA D

SCHOOL OF CHEMISTRY
UNIVERSITY OF HYDERABAD
HYDERABAD 500 046
INDIA

March 2016

Dedicated to

My Parents, Teachers

TABLE OF CONTENTS

School of Chemistry
University of Hyderabad
Central University P. O.
Hyderabad 500 046
India

STATEMENT

I hereby declare that the work embodied in this dissertation is the result of the investigations carried out by me in the School of Chemistry, University of Hyderabad, Hyderabad, under the supervision of **Prof. Abani K. Bhuyan**.

Ramakrishna D
(10CHPH12)

March, 2016

Statement Verified
(Prof. ABANI K. BHUYAN)
PROJECT SUPERVISOR

School of Chemistry
University of Hyderabad
Central University P. O.
Hyderabad 500 046
India

CERTIFICATE

Certified that the work embodied in this thesis entitled "**Studies on Thermodynamics and Kinetics of Protein Folding for Interpretation of Some Basic Assumptions**" has been carried out by **Mr. Ramakrishna D** under my supervision, and the work has not been submitted elsewhere for a Degree.

Prof. ABANI K. BHUYAN
(THESIS SUPERVISOR)

Dean
School of Chemistry

ACKNOWLEDGEMENTS

I offer my heartfelt gratitude to my research supervisor Prof. Abani K. Bhuyan for his extraordinary guidance and moral support throughout my thesis. I am extremely grateful to him for generously taking me into his laboratory, and for introducing me to the interface of Chemistry and Biology. I thank him for all his help, support, and encouragement in my professional as well as personal life.

I would like to express my gratitude to former Dean, Prof. M.V. Rajasekharan and the present dean Prof. M. Durga Prasad for providing excellent infrastructure and research environment.

I would like to special thank my Doctoral Committee members Prof. Lalitha Guruprasad, Prof. Pradeepta K. Panda and all other faculty members of the School of Chemistry for their support on various occasions during my Ph.D. tenure.

My special thanks to Dr. P. Nageswara Rao and Dr. Prakash Prabhu for their advice and encouragement.

I am extremely grateful to Dr. Karnati Roy, Dept. of Animal Sciences, for his help and support.

I was extraordinarily fortunate to work with a very good company of people in the laboratory. Many thanks to P. Sashikantha Reddy, Dr. U. Yasin, Dr. Babu Sudhamalla, P. Hima Girija, Sunil Kumar, and Dr. Aparna and Dr. B. Harihar for making my life happy and memorable all these days in the lab.

I would like to express my deep sense of gratitude to Raman Goud and Mahesh for their encouragement and moral support throughout my carrier.

I wish to express my heartfelt gratitude to my dear sir, Venugopal Reddy for his constant support and encouragement throughout my B. Sc.

I would like to thank all faculty members in the Department of Chemistry, NIT Warangal, for their encouragement and guidance up to this stage.

I am very pleased to thank my friends, colleagues and classmates Dr. V. Venkat rao, Dr. K. Mahesh, Dr. Kishore, Dr. Pavan, Dr. Thirupathi, Dr. Siva Ramakrishna, Sudheer Kumar, Bhanu, Deperna, Dr. G. Chandrashekar. Dr. Srinivas (ILS), Dr. Ramu Yadav, Dr. Naga Prasad, Dr. B. Ramakrishna, Dr. Karunakar, Rajender, Satheesh, Divya, Chandu, Ashok, Naidu, Vikranth, Ramana, Prasad, Lasya, Mohan Raj, T. Suresh, Tejaswini Naidu, Kiran. I thank all my school and college teachers and my college friends for their support.

I thank all the research scholars of School of Chemistry and especially who helped me in need. I would also acknowledge all the non-teaching staff, School of Chemistry and CIL for their help. Research fellowships and financial support from UGC-CSIR, and DST, Government of India, are gratefully acknowledged.

I express my sincere thanks to our lab technician G. Mahendher for his helping hand throughout my research.

I wish to express my deep sense of gratitude to my dearest brother Kumar being supportive and caring.

I would like to thank Kishore bava, Pallavi, Dr. Guru Raghavendra, Keerthi, Ramakrishna Anna and Radhika vadhina for their love and affection to me.

Where would I be without my family? My mother and father deserve special mention for their inseparable support and prayers. With all their love, blessings and sacrifice only this could be possible.

Finally my appreciation to my wife Sandhya Rani for her care and love. Collective and individual acknowledgments to all family members, friends and relatives.

Above all I would like to thank LORD who granted and bestowed blessings upon me.

RAMAKRISHNA D

ABBREVIATIONS

cyt c	cytochrome c
BSA	bovine serum albumin
GdnHCl	guanidinium hydrochloride
R_H	hydrodynamic radius
ΔG^o	protein conformational stability in water
$\Delta G(T)$	unfolding free energy at temperature T
$\Delta H(T)$	unfolding enthalpy at temperature T
$\Delta S(T)$	unfolding entropy at temperature T
ΔC_p	change of heat capacity of denaturation
m_g	differential protein-denaturant interactions in native and unfolded states
T_m	heat denaturation midpoint temperature
T_c	cold denaturation midpoint temperature
T_s	temperature of maximum stability
T_h	the temperature at which $\Delta H=0$
ΔH_m	change in enthalpy at transition midpoint
CD	circular dichroism
ΔASA	difference in solvent accessible surface areas in native and unfolded states
$< \delta E^2 >$	mean internal energy of the protein
α_i	fraction of the i-type group exposed to the solvent in the U state
$\Delta g_{tr,i}$	free energy of transfer of the i-type group from water to denaturant
λ_f	refolding rate
sLED-PFG	s-longitudinal encode-decode - pulsed field gradient
$m^{\ddagger}$	surface area buried in the transition state
U′	collapsed state of the unfolded chain
SAXS	Small-angle X-ray scattering
LFEM	linear free energy model
LEM	linear extrapolation method
SB	Santoro-Bolen
SMFRET	single-molecule fluorescence resonance energy transfer

CHAPTER 1

INTRODUCTION

To no contest, protein folding is the most difficult many-body problem known today. The basic difficulty is to know how the tertiary structure of the folded protein is encoded in the amino acid sequence of the initial polypeptide. The code is far from trivial, because many distantly related polypeptides which share only a few amino acids in common, in the case of globin for example, acquire the same 'globin-fold' tertiary structure as determined by X-ray crystallography.[1] The code is thus degenerate, but cracking it is vital in order to be able to produce proteins with desired folds and functions from designed amino acid sequences ab initio.

1.1 Levinthal Paradox, Structural Intermediates, and Folding Pathways

Although the complexity of protein denaturation – the reversible transition from the native to the denatured or unfolded state shown as N⇋D or better N⇋U – was known for a very long time,[2] and steady progress was made toward thermodynamic and kinetic description of the reaction,[3] the enormity of the problem surfaced some 50 years ago when Levinthal realized that the time for the U→N reaction would be astronomically long if the unfolded polypeptide has to randomly search the entire conformational space available in order to fold.[4] Levinthal made the point that the unfolded polypeptide has to be somehow guided through discrete steps toward achieving the native state within biologically relevant time. The thought influenced folding research immensely so as to find out the steps the unfolded polypeptide goes through. It became clear in a rather short course of time that the folding reaction largely involves sequential and perhaps preferential pathways with structural intermediates.[5,6] It has been realized widely that structural characterization of folding intermediates at atomic resolution can be of immense help in cracking the code, because such structures would show the decoded atomic interactions in a stepwise manner as folding proceeds.

Structural intermediates for a very large number of proteins, often at high resolution, have been described. The occurrence of intermediates is described by several mechanisms. In the polypeptide collapse or hydrophobic collapse mechanism, the hydrophobic residues of the unfolded chain are stated to collapse initially to produce a condensed state from which secondary structures evolve.[7,8] The framework model suggests initial formation of elements of local secondary structures,[5] which diffuse and collide and eventually coalesce to emerge as the native folded state. Some proteins on the other hand do not fold by detectable formation of intermediate structure – the so called two-state folding. The mechanism of two-state folding is described by nucleation growth or nucleation-condensation model, which envisages initial formation of a weak diffused nucleus that is reinforced by long range interactions perhaps on the way to the transition state.[9,10] Folding is rapid once the nucleus is condensed so that folding intermediates are not accumulated. A unifying folding mechanism due to Fersht and coworkers consists of initial formation of a nucleus braced by a native-like chain topology, collapse, and folding to the native state by gradual structure formation. Accumulation of folding intermediate(s) depends on the stability of the structural intermediate.[11]

1.2 Polypeptide Chain Collapse

It is often difficult to describe folding by the use of a specific model. Indeed, the sea of literature tends to point to the working of both collapse and framework model together. Studies of polypeptide collapse transition are based on the general recognition that the protein is a polymer, whose solvation properties are determined by the amino acid composition. The comparison of the protein chain with homopolymers allows application of some of the principles of polymer physics regarding the response of the protein as it is taken from a good to a poor solvent. In the parlance of test tube experiments of protein folding, the solvent quality refers to the level of denaturant in the medium. Thus, the solvent becomes increasingly better as the protein is placed in incrementally higher denaturant. When the unfolded protein chain initially prepared at

high concentration of a chemical denaturant is driven to fold by diluting out the denaturant, the chain collapses because of its placement in a bad solvent. The collapse contraction of the chain occurs due to unfavorable chain-solvent interactions.[12-14] Although it is still not clear as to what extent the polypeptide chain can be compared to a polymer, and whether all unfolded chains collapse when placed in bad solvent, a large volume of recent studies has considered polypeptide chain collapse as the earliest event in protein folding. Many questions exist regarding the kinetics and specificity of the collapse. For certain proteins, the collapse specifically leads to a productive intermediate,[15,16] and for some the collapse is non-specific.[17] Regardless of the nature of the collapse reaction, late intermediates can accumulate if the structure is sufficiently stable at low denaturant. Thus, a useful working model at present is

'unfolded chain $\rightarrow$ collapsed product $\rightarrow$ intermediate(s) $\rightarrow$ native protein'.

1.3 Thermodynamics of Protein Folding

The nature of forces and their relative contribution to the stability of native proteins, properties like solvophilicity, solubility, and compactness of globular proteins, location of polar and apolar surfaces within proteins, and the nature of their interactions with water are coded in protein thermodynamics. All forces of interactions are important because proteins are only marginally stable.[18] The reversibility of the N$\leftrightharpoons$U reaction at equilibrium has been studied for numerous proteins since a very long time[3,19-21] to determine Gibbs free energy, enthalpy, entropy, and heat capacity of native proteins. The most important application of the N$\leftrightharpoons$U reaction studied by the use of temperature and chemical denaturants is the determination of conformational stability of proteins (ΔG^o), which is the difference of Gibbs free energies of the unfolded and native states.[22] Perhaps the most outstanding result obtained is that the heat capacity change accompanying protein unfolding (ΔC_p) is large and positive, which is a direct reflection of predominance of hydrophobic surfaces in the protein interior that are exposed to the aqueous solvent in the unfolded state. The large value of ΔC_p also causes the unfolding enthalpy (ΔH) to

increase considerably with increasing temperature. In experiments using chemical denaturants, understanding the variation of Cp with denaturant level is of current interest.

1.4 Assumptions and Hypotheses in Protein Folding

Experimental studies of protein folding are based on assumptions and hypotheses that are necessitated partly due to the difficulty of performing experiments under required conditions. For example, experiments are often done with small model compounds mimicking protein groups,[2,3,23,24] and the results are extrapolated to obtain information regarding thermodynamic properties of proteins. The difficulty of determining the equilibrium constant (K) and kinetic rate constant (k_{obs} or λ) under very low and high concentrations of denaturants requires suppositions regarding their functional dependence on the denaturant. Listed below are a few assumptions that are relevant to the study of this thesis.

1.5 Linear Free Energy Model

In analogy with simple chemical reactions of small molecules the protein unfolding reaction is modeled by the two state N⇋U reaction, whose free energy change across the reaction coordinate is modeled almost universally by[22]

$$\Delta G = \Delta G^{o} - m_{g}[\mathrm{D}] \qquad (1)$$

where ΔG^{o} ($=G_U - G_N$) is the conformational stability of the protein, and m_g is an empirical parameter that measures how differently the unfolded protein interacts with the denaturant, D, compared to its interaction with the native state. The apparent rationale for widespread use of this linear relation is the sharp cooperative transition (all-or-none) associated with the native to unfolding transition, which is due to the involvement of weak forces of interaction in protein structure, and which appears to suggest that both native and unfolded states are structurally invariant to the content of denaturant in the reaction medium. However, there is not enough reason to believe that the protein exists in a single native conformation at all denaturant concentrations corresponding to the pre-transition region of the unfolding reaction. The same reasoning applies to the post-

transition region. On the other hand, the extent of susceptibility of the native structure to predenaturing amounts of the denaturant need not be compared with that at higher levels of the denaturant. In other words, it is not clear whether the K (=U/N) values that are readily obtained from the sigmoidal cooperative region of the denaturant-induced unfolding transition can be linearly extrapolated to the aqueous condition (i.e., without denaturant) so as to be able to calculate the ΔG^o value.

The linear extrapolation procedure appears in another guise. The value of ΔG^o can be calculated by the details of protein groups that are solvent-exposed in the unfolded state but not in the native state.[25] In the equation[25,26]

$$\Delta G = \Delta G^o + \sum_i n_i \alpha_i \Delta g_{\mathrm{tr},i} \qquad (2)$$

n_i is the total number of i type of groups present in the protein, α_i represents the fraction of the i-type group exposed to the solvent in the U state, and $\Delta g_{\mathrm{tr},i}$ measures the free energy of transfer of the i-type group from water to a given level of the chemical denaturant used. Computation of values of $\Delta g_{\mathrm{tr},i}$ is based on transfer free energy of model compounds.

1.6 Rate-Limited Chevron Rollover

The kinetic version of the assumption of free energy linearity is given by

$$\log \lambda_{\mathrm{f}} = \log \lambda_{\mathrm{f}}^{\mathrm{o}} - m_{\mathrm{f}}[D] \qquad (3)$$

where, λ_{f} is the observed refolding rate or the eigenvalue (often also written as k_{f}), $\lambda_{\mathrm{f}}^{\mathrm{o}}$ is the value in water (i.e., without denaturant), and m_{f} is called kinetic-m value ($RT\,\partial ln\lambda/\partial$[D]. Accordingly, the denaturant dependence of log λ should be linear with a negative slope for folding and positive for unfolding, so as to provide a chevron shape. The past 25 years of kinetic studies of protein folding have recorded numerous instances where the assumed linearity breaks down to variable extent along both folding and unfolding arms of the chevrons, although chevrons of some small and fast-folding proteins are linear. The reason for the breakdown, interpreted especially for the folding

arm curvature, is the accumulation of kinetic intermediates that become increasingly stabilized with lower denaturant level. The more stable the intermediates are, slower the rate of their conversion the native state, implying that it is not the U→N conversion (linear) but I→N conversion that limits the observable rate, and hence a curvature in the folding arm of the chevron.[27,28] There are other interpretations in terms of shifts at the transition state level.[29] However, many proteins which are known to fold without the accumulation of folding intermediate(s) also show chevron folding arm rollover. Further, curvature in the unfolding arm of the chevron is also widely prevalent. As yet, there does not appear a satisfactory interpretation of chevron curvature.

1.7 Homopolymer Attribute of the Unfolded Chain

As discussed in the context of polypeptide chain collapse above, the unfolded chain is assumed to behave like a homopolymer in its response to a change in denaturant level or temperature. However, all polypeptides do not contract/collapse the way the homopolymer theory suggests. Also, the collapse process immediately after denaturant dilution has not been resolved for all unfolded polypeptides, making it unclear as to what extent the unfolded chain may be compared to a homopolymer.

1.8 Objectives of This Work

This thesis describes experimental equilibrium and kinetic results for the folding of four proteins – cytochrome *c*, holomyoglobin, bovine serum albumin (BSA), and lysozyme. Equilibrium studies specifically delve into the validity of the linear free energy model (LFEM) in the determination of conformational stability of proteins, and refers to thermodynamic properties of these proteins at subdenaturing levels of temperature and chemical denaturants. Heat capacity values of native-like states for all four proteins under subdenaturing conditions have been measured. Refolding and unfolding kinetics resolved to millisecond have been measured under a variety of denaturant conditions to learn about structure formation in the submillisecond regime with reference to unfolded chain

collapse. All four proteins investigated show variable degree of chevron curvature along both folding and unfolding arms of the chevron. The chevron curvature is projected to continuous change of both structure and energy of the protein across the denaturant scale.

1.9 REFERENCES

1. Lesk, A. M., and Chothia, C. (1980) How different amino acid sequences determine similar protein structures: the structure and evolutionary dynamics of globins. *J. Mol. Biol. 136*, 225–270.
2. Kauzmann, W. (1959) Some factors in the interpretation of protein denaturation. *Adv. Protein Chem. 14*, 1–63.
3. Tanford, C. (1970) Protein denaturation. C. Theoretical models for the mechanism of denaturation. *Adv. Protein Chem. 24*, 1–95.
4. Levinthal, C. (1968) Are there pathways for protein folding? *J. Chim. Phys. 65*, 44–45.
5. Kim, R. F., and Baldwin, R. L. (1982) Specific intermediates in the folding reactions of small proteins and the mechanism of protein folding. *Annu. Rev. Biochem. 51*, 459–489.
6. Kim, R. F., and Baldwin, R. L. (1989) Intermediates in the folding reactions of small proteins. *Annu. Rev. Biochem. 59*, 631–660.
7. Go, N. (1984) The consistency principle in protein structure and pathways of folding. *Adv. Biophys. 18*, 149–164.
8. Agashe, V. R., Shastry, M. C. R., and Udgaonkar, J. B. (1995) Initial hydrophobic collapse in the folding of barstar. *Nature 377*, 754–757.
9. Fersht, A. R. (1997) Nucleation mechanism in protein folding. *Curr. Opin. Struct. Biol. 7*, 3−9.
10. Nolting, B., and Agard, D. A. (2012) How general is the nucleation-condensation mechanism? *Proteins 73*, 754–764.
11. Gianni, S., Guydosh, N. R., Khan, F., Caldas, T. D., Mayor, U., White, G. W. N.,

DeMacro, M. L., Daggett, V., and Fersht, A. R. (2003) Unifying features in protein folding mechanisms. *Proc*. *Natl*. *Acad*. *Sci*. *USA 100*, 13286−13291.

12. Dill, K. A. (1985) Theory for the folding and stability of globular proteins. *Biochemistry 24*, 1501-1509.
13. Dill, K. A., and Shortle, D. (1991) Denatured states of proteins. *Annu*. *Rev*. *Biochem*. *60*, 795-825.
14. England, J. L., and Haran, G. (2011) Role of salvation effects in protein denaturation: from thermodynamics to single molecules and back. *Annu*. *Rev*. *Phys*. *Chem*. *62*, 257-277.
15. Shastry, M. C. R., and Roder, H. (1998) Evidence for barrier-limited protein folding kinetics on the microsecond time scale. *Nat*. *Struct*. *Biol*. *5*, 385−392.
16. Lapidus, L. J., Yao, S., McGarrity, K. S., Hertzog, D. E., Tubman, E., and Bakajin, O. (2007) Protein Hydrophobic collapse and early folding steps observed in a microfluidic mixer. *Biophys*. *J*. *93*, 218−224.
17. Udgaonkar, J. B. (2013) Polypeptide chain collapse and protein folding. *Arch*. *Biochem*. *Biophys*. *531*, 24−33.
18. Dill, K. A. (1990) Dominant forces in protein folding. *Biochemistry 29*, 7133−7155.
19. Brandts, J. F. (1964) The thermodynamics of protein denaturation. I. The dnaturation of chymotrypsinogen. *J*. *Am*. *Chem*. *Soc*. *86*, 4291−4301.
20. Brandts, J. F. (1964) The thermodynamics of protein denaturation. II. A model of reversible denaturation and interpretations regarding the stability of chymotrypsinogen. *J*. *Am*. *Chem*. *Soc*. *86*, 4302−4314.
21. Privalov, P. L. (2008) Microcalorimetry of proteins and their complexes. *Methods Mol*. *Biol*. *49*, 7764-7773.
22. Greene, R. F., and Pace, C. N. (1974) Urea and guanidine hydrochloride denaturation of ribonuclease, lysozyme, α-chymotrypsin, and β-lactoglobulin. *J*. *Biol*. *Chem*. *249*, 5388−5393.
23. Tanford, C. (1962) Contribution of hydrophobic interactions to the stability of the

globular conformation of proteins. *J*. *Am*. *Chem*. *Soc*. *84*, 4240–4247.

24. Auton, M., and Bolen, D. W. (2005) Predicting the energetic of osmolyte-induced protein folding/unfolding. *Proc*. *Natl*. *Acad*. *Sci*. *USA 102*, 15065−15068.
25. Tanford, C. (1964) Isotermal Unfolding of Globular Peoteins in Aqueous Urea Solutions. *J*. *Am*. *Chem*. *Soc*. *86*, 2050-2059.
26. Tanford, C. (1969) Protein Denaturation: Part C. Theoretical Models for the Mechanism of Denaturation. *Adv*. *Protein Chem*. *24*, 1-95.
27. Matouschek, A., Kellis, J. T., Serrano, L., Bycroft, M., Fersht, A. R. (1990) Transient folding intermediates characterized by protein engineering. *Nature 346*, 440–445.
28. Baldwin, R. L. (1996) On-pathway versus off-pathway folding intermediates. *Fold*. *Design 1*, R1–R8.
29. Otzen, D. E., Kirstensen, O., Proctor, M., and Oliveberg, M. (1999) Structural changes in the transition state of protein folding: alternative interpretations of curved chevron plots. *Biochemistry 38*, 6499–6511.

CHAPTER 2

Protein Folding Energy is Not Universally Linear with Denaturant: A Revisit to the Linear Free Energy Model

2.1 ABSTRACT

Conformational stability of proteins is determined invariably from denaturant-induced isothermal unfolding transitions by the premise of the linear free energy model (LFEM). It is also known that the assumption of the linear dependence of stability on denaturant molarity breaks down for some proteins, a satisfactory interpretation of which is not available. Here, the problem is revisited with four proteins by isothermal experiments employing two chemical denaturants concurrently, and heat denaturation experiments in the presence of a single chemical denaturant at variable pH. Plots of Gibbs free energy of folding with denaturant are categorized into linear (cytochrome *c*), curved upward (myoglobin), moderately rolled over (lysozyme), and curved downward (BSA), implying that the linear proportionality of equilibrium folding parameters on denaturant concentration does not hold universally. The key to interpret the denaturant dependence of protein folding is the effect of denaturant binding on conformational and energy fluctuations that assume critical significance under native-like subdenaturing conditions. Binding of denaturants to similar and independent sites on the protein brings about energy variation in a protein specific manner, which is reflected in the observed dependence of folding parameters on denaturant concentration. There is no confidence that linear extrapolation of folding free energies from the transition region to the denaturant-stripped condition provides the true conformational stability. The actual value is determined by experiments that use more than one denaturing agent concurrently. The accompanying article suggests that the breakdown of the LFEM is a major factor for curvatures in protein folding chevron.

2.2 INTRODUCTION

The basic and the most practical utility of the equilibrium unfolding reaction measured by using GdnHCl or urea is the determination of protein conformational

stability or folding free energy, ΔG^{o}. In general, the highly cooperative transition provides only a narrow window to calculate the equilibrium constant of the reaction, which is most often considered two-state (N⇌U). It was Greene and Pace[1] who experimentally found that Gibbs free energy of folding in water can be determined by linearly extrapolating the transition-region free energy values to 'zero' GdnHCl or urea concentration, and hence the procedure is referred to as linear extrapolation method (LEM). The 'Pace procedure' has not only drawn further attention of theorists,[2–5] but also greatly influenced analysis of isothermal denaturation experiments that has become a convenient and standard procedure for estimation of protein conformational stability.[6] The stability of a very large number of proteins determined in different laboratories by LEM has already been collated by Pfeil,[7–9] and the number continues to grow.

Because of the influence of LEM, which is essentially coded in the linear free energy model (LFEM), and to provide an overview of the problem studied, the basic idea of the practiced procedure is briefly introduced here. According to the general requirement for the calculation of ΔG, one needs to evaluate the fractions of native (N) and unfolded (U) proteins so as to determine the equilibrium constant K (=U/N), which is sizable and best determined in the transition region. Calculation of values of N and U in the transition region however requires determination of native- and unfolded signal values across this region which can be done by extrapolating both native- and unfolded-state signals into the transition region. Such extrapolation is fraught with some uncertainty however, because the actual denaturant dependence of signals passing from pre- and post-transition regions into the transition of the unfolding curve is not known accurately and is judged by inspection only. Depending on the inspection-based linearity or nonlinearity, the denaturant dependence of pre- and post-transition baselines is written as

$$S(D) = S^{\circ} + m[D] \text{ or } S(D) = S^{\circ} + m_1[D] + m_2[D]^2 \quad (1)$$

where $[D]$ and m are denaturant concentration and associated coefficients, and S^{o} is the signal value in water alone. Thus, the pre- and post-transition baselines can be approximated by 1º or 2º polynomial in order to extrapolate to the transition region.

These baseline values are used to calculate the folding equilibrium constant by

$$K = \frac{S_{obs} - (S_N^o + m_N[D])}{(S_U^o + m_U[D]) - S_{obs}} \quad \text{or} \quad K = \frac{S_{obs} - (S_N^o + m_{N,1}[D] + m_{N,2}[D]^2)}{(S_U^o + m_{U,1}[D] + m_{U,2}[D]^2) - S_{obs}} \qquad (2)$$

where S_{obs} is the observed signal at a given concentration of the denaturant, and S^o_N and S^o_U refer to signal values of N and U states in water. The data set is then normalized as fraction unfolded as a function of denaturant molarity, and the free energy difference between native and unfolded states evaluated by

$$\Delta G = -RT\, lnK \qquad (3)$$

The ΔG dependence of the denaturant is now extrapolated from the transition region to the ordinate by

$$\Delta G = \Delta G^o - m_g[D] \qquad (4)$$

where ΔG^o is the folding energy in water or the conformational stability of the protein, and m_g represents the differential protein-denaturant interactions in native and unfolded states.[2] This is the essence of the linear free energy model (LFEM), and the method of estimating ΔG^o from the *y*-intercept of ΔG vs denaturant is called linear extrapolation method (LEM) first used by Greene and Pace,[1,6] and is still used indiscriminately to measure conformational stability of proteins. To avoid uncertainty due to rather long extrapolation from the transition region to the ordinate, one can extract the ΔG^o value directly by rewriting Equation 4 as

$$K = \exp\left(\frac{-\Delta G^o + m_g[D]}{RT}\right) \qquad (5)$$

and equating it with the K expression given in Equation 2. For example, if a 1º polynomial is chosen to simulate both native and unfolded baselines of the transition curve, one obtains

$$\frac{S_{obs} - (S_N^o + m_N[D])}{(S_U^o + m_U[D]) - S_{obs}} = \exp\left(\frac{-\Delta G^o + m_g[D]}{RT}\right)$$

$$S_{obs} = \frac{(S_N^o + m_N[D]) + (S_U^o + m_U[D]) \exp\left(\frac{-\Delta G^o + m_g[D]}{RT}\right)}{1 + \exp\left(\frac{-\Delta G^o + m_g[D]}{RT}\right)} \quad (6)$$

This idea due to Santoro and Bolen (SB) provides an approach to evaluate ΔG^o by a nonlinear least square analysis of the primary data alone,[10] unlike LEM which requires determination of denaturant dependence of ΔG in the transition region followed by a long extrapolation which significantly underestimates the error. Hence, the value of ΔG^o obtained by the SB approach would appear improved, even though this approach also relies on LFEM (Equations 4-6).

An outstanding issue is however the validity of LFEM itself. There has been overwhelming support for the LEM procedure,[6,11–14] which is consistent with Tanford's transfer model,[15,16] but the enormous importance of protein stability measurement itself stipulates elaborate scrutiny of the practiced procedure. Should experimental folding parameters vary linearly with denaturant? Little consensus has emerged from studies to date; linearity is good for some proteins but not for others.

Despite being LFEM-based, the SB analysis can be objectively used to examine the validity of the linear free energy model ($\Delta G=\Delta G^o-m_g[D]$) in protein folding. The idea here is to determine values of ΔG^o from a series of unfolding transitions where the primary denaturant is held constant at different pretransition levels and a secondary perturbant, which could be another chemical denaturant or temperature, is added incrementally to unfold the protein. The approach is quite general, and has been exploited in many studies directed toward testing LEM.[17-22] As will be shown below, the ΔG^o values obtained for the pretransition region of the primary denaturant are mapped onto the transition-region ΔG values determined by the use of the primary denaturant alone. This work revisits the assumption of LFEM through very basic unfolding experiments with cytochrome *c*, myoglobin, BSA, and lysozyme. These four commercially available proteins are archetypal for folding studies, and results can be easily compared across laboratories. It is shown that the linear free energy model cannot be applied indiscriminately for stability determination.

2.3 MATERIALS AND METHODS

Experiments were performed using commercially available horse myoglobin (Sigma), horse heart cytochrome *c* (Sigma), BSA (Sigma), and hen egg white lysozyme (Calbiochem or HiMedia) without further purification. The use of monomeric form of BSA was ensured often by Sephadex G75 gel filtration. Urea, GdnHCl, and buffer components were ultrapure. Urea solutions were prepared for use within 24 hours.

To study denaturant-induced unfolding reactions, samples were prepared by mixing only two solutions one containing the native protein, and another the unfolded protein. These two stock solutions were identical in composition and pH, except that the one corresponding to the unfolded state also contained the denaturant at the highest level. In doubly perturbed experiments involving both GdnHCl and urea, where concentration of one of the denaturants was held constant and the other varied, the two stock protein solutions identically contained the denaturant that was held constant. This procedure of sample preparation not only ensures uniform protein concentration, but also forms a test of reversibility of the folding-unfolding reaction. The final protein concentration in a set of samples was in the 5−25 μM range depending on the protein type, the measurement probe, and the optical pathlength employed. Buffers used were 100 mM sodium phosphate, pH 7 (cytochrome *c*), 20 mM sodium phosphate, pH 7 (myoglobin), 50 mM sodium phosphate, pH 7 (BSA), and 20 mM sodium acetate, pH 5 (lysozyme). Samples were equilibrated at 25ºC for ~12 hours before spectral measurements at the same temperature using thermostated Fluoromax 4P (Horiba) and Jasco FP-8300 instruments for fluorescence, and AVIV SF420 for CD. After these measurements, refractive index of each sample was determined using a ABBE-3L (Thermo Spectronic) refractometer to calculate the actual concentration of the denaturant.

Samples for heat denaturation experiments were prepared by mixing a constant volume of the native protein solution with a concentrated denaturant solution and buffer so as to obtain different denaturant levels but uniformity in protein concentration across samples of the same protein. Buffer systems were same as described above for isothermal denaturant-induced unfolding experiments, although

they were used at different pH values in order to determine heat capacity changes. Since intrinsic fluorescence emission intensity generally decreases with temperature due to increased rate of internal conversion in the excited state, heat denaturation experiments here were probed by far-UV CD alone. Ellipticity values were recorded at temperature interval of 1.5 or 2(±0.2)ºC with a dwell time (incubation) of 30-60 seconds at each temperature. Signal averaging time was 15 seconds. Thermal unfolding was found reversible for all conditions of mild perturbation of the proteins with low concentrations of denaturants.

For determination of ΔC_p, thermal unfolding experiments were carried out at different denaturant levels, and at different pH values for each denaturant concentration. The pH values were 7.5, 6.5, 5.5, and 4.5 for cytochrome c, 7.0, 6.0, 5.7, 5.3, and 5.0 for myoglobin, 7.0, 6.0, 4.5, and 4 for BSA, and 5.0, 4.5, and 3.6 for lysozyme. Solutions at pH<6 were buffered with sodium acetate.

2.4 RESULTS

2.4.1 Linearity of Folding Free Energy of Cytochrome *c* with GdnHCl: A Benchmark of LFEM. Although the linear relation of ΔG of cytochrome *c* with denaturants could be surmised from numerous earlier results, the value of ΔG at very low denaturant was not measured by the use of a global probe. To generate a complete graph of ΔG vs GdnHCl concentration, unfolding experiments were conducted using GdnHCl and urea as primary and secondary perturbants, respectively. The GdnHCl-induced transitions monitored by far-UV CD and fluorescence are apparently identical yielding indistinguishable dependence of ΔG on the denaturant (m_g=3.4 kcal mol^{-1} M^{-1}) across the transition region of unfolding (Figure 1a). To determine the variation of ΔG in the pretransition region of unfolding, we generated a series of urea unfolding curves by holding the concentration of the primary denaturant GdnHCl constant in the 0−2 M range, and analyzed them individually by Equation 6 (Figure 1b, Table 1). These values of ΔG and those obtained from Figure 1a are combined in the plot of folding free energy in the 0−3 M range of GdnHCl (Figure 1c), clearly showing that folding energy under subdenaturing conditions can be obtained by linear extrapolation of ΔG values from the transition region. The dependence of ΔG on GdnHCl is

characterized by the slope of the line (m_g=3.3 kcal mol^{-1} M^{-1}), which is >95% recovery of the m_g-value obtained by fitting the GdnHCl-induced unfolding transitions to Equation 6 (Figure 1a). It is concluded that cytochrome *c* unfolding is a paradigm of LFEM.

Double perturbation experiments also provide a set of m_g values associated with the nature of the secondary perturbant. Each urea-induced transition in the presence of a constant GdnHCl yields a m_g value (Figure 1d), which is invariably less than half of that obtained from GdnHCl dependence of ΔG (Figure 1c). It is well known that m_g values measured by urea unfolding of proteins are generally smaller than the ones measured using GdnHCl. A slight increase in the urea-measured m_g value with GdnHCl is also notable (Figure 1d). This is due to increased interaction of the denatured state of the protein with urea when coupled to the rising level of GdnHCl in the unfolding medium, the net result of which is more solvent exposure of protein groups.

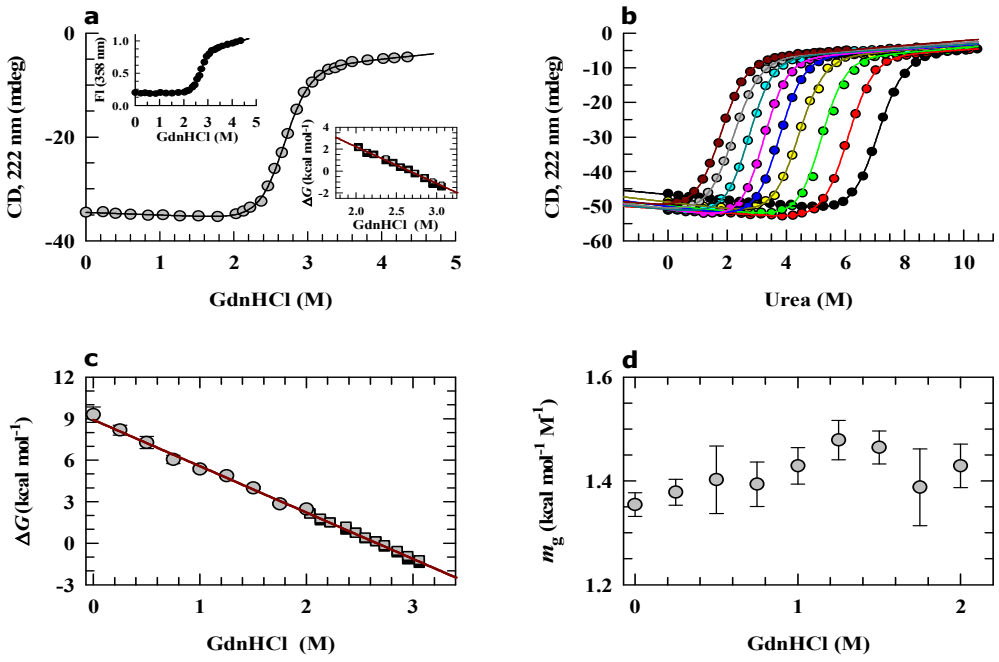

Figure 1. Unfolding of cytochrome *c* in 0.1 M sodium phosphate buffer, pH 7, 25 ºC. (a) Transitions measured by CD (●) and fluorescence (●, *upper inset*) analyzed with Equations 1-4 yield nearly identical dependence of ΔG on GdnHCl (*lower inset*: □ and ■, calculated from CD and fluorescence,

respectively). (b) Urea unfolding transitions in the presence of (from right to left) 0, 0.25, 0.5, 0.75, 1.0, 1.25, 1.5, 1.75, and 2.0 M GdnHCl. The transitions are fitted to Equation 6 or SB analysis, and ΔG^o and m_g values obtained are listed in Table 1. (c) These ΔG^o values (●) are mapped onto the set of ΔG (■ and ■) that are shown in the *lower inset* of panel *a*. Note that the unfolding energy is labeled ΔG^o for each urea-unfolding curve in panel *b* by virtue of SB analysis, but when this value is shown at the corresponding molarity of the primary denaturant GdnHCl, it is labeled ΔG. The slope of the straight line through these data (r^2=0.99) provides ΔG^o=8.9 kcal mol^{-1}, and m_g=3.35 kcal mol^{-1} M^{-1}. (d) GdnHCl dependence of m_g values obtained from SB analysis of urea unfolding curves shown in panel *b*. These m_g values are also listed in Table 1.

Table 1. Fit parameters to Equation 6 for CD-measured double perturbation unfolding transitions of cytochrome *c* with GdnHCl as the primary and urea as the secondary perturbant.

GdnHCl (M)	ΔG (kcal mol^{-1})	m_g (kcal mol^{-1} M^{-1})
0.00	9.30	1.35
0.25	8.20	1.38
0.50	7.25	1.40
0.75	6.05	1.39
1.00	5.35	1.43
1.25	4.85	1.48
1.50	4.00	1.46
1.75	2.85	1.38
2.00	2.45	1.43

2.4.2 Nonlinearity of Folding Free Energy of Myoglobin with GdnHCl: A Case of Upward Curvature. Isothermal experiments with myoglobin at pH 7 involved GdnHCl as the primary perturbant and urea the secondary. The unfolding transition was studied by fluorescence and far-UV CD, initially by varying GdnHCl alone (Figure 2a,b), and then by varying urea in the presence of constant GdnHCl (Figure 2c,d). Analyses of transition curves (Equations 2,6) required the use of a linear unfolded baseline, and occasional use of a 2º polynomial to simulate the native-state baseline. Variations in iterated values of ΔG and m_g (Table 2) caused by simulation of the native-state baseline are included in the estimation of errors for these parameters.

Figure 2e shows that ΔG values for pretransition levels of GdnHCl are simply not contained in the line drawn by linear extrapolation of ΔG values from the transition region. This result, obtained by both fluorescence and CD measurements, strongly undermines the validity of LFEM. The magnitude and the trend of GdnHCl dependence of the m_g value measured with the secondary perturbant urea (Figure 2f) are similar to the observations made earlier for cytochrome *c*.

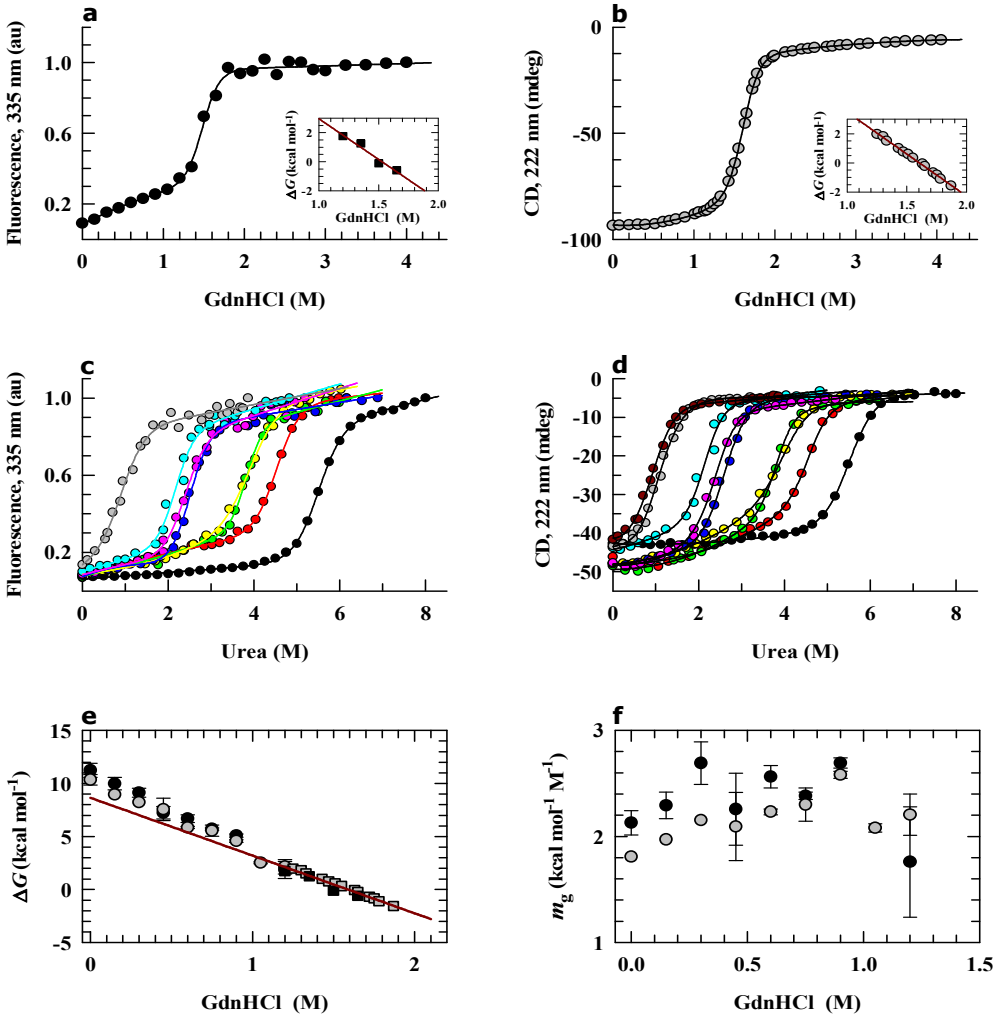

Figure 2. Unfolding of myoglobin in 20 mM sodium phosphate buffer, pH 7, 25 ºC. (a) Fluorescence (●), and (b) CD (●) measured unfolding by GdnHCl. In each panel the *inset* shows ΔG values across the transition region calculated by Equations 1-4. (c) Fluorescence-, and (d) CD-monitored urea unfolding transitions in the presence of (from right to left) 0, 0.15, 0.3, 0.45, 0.6, 0.75, 0.9, 1.05 (CD

alone), and 1.2 M GdnHCl. Each curve is analyzed by Equation 6, and ΔG^o and m_g values are listed in Table 2. (e) The ΔG^o values so obtained are plotted with different molarities of GdnHCl (●, fluorescence, and ●, CD) along with ΔG values calculated from the transitions measured by the use GdnHCl alone, as shown in panels *a* and *b* (■, fluorescence, and ■, CD). The solid line drawn through the transition region data (r^2-0.96) yields the ΔG^o=8.65 kcal mol^{-1}, and m_g=5.43 kcal mol^{-1} M^{-1}.

Table 2. Fit parameters to Equation 6 for fluorescence- and CD-measured urea unfolding of myoglobin in the presence of different concentrations of GdnHCl.

GdnHCl (M)	ΔG (kcal mol^{-1})		m_g (kcal mol^{-1} M^{-1})	
	Fluorescence	CD	Fluorescence	CD
0.00	11.25	9.95	2.13	1.81
0.15	10.80	8.95	2.30	1.97
0.30	11.15	8.15	2.69	2.15
0.45	6.10	6.05	2.26	2.10
0.60	6.70	5.75	2.56	2.23
0.75	5.80	5.15	2.40	2.30
0.90	5.80	5.48	2.70	2.60
1.05		2.15		2.08
1.20	2.00	2.15	1.76	2.20

The upward curvature of ΔG observed here is qualitatively consistent with an earlier study of myoglobin that employed the double perturbation method, but restricted the analysis to the linear extrapolation alone.[18] Also, ΔG values reported there are underestimates, perhaps due to the use of Soret heme absorbance, which is not a global probe. At this stage, we do not attempt to fit the upward curvature of the ΔG vs GdnHCl plot (Figure 2e) to any model, because denaturant-induced deformation of the energy surface discussed later would render model-based description redundant.

2.4.3 Nonlinearity of Folding Free Energy of BSA with GdnHCl: A Case of Downward Curvature. To study unfolding of BSA, we engaged GdnHCl and urea as primary and secondary perturbants, respectively, as was done for cytochrome *c* and

myoglobin described above. Both fluorescence and CD-monitored transitions due to the primary perturbant GdnHCl appear conspicuous (Figure 3a,b) conveying as though the unfolding process is multi-state. Relying on earlier evidences of two-state unfolding for both human and bovine serum albumin at neutral pH,[23,24] we simulated the baselines by a 2º polynomial to analyze the transitions by the use of Equations 2-6, and obtained ΔG^{o}=9.2(±0.8) kcal mol^{-1} and m_g=4.9(±0.5) kcal mol^{-1} M^{-1}. A series of urea unfolding transitions were then recorded in the presence of different GdnHCl (Figure 3c,d).

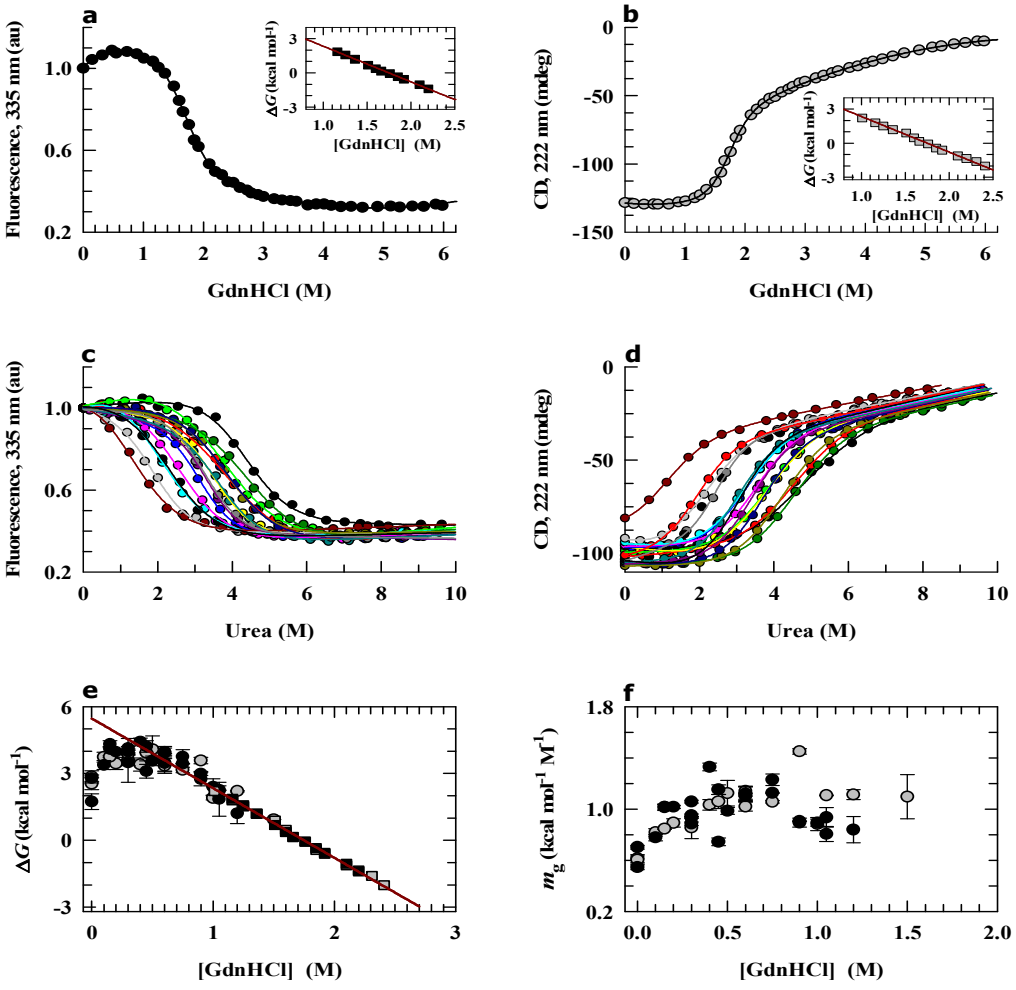

Figure 3. Unfolding of BSA monomer in 50 mM phosphate, pH 7, 25 ºC. (a) Fluorescence (●), and (b) CD (●) monitored unfolding due to the primary denaturant GdnHCl. The *inset* in each panel shows the linearity of ΔG vs GdnHCl in the transition region. The curves were analyzed by Equations 1-4. (c)

Fluorescence- and (d) CD-measured urea unfolding transitions in the presence of (from right to left) 0.1, 0.15, 0.2, 0.3, 0.4, 0.45, 0.5, 0.6, 0.75, 0.9, 1.0, 1.05, 1.2, and 1.35 M GdnHCl. Each curve is fitted to Equation 6, and ΔG^{o} and m_g values obtained are collected in Table 3. (e) Mapping the ΔG dependence of GdnHCl (●, fluorescence, and ⬤, CD) observed by the double perturbation procedure (panels *c* and *d*, and Table 3) onto the ΔG dependence determined by the use of the primary denaturant alone (■, fluorescence, and ▣, CD) as shown in panels *a* and *b*. (f) GdnHCl dependence of mg values calculated from the double perturbation curves (panels *c* and *d*) by Equation 6 (●, fluorescence, and ⬤, CD).

Table 3. Fit parameters to Equation 6 for fluorescence- and CD-measured urea unfolding of BSA in the presence of different concentrations of GdnHCl.

GdnHCl (M)	ΔG (kcal mol^{-1})		m_g (kcal mol^{-1} M^{-1})	
	Fluorescence	CD	Fluorescence	CD
0.00	1.75, 2.79	2.85, 2.54	0.55, 0.70	0.62, 0.60
0.10	4.10	3.74	0.78	0.82
0.15	4.32	3.75	1.00, 1.02	0.85
0.20	3.45	3.45	1.02	0.89
0.30	4.15, 4.00	3.85, 3.60	0.89, 1.06	0.85, 0.93
0.40	4.43	3.40	1.33	1.03
0.45	4.20, 3.10	3.95	1.15, 0.74	1.06
0.50	4.10	4.10	0.98	1.12
0.60	3.45, 3.96	3.94, 3.35	1.12, 1.10	1.02, 1.14
0.75	3.45, 3.75	3.20	1.12, 1.22	1.06
0.90	2.75, 3.00	3.59	0.89, 0.90	1.45
1.00	2.22	1.90	0.89	0.88
1.05	1.85, 2.22	2.25	0.93, 0.80	1.11
1.20	1.22	2.20	0.84	1.10
1.50		0.95		1.10

Interestingly, values of ΔG obtained from these double perturbation measurements (Table 3) are lower than expected from the linear free energy model. By mapping these ΔG values onto those measured in the transition region of the primary perturbant curves (Figure 3a,b) one finds a gradual downward curvature in the ΔG vs GdnHCl

plot under decreasing subdenaturing conditions, and a smooth turn to produce negative slope as strongly native-like conditions are approached (Figure 3e). This unprecedented observation was puzzling to us initially, but repeated recovery of the same result in multiple experiments confirms the result. Even if the apparent turn to produce negative slope is ignored, the rollover of ΔG under subdenaturing conditions provides evidence to argue against the operation of LFEM. The m_g values obtained from urea transitions at constant GdnHCl (Table 3) are at most one-fourth of the m_g value obtained from the transition induced by GdnHCl alone (Figure 3f), suggesting again that urea-associated m_g value is significantly lower than the GdnHCl-associated, and is probably related to less complete interaction of the unfolded protein with urea.

2.4.4 Nonlinearity of Folding Free Energy of Lysozyme with Urea: Another Case of Downward Curvature. Continuing with earlier work on the nonlinear dependence of folding energy of lysozyme on denaturant,[22] we have consolidated the results. Although lysozyme at pH 5 does not unfold completely within the limit of aqueous solubility of urea, the protein fluorescence gradually quenches to zero with subdenaturing levels of urea before the global unfolding sets in (Figure 4a). The CD signals however remain constant before approaching the transition region (Figure 4b) suggesting some tertiary structural changes in the subdenatured protein. Hence, folding free energy as a function of urea was measured using GdnHCl as the secondary perturbant. Fluorescence-monitored GdnHCl transitions display sharp and linear baselines for the unfolded state, probably related to continuous expansion of the unfolded chain that reduces fluorescence quenching by separating the quenchers further from the side chain fluorophores (Figure 4c). The CD transitions are relatively simple, urea dependence of ΔG extracted from these transitions by using Equation 6 rolls over under subdenaturing conditions (Figure 4e), providing another example that invalidates LFEM. Since the secondary perturbant for lysozyme experiments is GdnHCl, the m_g values obtained from double perturbation experiments (Figure 4f, Table 4) are comparable with the m_g value ($\approx$2.5 kcal mol^{-1} M^{-1}) for the transition in the presence of GdnHCl alone. Further, the slope of the GdnHCl dependence of m_g is not positive as were recorded for the other three proteins described above for which

urea was the secondary perturbant. The lysozyme data show little dependence of m_g on GdnHCl within the measurement error (Figure 4f).

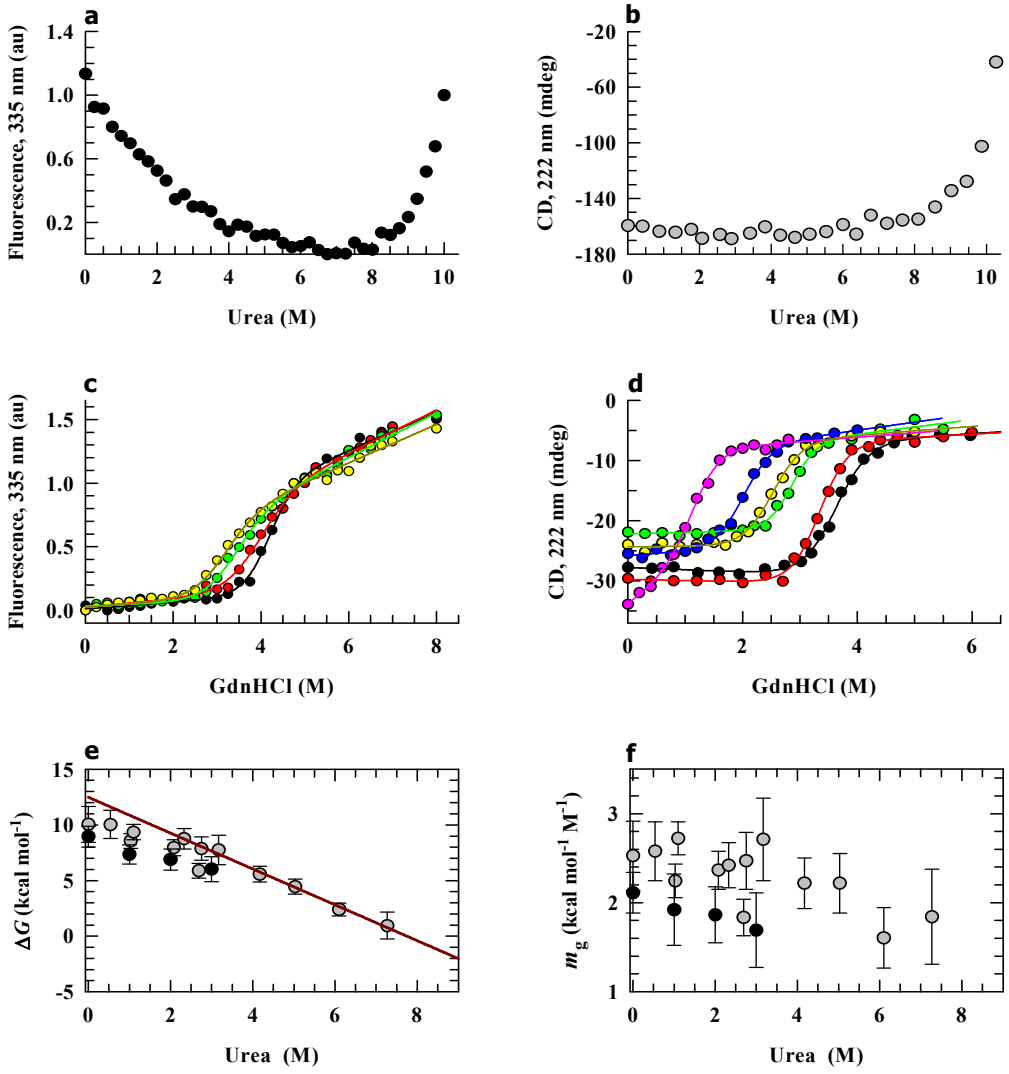

Figure 4. Unfolding of lysozyme in 20 mM sodium acetate, pH 5, 25 ºC. (a) Fluorescence (●), and (b) CD (●) measurements indicate incomplete unfolding of the protein within the solubility limit of urea. (c) Fluorescence-measured unfolding by the secondary denaturant GdnHCl in the presence of (from right to left) 0, 1, 2, and 3 M urea. (d) CD-measured GdnHCl unfolding in the presence of (from right to left) 1, 2.1, 3.2, 4.2, 5.0 and 7.3 M urea. The ΔG^{o} and m_g values obtained by fitting these curves to Equation 6 are collated in Table 4. (e) Urea dependence of ΔG measured by the double perturbation procedure (●, fluorescence, and ●, CD). The solid line emphasizes on the nonlinear dependence of ΔG on urea.

Table 4. Fit parameters to Equation 6 for fluorescence- and CD-measured GdnHCl unfolding of lysozyme in the presence of different concentrations of urea.

Urea (M)	ΔG (kcal mol^{-1})		m_g (kcal mol^{-1} M^{-1})	
	Fluorescence	CD	Fluorescence	CD
0.00	8.95	10.05	2.11	2.53
0.55		10.00		2.58
1.00	7.35		1.92	
1.05		8.55		2.24
1.10		9.35		2.72
2.00	6.90		1.86	
2.10		7.95		2.36
2.30		8.76		2.42
2.70		5.85		1.83
2.75		7.90		2.47
3.00	6.05		1.69	
3.20		7.75		2.71
4.20		5.56		2.22
5.05		4.45		2.21
6.10		2.40		1.60
7.30		0.95		1.84

2.4.5 Temperature and Denaturant Coupled Unfolding Experiments. Heat denaturation measurements have held central importance in the understanding of protein response to destabilizing conditions. To test the validity of LFEM further, we performed an extended series of double perturbation experiments, where thermodynamic properties of the protein in the presence of subdenaturing levels of GdnHCl or urea are measured by temperature-induced global unfolding. Thermal unfolding measurements were taken up as a substitute for differential scanning calorimetry, since thermodynamic quantities derived from the two methods are known to be equivalent.[13] Since temperature alters fluorescence quenching, thermal unfolding processes were probed by far-UV CD for cytochrome c, myoglobin, and BSA, and

near-UV CD for lysozyme.

Thermal unfolding transitions in the presence of different subdenaturing concentrations of GdnHCl or urea are shown in Figure 5a,d,g,j. The transitions were initially fitted to the Gibbs-Helmholtz equation.

$$\theta(T) = \frac{(c_N + m_N T) + (c_U + m_U T)\exp\left[\dfrac{\Delta H_m\left(\frac{T}{T_m} - 1\right) + \Delta C_p[T_m - T + T\ln\left(\frac{T}{T_m}\right)]}{RT}\right]}{1 + \exp\left[\dfrac{\Delta H_m\left(\frac{T}{T_m} - 1\right) + \Delta C_p[T_m - T + T\ln\left(\frac{T}{T_m}\right)]}{RT}\right]} \quad (7)$$

to extract the temperature midpoint of transition, T_m, the midpoint enthalpy change, ΔH_m, and an apparent initial value (highly error prone) of heat capacity change, ΔC_p. In individual analysis of traces, pre- and post-transition baselines are parameterized by ordinate intercepts, c_N and c_U, respectively, and corresponding slopes, m_N, and m_U.

Denaturant dependence of T_m (Figure 5b,e,h,k, Table 5) are realistic reflection of what were observed earlier for the four proteins (Figures 1-4), because the effect of low concentrations of denaturants on the stability of proteins is revealed in changes in temperature midpoint of thermal unfolding.[25] For all of them except the LFEM benchmark cytochrome *c*, for which T_m varies linearly with GdnHCl (Figure 5b), the T_m vs denaturant plot is noticeably curved (Figure 5e,h,k), and in each case the direction and extent of curvature qualitatively matches those observed earlier by isothermal denaturant-induced unfolding experiments (Figures 2e, 3e, 4e). This is an important result because it establishes agreement, within experimental error, of ΔG values measured by thermal unfolding and denaturant-induced unfolding data. The protein-specific curvatures are uniformly and even more conspicuously maintained in ΔH_m vs denaturant graphs (Figure 5c,f,i,l, Table 5). It is easy to see that $\Delta H_U(T)$, the unfolding enthalpy at temperature T, has the same functional dependence on the denaturant as does ΔH_m, because $\Delta H_U(T) = \Delta H_m + \Delta C_p\ (T - T_m)$, where ΔC_p is linear with denaturant (see below), and therefore $\Delta H_U(T) = \Delta H_m$ + constant. These results thus provide apparent validation of LFEM in the case of cytochrome *c* unfolding, but not for myoglobin, BSA, and lysozyme.

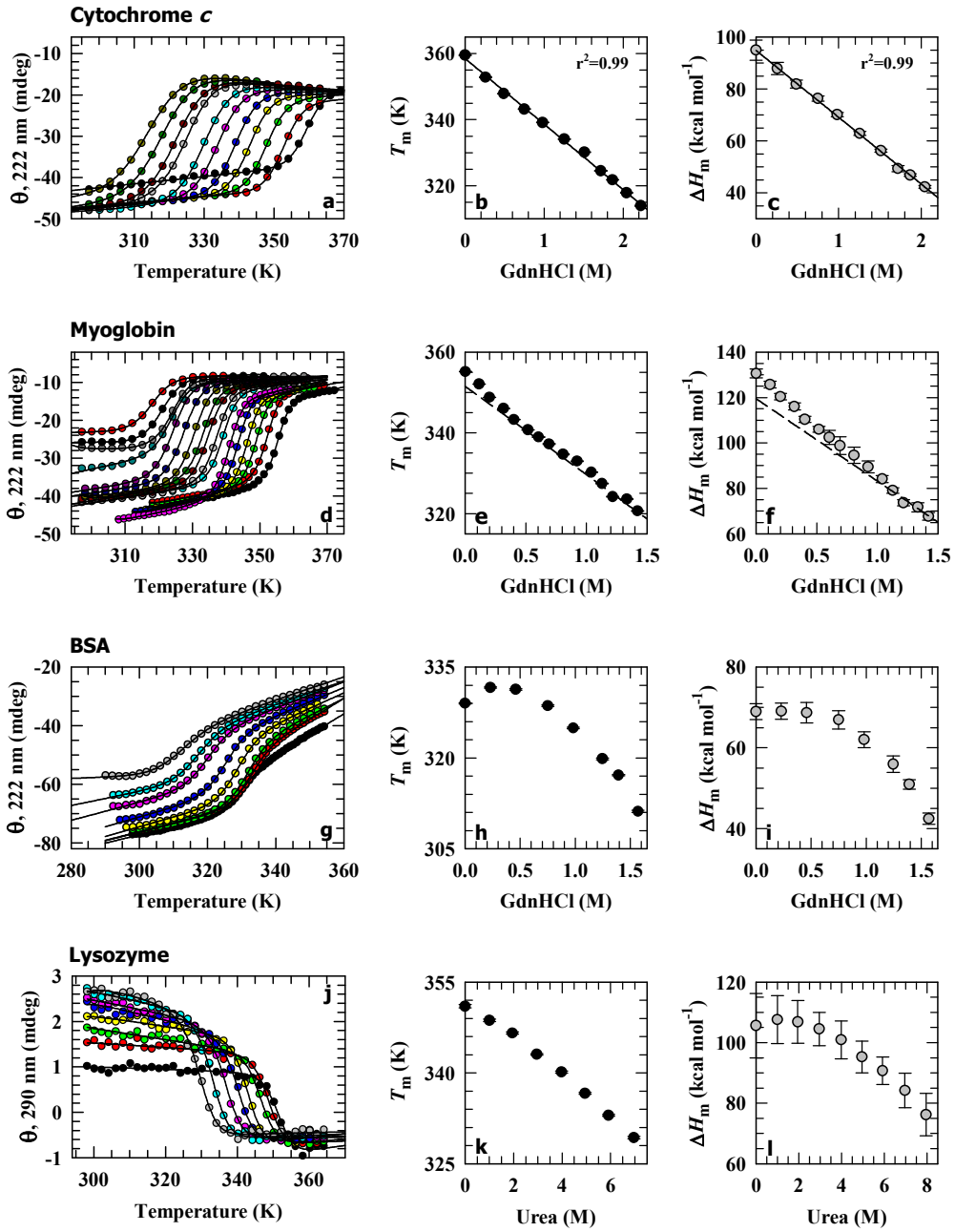

Figure 5. Temperature unfolding of (a) cytochrome *c*, (d) myoglobin, and (g) BSA at different molarity of GdnHCl, and (j) lysozyme at different urea. The transitions move to the left with increasing level of denaturants that are given in Table 5. Transitions were fit to Gibbs-Helmholtz equation as described in the text, and values of ΔC_p, ΔH_m, and T_m are listed in Table 5. Variation of Tm with GdnHCl: (b) cytochrome *c*, (e) myoglobin, (h) BSA, and (k) lysozyme. The dashed line in panel *e*, drawn approximately by using the transition region data points, is indicative of the deviation from linearity

which is apparent also for BSA (panel *h*) and lysozyme (panel *k*). Behavior of ΔH_m with GdnHCl: (c) cytochrome *c*, (f) myoglobin, (i) BSA, and (l) lysozyme. The deviation of myoglobin data from linearity is shown by the dashed line drawn by using the transition data approximately. Nonlinearity for BSA and lysozyme data is clearly evident.

Table 5. Fit parameters[#] of denaturant-variable thermal unfolding transitions to Gibbs-Helmholtz equation for all four proteins

Cytochrome *c*				Myoglobin				BSA				Lysozyme			
GdnHCl	ΔC_p	T_m	ΔH_m	GdnHCl	ΔC_p	T_m	ΔH_m	GdnHCl	ΔC_p	T_m	ΔH_m	Urea	ΔC_p	T_m	ΔH_m
0.00 M	*	359.5	94.9	0.00 M	5.62	355.2	130.6	0.00 M	1.04	329.0	68.9	0.00 M	3.37	351.0	105.6
0.25	*	352.8	87.9	0.10	5.83	352.1	125.7	0.23	1.99	331.6	69.1	1.00	3.20	348.6	107.6
0.50	*	347.8	81.9	0.20	5.79	348.8	120.4	0.45	0.15	331.3	68.7	1.95	3.45	346.5	106.8
0.75	0.31	343.2	76.3	0.30	5.40	346.0	116.0	0.75	0.07	328.6	66.9	2.95	3.68	343.0	104.5
1.00	0.23	339.1	70.1	0.40	5.58	343.3	110.3	1.00	1.03	324.9	62.0	4.00	3.76	340.1	100.9
1.25	0.50	334.1	62.7	0.50	4.95	340.7	105.9	1.25	0.05	319.8	56.0	4.95	3.37	336.6	95.3
1.50	0.70	330.2	56.2	0.60	1.97	338.9	102.4	1.40	*	317.1	51.0	5.90	3.38	333.0	90.7
1.75	1.77	324.5	49.3	0.70	1.53	337.2	98.8	1.55	*	311.2	42.4	6.95	4.20	329.3	84.2
1.90	0.87	321.8	46.8	0.80	0.75	334.7	94.6	1.70	0.53	304.4	32.8	7.95	4.27	326.3	76.2
2.05	0.77	317.9	42.3	0.90	4.05	332.9	89.4	1.85	*	300.9	26.4	8.95	4.02	324.5	69.6
2.20	0.53	313.9	37.5	1.00	3.76	330.2	84.1					9.95	2.32	323.8	63.6
2.35	0.54	309.6	33.4	1.10	1.70	327.4	79.1								
2.50	*	307.4	29.9	1.20	1.83	324.2	73.7								
2.65	*	305.0	26.5	1.30	0.79	323.6	71.7								

[#]ΔC_p, T_m, and ΔH_m are in kcal/mol K^{-1}, K, and kcal/mol, respectively; * indicates negligible value; Mean of standard error for T_m and ΔH_m are 0.1, 0.15, 0.2, and 0.2 K, and 2.0, 2.6, 1.8, and 6.7 kcal/mol for cytochrome *c*, myoglobin, BSA, and lysozyme, respectively.

2.4.6 Temperature, Denaturant, and pH Coupled Unfolding Experiments for Determination of ΔC_p and ΔG. Calculation of unfolding free energy from heat denaturation data requires accurate determination of ΔC_p, whose values is not reliable when extracted from fits of thermal transitions by the Gibbs-Helmholtz relation (Equation 7). A more reliable method is the use of the Kirchoff equation,[26]

$$\Delta C_p = \frac{\delta \Delta H_m}{\delta T_m} \tag{8}$$

which requires a set of ΔH_m and corresponding T_m values measured for a fixed concentration of the denaturant. The set of ΔH_m and T_m are generated by thermal unfolding experiments with the protein held at different pH, but at a known fixed denaturant concentration. The choice of the range of pH values is constrained so as to avoid considerable protein conformational change. This approach was used to determine ΔC_p values for all four proteins at different subdenaturing level of the denaturant.

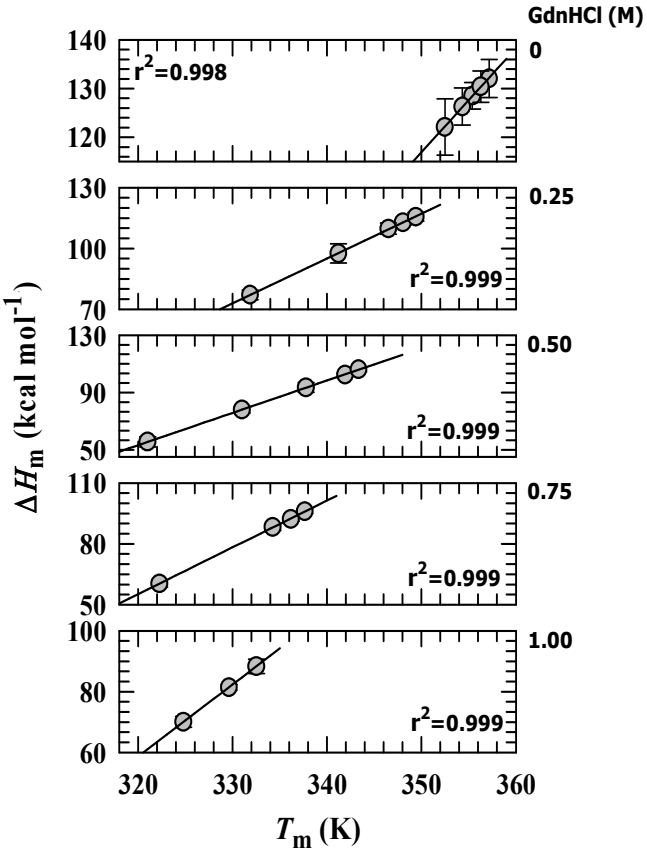

Figure 6. Representative data obtained from three-perturbant (denaturant, pH, and temperature) unfolding experiments for determination of ΔC_p under subdenaturing conditions, illustrated here with myoglobin results. The thermal melts are of sufficiently high quality, but are not shown here to avoid redundancy. ΔH_m and T_m are determined from thermal unfolding experiments at pH values 7.0, 6.0, 5.7, 5.3, and 5.0 for each indicated concentration of GdnHCl, and the slope of the plots provide the ΔC_p values at these denaturant

molarities (Equation 8). At higher denaturant (0.75 and 1.0 M GdnHCl) the protein is relatively destabilized, and low pH values are not used for experiments. Hence, there are only four and 3 data points at 0.75 and 1 M GdnHCl, respectively.

Table 6. ΔC_p values at different concentrations of denaturants for all four proteins. Calculations were done according to Equation 8.[#]

GdnHCl(M)	ΔC_p (kcal mol^{-1} K^{-1})			Urea(M)	ΔC_p (kcal mol^{-1} K^{-1})
	Cytochrome *c*	Myoglobin	BSA		Lysozyme
0.0	0.98	2.13	1.66	0.00	1.45
0.25	1.07	2.20	1.89	0.50	1.50
0.50	1.13	2.25	0.93	1.00	1.53
0.75	1.20	2.30	1.07	1.50	1.58
1.00	1.28	2.36	1.76	2.00	1.62
			2.50	1.66	
			3.00	1.70	
			3.50	1.73	
			4.00	1.78	

pH values at each concentration of the denaturant used for data measurement were 7.5, 6.5, 5.5, and 4.5 for cytochrome *c*, 7.0, 6.0, 5.7, 5.3, and 5.0 for myoglobin, 7.0, 6.0, 4.5, and 4.0 for BSA, and 5.0, 4.5, and 3.6 for lysozyme. The proteins presumably do not undergo a major conformational change under the corresponding pH conditions.

Figure 6 shows a sample data set measured for myoglobin at pH values 7, 6, 5.7, 5.3, and 5 at the indicated concentrations of GdnHCl. The slopes provide ΔC_p values, whose dependence on the denaturant is credibly linear for all proteins except BSA (Figure 7a,c,e,g, Table 6). The outlying dependence observed for BSA may arise from a number of factors, including a shift from two- to three-state unfolding transition at pH values below 7. The linear dependence of ΔC_p on subdenaturing concentration of denaturants is consistent with earlier data for several proteins,[27,28] and has been proposed to arise from protein-denaturant interactions whereby the protein is solvated by the denaturant.[28–31] The linear increase in ΔC_p at low concentrations of denaturants can hardly be used to sense the response of protein

conformation to subdenaturing conditions, because any minor change in the heat capacity of the native-like states, which may arise from weakening of a hydrogen bonding interaction or a small change in entropy, is overwhelmed by heat effects of protein-denaturant interactions. The ΔC_p values can nonetheless be used to evaluate $\Delta H(T)$ and $\Delta S(T)$ at temperature T so as to obtain $\Delta G(T)$.

$$\Delta H(T) = \Delta H_m + \int_{T_m}^{T} dT \Delta C_p(T) \quad (9)$$

$$\Delta S(T) = \Delta S_m + \int_{T_m}^{T} d\,(\ln T) \Delta C_p(T) \quad (10)$$

If $\Delta C_p(T)$ is considered constant, especially near physiological temperature where it appears temperature independent,[32]

$$\Delta H(T) = \Delta H_m + \Delta C_p(T - T_m) \quad (11)$$

$$\Delta S(T) = \frac{\Delta H_m}{T_m} + \Delta C_p ln\left(\frac{T}{T_m}\right) \quad (12)$$

$$\Delta G(T) = \Delta H(T) - T\Delta S(T) = \Delta H_m \left(1 - \frac{T}{T_m}\right) + \Delta C_p \left\{T - T_m - T\ ln\left(\frac{T}{T_m}\right)\right\} \quad (13)$$

The denaturant dependence of ΔG calculated at T=298 K (Figure 7b,d,f,h, Table 7) qualitatively reproduces the dependence observed in isothermal denaturant-induced unfolding experiments for all four proteins described earlier (compare with Figures 1c, 2e, 3e, 4e), providing further evidence that LFEM is not universally applicable.

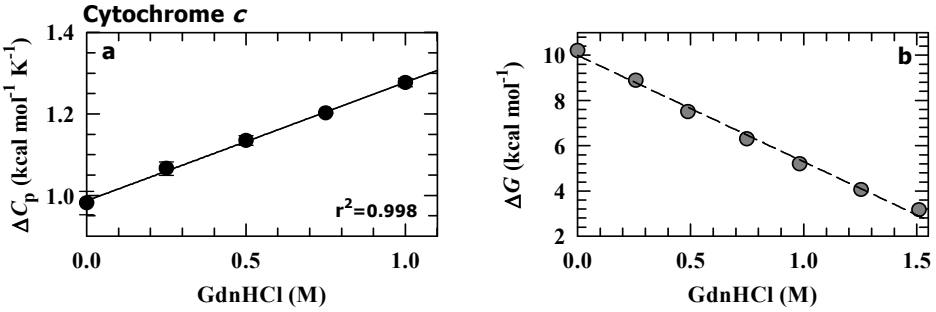

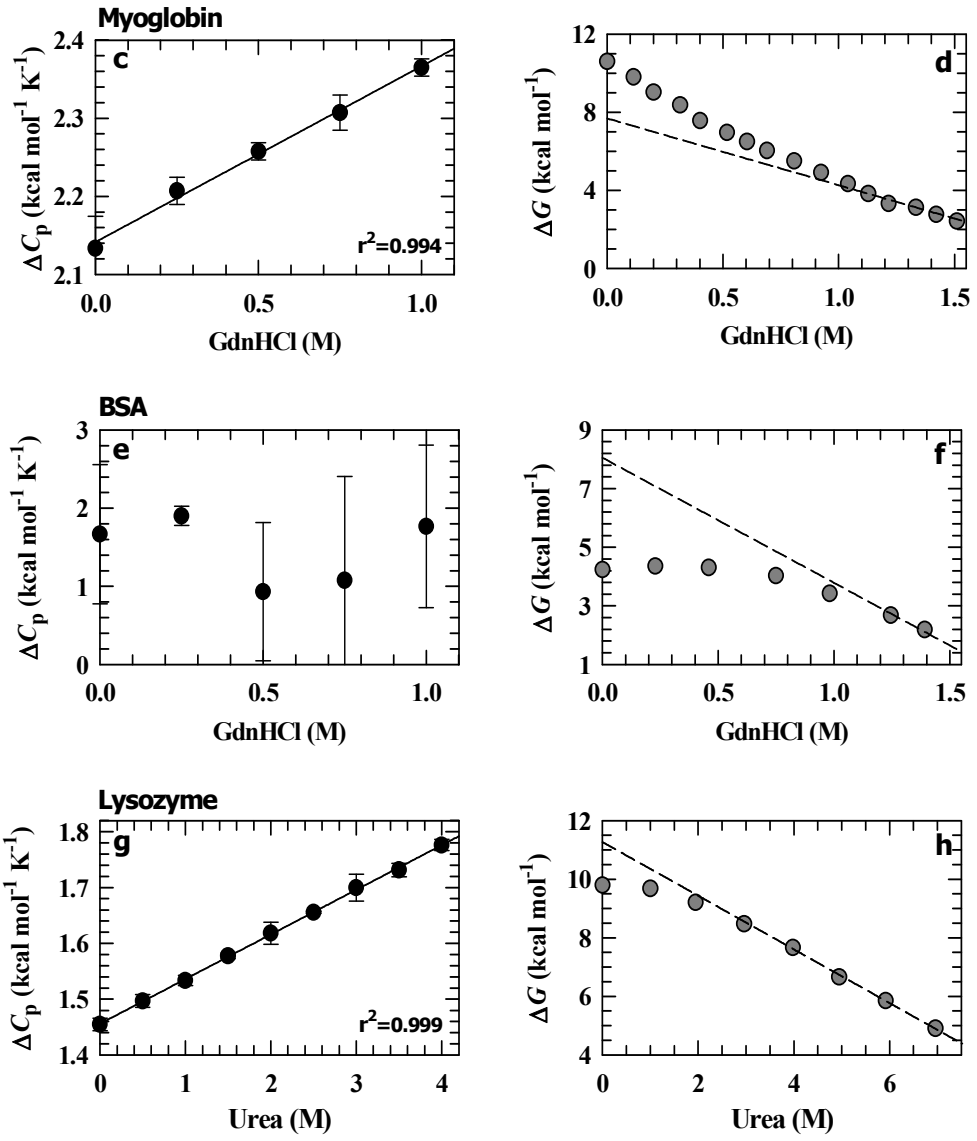

Figure 7. Three-perturbant (denaturant, pH, and temperature) unfolding experiments for determination of ΔC_p, and ΔG (Equations 8 and 13) under subdenaturing conditions. Values of ΔC_p, and ΔG and corresponding denaturant concentrations are listed in Tables 6 and 7, respectively. ΔC_p dependence on GdnHCl for (a) cytochrome *c* and (c) myoglobin and on urea for (e) lysozyme is perfectly linearly with a positive slope. (g) Variation of ΔC_p on GdnHCl for BSA is not determined accurately, due to considerable perturbation of BSA conformation by lower pH. The denaturant dependence of ΔG on denaturant: (b) cytochrome *c*, (d) myoglobin, (f) BSA, and (h) lysozyme.

Table 7. Δ*G* (298 K) values in kcal mol^{-1} at different concentrations of denaturants for all four proteins calculated from heat unfolding transitions in conjunction with ΔC_p values (Equation 13). [#]

Cytochrome *c*		Myoglobin		BSA		Lysozyme	
GdnHCl (M)	Δ*G*	GdnHCl (M)	Δ*G*	GdnHCl (M)	Δ*G*	Urea (M)	Δ*G*
0.00	10.2 (9.30)	0.00	10.6 (9.95)	0.00	4.25 (2.85)	0.00	9.80 (10.05)
0.25	8.88 (8.20)	0.10	9.80	0.23	4.35 (3.45)	1.00	9.70
0.50	7.50 (7.25)	0.20	9.00	0.45	4.30 (3.95)	1.95	9.20
0.75	6.30 (6.05)	0.30	8.40 (8.15)	0.75	4.00 (3.20)	2.95	8.50
1.00	5.20 (5.35)	0.40	7.60	1.00	3.40 (1.90)	3.00	7.70
1.25	4.05 (4.85)	0.50	7.00	1.25	2.70	4.95	6.65 (4.45)
1.50	3.20 (4.00)	0.60	6.50 (5.75)	1.40	2.20	5.90	5.85
		0.70	6.00	1.60	1.35	7.00	4.90
		0.80	5.50	1.70	0.60	7.95	3.95
		0.90	4.90 (5.48)	1.85	0.25	8.95	3.25
		1.05	4.35 (2.15)			9.95	2.70
		1.10	3.85				
		1.20	3.35 (2.15)				
		1.35	3.15				
		1.40	2.75				
		1.50	2.40				
		1.60	2.20				
		1.70	1.85				
		1.80	1.65				

#, parentheses contain Δ*G* values at the corresponding denaturant molarity obtained from CD-measured unfolding at 298 K.

2.4.7 Temperature Stability Curves. The $\Delta G(T)$ function is often used to determine protein stability curves when ΔC_p is known reliably regardless of whether the heat capacity change is temperature dependent or independent.[29,33] The curves were calculated at different concentrations of GdnHCl and urea, where temperatures at which ΔG=0 correspond to midpoint temperatures of cold denaturation, T_c, and heat denaturation, T_m (Figure 8). Clearly, all four proteins undergo cold denaturation − a general phenomenon recognized from extensive thermodyna- mic studies of Privalov and others.[29,33–39] Values of T_c and T_m read from the curves are listed in Table 8, which shows consistency of T_m values calculated directly from Gibbs-Helmholtz fits of thermal unfolding transitions (Figure 5b,e,h,k). The results also show higher values of T_c with larger ΔC_p values, a fact known since early days of the discovery of cold denaturation.[29,35] Amongst the four proteins studied, ΔC_p of myoglobin is largest at all concentrations of the denaturant (Figure 7, Table 6), which facilitates experimental studies of cold denaturation[35] under solvent conditions and temperatures that are relatively easily accessible than those required for cytochrome *c*.[39]

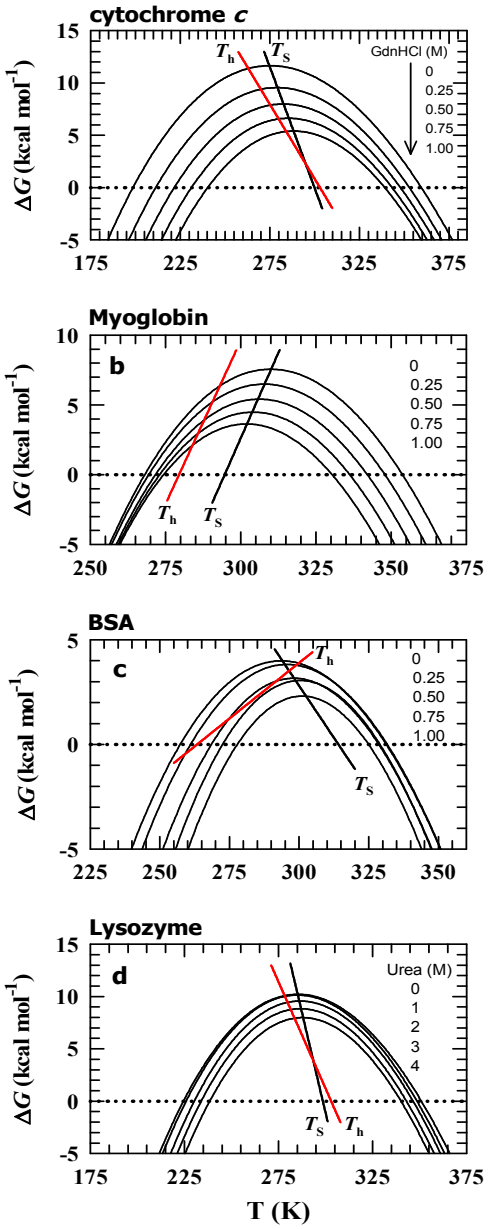

Figure 8. Stability curves at indicated denaturant concentrations calculated according to Equation 13. Straight lines labeled T_S and T_h show temperatures of maximum stability and ΔH=0, respectively.

Table 8. Midpoint temperature for cold and heat denaturation (T_c and T_m, respectively), temperature of maximum stability (T_S), and the temperature at which $\Delta H=0$ (T_h) for the four proteins at subdenaturing levels of denaturant concentration. Unit Kelvin.

	Cytochrome *c*				Myoglobin				BSA					Lysozyme			
GdnHCl	T_c	T_m	T_S	T_h	T_c	T_m	T_S	T_h	T_c	T_m	T_S	T_h	Urea	T_c	T_m	T_S	T_h
0 M	198.5	359.5	275.0	262.5	268.0	354.0	310.0	292.5	272.5	329.0	300.5	287.5	0 M	224.5	351.0	285.5	278.0
0.25	211.5	353.0	279.0	271.0	269.5	348.0	308.0	291.0	261.0	332.0	295.5	295.5	1	226.0	348.5	285.0	278.5
0.50	221.5	348.0	282.5	275.5	271.5	342.0	306.0	288.5	275.5	331.5	293.5	257.5	2	230.5	346.5	286.5	280.5
0.75	231.5	343.0	285.5	279.5	273.0	336.5	304.0	286.0	268.5	328.5	298.0	266.0	3	234.0	343.0	287.0	281.5
1.00	240.5	339.0	288.5	284.0	274.5	330.5	302.0	284.0	278.0	325.0	301.0	290.0	4	238.5	340.0	288.0	283.5

The stability curves allow estimation of two other parameters: T_S, the temperature of maximum stability (ΔG_S), and T_h, the temperature at which ΔH=0. The T_S value corresponds to the temperature of maximum ΔG in the curve, and T_h is calculated by[33]

$$T_h = T_m - \frac{\Delta H_m}{\Delta C_p} \quad (14)$$

Values of T_S and T_h at all concentrations of denaturants used are given in Table 8, and are shown by straight lines in Figure 8.Since ΔG_S=ΔH at T_S, and ΔH=0 at T_h,[33] the temperature and the denaturant concentration at which the lines intersect should correspond to a condition at which ΔG=0. This fulfillment is not observed in data sets present, most likely due to nonlinearity of one or both of T_S and T_h on GdnHCl.

2.5 DISCUSSION

2.5.1 Degree and Direction of Nonlinearity of Δ*G*. Results here provide evidence that the ΔG vs denaturant plot could be linear or nonlinear, and there is no way of knowing a priori which track would be observed. Regarding nonlinearity, the course of deviation may be upward or downward, and observations made for BSA and lysozyme imply that the extent of curvature may vary from one protein to another.

Table 9. Nonlinearity in the Δ*G*–denaturant plot for some proteins.

Protein	Denaturant	Solvent conditions	Curvature[#]	Reference
Myoglobin	GdnHCl	pH 7, 25ºC	++	*18*,*40*,*41*,this work
Barnase	pH	25ºC	−−	*42*
	Urea	pH 6.3	++	*31*
Ubiquitin	GdnHCl	pH 2	−−−	*43*
RNase A	Urea	pH 3.6, 25ºC	+	*44*
RNase T1	GdnHCl	pH 7, 25ºC	+	*44*
SNase mutants	Urea	pH 8, 20ºC	−−	*45*,*46*
	NaSCN	pH 8, 20ºC	+−	*45*,*46*
β1	GdnHCl	pH 5, 25ºC	−	*47*
Bacteriorhodpsin	SDS	pH 7	−−−	*48*
BSA	GdnHCl	pH 7, 25ºC	−−−	this work
Lysozyme	Urea	pH 5, 25ºC	−−	*22*, this work

#, Upward and downward curvatures are denoted by + and −, respectively. The number of '+' or '−' signs qualitatively indicates the extent of curvature.

Reports on nonlinearity and the extent of curvature in the ΔG vs denaturant plot (Table 9) may seem relatively scanty, apparently due to incomplete ΔG measurement of investigated proteins under subdenaturing concentrations of denaturant. But evidences are compelling that folding energy be measured over an extended range of denaturant concentration not only for improved estimation of protein stability in a model-independent manner, but also to develop a data base that might provide clues to the basis of the ΔG−denaturant relation.

2.5.2 Inadequacy of LFEM. The observations that LEM works for some proteins exemplified here by cytochrome *c*, but not for others, including those listed in Table 9, pose a fundamental difficulty regarding the use and interpretation of this widely employed method that holds that the dependence of Gibbs energy of folding on chemical denaturant is determined by the parameter m_g, which is constant at all levels of the denaturant.[6] But, in the denaturant dependence of the isothermal folding equilibrium constant, $(\partial \ln K/\partial D) \cong m_g$, the parameter m_g is related to the excess free energy due to protein-denaturant interaction, and since the interaction is expected to vary across the denaturant scale, m_g must also be a function of the denaturant. The functional dependence of m_g on the denaturant is difficult to know from a single experiment, which allows evaluation of the equilibrium constant only across the narrow unfolding transition region.[2] There is little assurance that m_g will remain constant at all concentrations of the denaturant. The nonlinear dependence of Gibbs energy of protein interactions with denaturant, where the nonlinearity is more pronounced with GdnHCl than urea,[28] also suggests that m_g should be nonlinear with denaturants. Therefore, m_g need not be considered a parameter value. Strictly, $(\partial \ln K/\partial D) \cong m_g$ and its linear free energy form, $\Delta G = \Delta G^o - m_g[D]$, should be used only at the transition midpoint or, at most, across the steep unfolding transition where the equilibrium constant is substantial in magnitude and measured easily. Within this narrow interval of denaturant concentration the denaturant-dependent 'm_g-function' may be approximated by a 'm_g-value', but there is little scope of using this value all across the denaturant scale. Makhatadze and Privalov have also reasoned that the m_g-

parameter ($\cong\partial\Delta G/\partial D$) need not be a constant.[28] Their estimation of deviation from linearity is marginal for urea, but amounts to roughly 10 to 15% when GdnHCl-measured ΔG values are extrapolated to zero denaturant concentration.

The m_g-value in the context of LEM is also correlated with the difference in solvent accessible surface areas in native and unfolded states (ΔASA) that are calculated from crystal structures of native proteins and appropriate peptide surfaces.[41] Although this relation is approximately, but not exactly, obtained in theoretical models as well,[2,4] the fact resurfaces that the denaturant functional dependence of m_g should also be reflected in ΔASA. In another study, Thirumalai and coworkers claim that Tanford's transfer model and hence the linearity of ΔG vs denaturant holds, in spite of the fact that their calculated curve is largely nonlinear.[49] In a similar study of analysis of SMFRET data, folding free energy of some proteins are not found to vary linearly with denaturant molarity.[50] Therefore, difference in surface exposure, m_g, and ΔG of protein folding need not invariably be linear functions of the denaturant concentration. Some earlier reports on proteins showing nonlinear dependence of folding energy on denaturant have treated them as special cases with interpretations in a protein and solvent specific model-dependent manner. Curvatures noticed for barnase,[31,42] myoglobin,[18,40,41] RNases A and T1,[44] and SNase mutants[45,46] have been interpreted by invoking the denaturant binding model, which is known to yield a higher value of protein stability than does LEM,[51] or unusual chaotrope-protein interaction in the denatured state or deviation from two-state folding. There also is an impression that ionic nature of GdnHCl may contribute to some rollover in folding energy, of thioredoxin, for example.[47] The ionic nature of GdnHCl cannot be overemphasized however, since neutral salt like NaCl is known to stabilize[11,12,25,43,52,53] or destabilize[47] proteins. For myoglobin, a detailed calorimetric study of Kelly and Holladay finds that none of the models used for estimation of folding free energy is adequate.[41] No model at present appears universal that can be used to estimate ΔG irrespective of the protein identity.

2.5.3 Model Independence: Denaturant Effect on Structural, Conformational, and Energetic Fluctuations. It is now widely believed that denaturants bind to

independent and similar sites on proteins, often referred to as 'simple binding'.[28] Existing evidences suggest direct protein-denaturant interactions,[55−58] by both van der Waals and multiple hydrogen-bonding interactions of denaturant atoms with protein backbone and side chain atoms.[59−61] Often a denaturant molecule forms hydrogen bonds with amino acids from different parts of the protein, thereby mediating additional intramolecular interactions.[61] At the same time, some native-state intramolecular contacts may be weakened or abolished. These modes of binding have at least three critical consequences on conformation, motions, and energy of proteins even in the presence of subdenaturing levels of denaturant concentration. First, the binding is not weak and selective, implying that Gibbs energy of denaturant binding as well as protein unfolding energy should not vary linearly with denaturant concentration.[28] Second, denaturant-mediated intramolecular crosslinks serve to restrict conformational dynamics of the protein molecule, resulting in a decrease in configurational entropy.[53,62] Third, denaturant binding significantly affects intramolecular vibrations by shifting the fundamental frequencies of internal modes.[63] In addition to these, denaturants affect both structure of water and surface hydration of protein.[64-66] It is important to note that manifests of the denaturant effect essentially depend on the concentration of the denaturant itself. The effects on protein energy and conformational fluctuations considered here assume larger significance in the subdenaturing limit of denaturant concentration where only a few of them are bound to the protein, so the average protein conformation is not very different from that of the native state. But at higher concentrations of the denaturant, the protein unfolding effect sets in due to binding of more denaturant molecules. Large-amplitude unfolding motions now overrun the initial effects observed in the subdenaturing regime. This note, partly presented earlier,[53] also appears to argue against the linearity of Gibbs energy of folding on denaturant.

Of the three outcomes of denaturant binding at the subdenaturing level, entropy decrease and shift of fundamental frequencies of internal modes of vibrations to different values have considerable influence on conformational fluctuations and average energy spectrum of the protein. Because fluctuations in native-state proteins allow for sampling of multiple conformational states whose energies are spread over a

wide range, a decrease in entropy is expected to limit fluctuations to a fewer conformational states, resulting in a lower mean square energy of the protein. Likewise, the shift of vibrational frequencies to lower values due to denaturant binding allows thermal excitation of lower energy modes, producing less average energy. However, the denaturant cross-linked protein is not homogenous; it is also likely that fundamental frequencies of some protein oscillators shift to higher values. The general implication of initial denaturant binding is perturbation of the average energy to variable extent as native-like states are populated. The perturbation should be specific for a protein considered, and whether the energy increases, decreases or stays near zero is determined by factors including changes in intramolecular contacts, entropy, and frequencies of oscillator vibrations. This thinking is similar to the finding of Yang and Honig that the contribution of pairwise charge-charge electrostatic interactions to protein stability may be positive negative or close to zero depending on the solvent pH and charge distribution on the protein surface.[19,67] The point of importance is the outcome of the interaction which is protein specific in the pretransition region. The significance of the energy variation in the subdenaturing regime disappears across the transition region of denaturant where large-amplitude unfolding motions dominate, and the average energy of the native-like ensembles increases. Denaturant sensitivity of the energy of the unfolded state is generally not substantial, because virtually all structural elements, including van der Waals interactions and hydrogen bonds are fully disrupted.

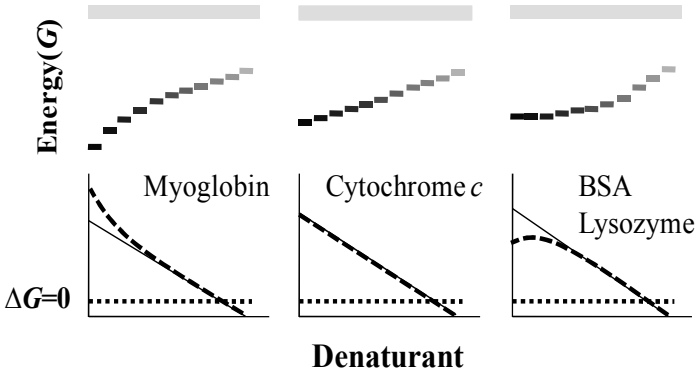

Figure 9. Schematic of denaturant-induced changes in Gibbs energy for the three different variations of ΔG on denaturant. Horizontal gray bars indicate relatively less sensitivity of the denatured state energy to the presence of denaturant. *Left*, upward curvature observed for myoglobin. *Middle*, the linear free energy dependence exemplified by cytochrome *c*. *Right*, downward curvature or rollover seen for BSA and lysozyme.

Apart from certain protein specific cases where nonrandom residual structure or non-native interactions occur,[46,68–72] the unfolded-state energy is unlikely to vary considerably with the denaturant. It follows that the denaturant dependence of folding energy is determined by protein specific response of structure and conformational fluctuations of native-like states to denaturant binding. This analysis is schematized in Figure 9 showing the correspondence with the experimental results of protein stability versus denaturant obtained.

2.5.4 Changes in Protein Heat Capacity with Denaturant Binding. Because the premise of the model is a change in the average energy of the protein due to denaturant binding and consequent restricted conformational fluctuations under subdenaturing conditions, the heat capacity of the protein should change commensurately. The spread about the mean internal energy of the protein is related to heat capacity by[73–77]

$$< \delta U^2 > \equiv < \delta E^2 > = k_B T^2 C_V \approx k_B T^2 C_P \qquad (15)$$

Therefore, the specific heat upon subdenaturing level of denaturant binding should increase substantially for the case of upward curvature of ΔG vs [D] (myoglobin), increase proportionately for the linear curve (cytochrome *c*), decrease largely for the downward curvature (BSA), and decrease moderately for the case of modest rollover (lysozyme). This is a challenging demand, and we have no data to substantiate at present. Limited studies have reported variable increase in specific heat of protein titration with denaturants in cases of cytochrome *c*, lysozyme, and RNase A,[28] but a decrease for several hydrophobic amino acids, dipeptides, and ovalbumin in the presence of urea.[78] It appears that the dependence of C_p on denaturant may vary in protein, cosolvent, and buffer specific manners in a way similar to results of differential scanning microcalorimetry.[79] Available C_p data for cytochrome *c* and lysozyme at different denaturant concentrations appears fairly consistent with our ΔG vs denaturant data. A recent study of calculations based on molecular transfer model has shown that C_v values for protein L and CspTm increase with urea, which is somewhat consistent with the calculated ΔG vs urea curve for protein L, but not for

the other protein.[49] Clearly, more isothermal calorimetry results of protein-denaturant titration will be needed to examine the correlations of C_p vs denaturant and ΔG vs denaturant curves.

2.6 CONCLUSIONS

Theory does not provide direct support for the linear free energy transfer model, and the determination of conformational stability of proteins (ΔG^o) by linear extrapolation from the transition region to the ordinate is burdened with huge uncertainty. Although SB procedure of nonlinear least square analysis of the entire transition curve appears to ameliorate the problem to an extent, the uncertainty about the actual denaturant dependence of pre- and post-transition baselines is likely to introduce error in the ΔG^o value. Accurate determination ΔG^o involves the use of two or more denaturing agents, where the primary denaturant alone provides ΔG values across the unfolding transition, and transitions measured by varying the secondary denaturant at fixed concentrations of the primary denaturant yield ΔG values in the subdenaturing region. All of these transitions are analyzed by SB method. Results of such a complete set of experiment would tell whether the dependence of ΔG on denaturant is linear, near-linear or curved for a given protein. The denaturant effect on protein stability is made complex by changes in protein fluctuations and intramolecular interactions brought about by denaturant binding interactions, and thus modulating the internal energy.

2.7 REFERENCES

1. Greene, R. F., and Pace, C. N. (1974) Urea and guanidine hydrochloride denaturation of ribonuclease, lysozyme, α-chymotrypsin, and β-lactoglobulin. *J. Biol. Chem. 249*, 5388–5393.
2. Schellman, J. A. (1978) Solvent denaturation. *Biopolymers 17*, 1305–1322.
3. Schellman, J. A. (1987) Selective binding and solvent denaturation. *Biopolymers 26*, 549–559.
4. Alonso, D. O. V, and Dill, K. A. (1991) Solvent denaturation and stabilization of globular proteins. *Biochemistry 30*, 5974–5985.

5. Schellman, J. A. (2002) Fifty years of solvent denaturation. *Biophys*. *Chem*. *96*, 91–101.
6. Pace, C. N., and Shaw, K. L. (2000) Linear extrapolation method of analyzing solvent denaturation curves. *PROTEINS*: *Struct*. *Func*. *Genet*. *Suppl*. *4*, 1–7.
7. Pfeil, W. (1998) *Protein Stability and Folding*. *A collection of Thermodynamic Data*, Springer-Verlag, Berlin Heidelberg.
8. Pfeil, W. (1998) *Protein Stability and Folding Supplement 1*. *A collection of Thermodynamic Data*, Springer-Verlag, Berlin Heidelberg.
9. Maxwell, K. L., Wildes, D., Zarrine-Afsar, A., de Los Rios, M A., Brown, A. G., Friel, C. T., Hedberg, L., Horng, J-C., Bona, D., Miller, E. J., Vallee-Belisle, A., Main, E. R. G., Bemporad, F., Qiu, L., Teilum, K., Vu, N-D., Edwards, A. M., Ruczinski, I., Poulsen, F. M., Kragelund, B. B., Michnick, S. W., Chiti, F., Bai, Y., Hagen, S. J., Serrano, L., Oliveberg, M., Raleigh, D. P., Wittung-Stafshede, P., Radford, S. E., Jackson, S. E., Sosnick, T. R., Marqusee, S., Davidson, A. R., and Plaxco, K. W. (2005) Protein folding: defining a "standard" set of experimental conditions and a preliminary kinetic data set of two-state proteins. *Protein Sci*. *14*, 602−616.
10. Santoro, M. M., and Bolen, D. W. (1988) Unfolding free energy changes determined by the linear extrapolation method. 1. Unfolding of phenylmethanesulfonyl α-chymotrypsin using different denaturants. *Biochemistry 27*, 8063–8068.
11. Santoro, M. M., and Bolen, D. W. (1992) A test of linear extrapolation of unfolding free energy changes over an extended denaturant concentration range. *Biochemistry* 31, 4901−4907.
12. Santoro, M. M., and Bolen, D. W. (1995) How valid are denaturant-induced unfolding free energy measurements? Level of conformance to common assumptions over an extended range of ribonuclease A stability. *Biochemistry 34*, 3771−3781.
13. Pace, C. N., Grimsley, G. R., Thomas, S. T., and Makhatadze, G. I. (1999) Heat capacity change for ribonuclease A folding. *Protein Sci*. *8*, 1500−1504.
14. Greenfield, N. J. (2006) Determination of the folding of proteins as a function of

denaturants, osmolytes or ligands using circular dichroism. *Nature Protoc*. *1*, 2733−2741.

15. Tanford, C. (1968) Protein denaturation. *Adv*. *Protein Chem*. *23*, 121–282.
16. Tanford, C. (1970) Protein denaturation. C. Theoretical models for the mechanism of denaturation. *Adv*. *Protein Chem*. *24*, 1–95.
17. Ahmad, F., Taneja, S., Yadav, S., Haque, S. E. (1994) A new method for testing the functional dependence of unfolding free energy changes on denaturant concentration. *J. Biochem*. *115*, 322–327.
18. Gupta, R., Yadav, S., and Ahmad, F. (1996) Protein stability: urea-induced versus guanidine-induced unfolding of metmyoglobin. *Biochemistry 35*, 11925–11920.
19. Ibarra-Molero, B., and Sanchez-Ruiz, J. M. (1996) A model-independent, nonlinear extrapolation procedure for the characterization of protein folding energetics from solvent-denaturation data. *Biochemistry 35*, 14689–14702.
20. Gupta, R., and Ahmad, F. (1999) Protein stability: functional dependence of denaturational Gibbs energy on urea concentration. *Biochemistry 38*, 2471–2479.
21. Fung, A., Li, P., Godoy-Ruiz, R., Sanchez-Ruiz, J. M., and Munoz, V. (2008) Expanding the realm of ultrafast protein folding: gpW, a midsize natural single-domain with α+β topology that folds downhill. *J. Am*. *Chem*. *Soc*. *130*, 7489–7495.
22. Yasin, U. M., Sashi, P., and Bhuyan, A. K. (2014) Free energy landscape of lysozyme: multiple near-native conformational states and rollover in the urea dependence of folding energy. *J. Phys*. *Chem*. *B 118*, 6662–6669.
23. Farruggia, B., and Pico, G. A. (1999) Thermodynamic features of the chemical and thermal denaturations of human serum albumin. *Int*. *J. Biol*. *Macromolecules 26*, 317-323.
24. Norberto, D. R., Vieira, J. M., de Souza, A. R., Bispo, J. A. C., Bonafe, C. F. S. (2012) Pressure- and urea-induced denaturation of bovine serum albumin: considerations about protein homogeneity. *Open J. Biophys*. *2*, 4-14.
25. Mayr, L. M., and Schmid, F. X. (1993) Stabilization of a protein by guanidinium chloride. *Biochemistry 32*, 7994–1998.
26. Privalov, P. L. (1979) Stability of proteins: small globular proteins. *Adv*. *Protein*

Chem. *33*, 167–241.

27. Pfeil, W., and Privalov, P. L. (1976) Thermodynamic investigations of proteins. 1. Standard functions for proteins with lysozyme as an example. *Biophys*. *Chem*. *4*, 23–32.
28. Makhatadze, G. I., and Privalov, P. L. (1992) Protein interactions with urea and guanidinium chloride. A calorimetric study. *J*. *Mol*. *Biol*. *226*, 491–505.
29. Privalov, P. L. (1990) Limited internal friction in the rate-limiting step of a two-state protein folding reaction. *Crit*. *Rev*. *Biochem*. *Mol*. *Biol*. *25*, 281–305.
30. Griko, Y. V., and Privalov, P. L. (1992) Calorimetric study of the heat and cold denaturation of β-lactoglobulin. *Biochemistry 31*, 8810–8815.
31. Johnson, C. M., and Fersht, A. R. (1995) Protein stability as a function of denaturant concentration: the thermal stability of barnase in the presence of urea. *Biochemistry 34*, 6795-6804.
32. Privalov, P. L., and Khechinashvili, N. N. (1974) A thermodynamic approach to the problem of stabilization of globular protein structure: a calorimetric study. *J*. *Mol*. *Biol*. *86*, 665–684.
33. Becktel, W. J., and Schellman, J. A. (1987) Proetin stability curves. *Biopolymers 26*, 1859–1877.
34. Chen, B.-L, and Schellman, J. A. (1989) Low-temperature unfolding of a mutant of phage T_4 lysozyme. 1. Equilibrium studies. *Biochemistry 28*, 685–691.
35. Privalov, P. L., Griko, Yu. V., Venyaminov, S. Yu., and Kutyshenko, V. P. (1986) Cold denaturation of myoglobin. *J*. *Mol*. *Biol*. *190*, 487–498.
36. Griko, Yu. V., and Privalov, P. L. (1986) Cold denaturation of myoglobin in alkaline solutions. *Dokl*. *Acad*. *Nauk S.S.S.R*. *291*, 709–711.
37. Cho, K. C., and Chan, K. K. (1984) Kinetics of cold-induced denaturation of metmyoglobin. *Biochim*. *Biophys*. *Acta 786*, 103–108.
38. Chen, B.-L, Baase, W. A., and Schellman, J. A. (1989) Low-temperature unfolding of a mutant of phage T4 lysozyme. 2. Kinetic investigations. *Biochemistry 28*, 691–699.
39. Kumar, R., Prabhu, N. P., Rao, D. K., and Bhuyan, A. K. (2006) The alkali molten globule state of horse ferricytochrome c: observation of cold denaturation. *J*. *Mol*.

Biol. *364*, 483–495.

40. Pace, C. N. and Vanderburg, K. E. (1979) Determining globular protein stability: guanidine hydrochloride denaturation of myoglobin. *Biochemistry 18*, 288–292.
41. Myers, J. K., Pace, C. N., and Scholtz, M. (1995) Denaturant *m* values and heat capacity changes: relation to changes in accessible surface areas of protein unfolding. *Protein Sci*. *4*, 2138–2148.
42. Pace, C. N., Laurents, D. V., and Erickson, R. E. (1992) Urea denaturation of barnase: pH dependence and characterization of the unfolded state. *Biochemistry 31*, 2728–2734.
43. Makhatadze, G. I. (1999) Thermodynamics of protein interactions with urea and guanidinium hydrochloride. *J*. *Phys*. *Chem*. *103*, 4781−4785.
44. Pace, C. N., Laurents, D. V., and Thomson, J. A. (1990) pH dependence of the urea and guanidine hydrochloride denaturation of ribonucleasse A and ribonuclease T1. *Biochemistry 29*, 2564–2572.
45. Shortle, D., Meeker, A. K., and Gerring, S. L. (1989) Effects of denaturants at low concentrations on the reversible denaturation of staphylococcal nuclease. *Arch*. *Biochem*. *Biophys*. *272*, 103–113.
46. Shortle, D. (1996) The denatured state (the other half of the folding equation) and its role in protein stability. *FASEB J*. *10*, 27–34.
47. Ferreon, A. C. M., and Bolen, D. W. (2004) Thermodynamics of denaturant-induced unfolding of a protein that exhibits variable two-state denaturation. *Biochemistry 43*, 13357−13369.
48. Chang, Y-C., and Bowie, J. U. (2014) Measuring membrane protein stability under native conditions. *Proc*. *Natl*. *Acad*. *Sci*. *USA 111*, 219-224.
49. O'Brien, E. P., Ziv, G., Haran, G., Brooks, B. R., and Thirumalai, D. (2008) Effects of denaturants and osmolytes on proteins are accurately predicted by the molecular transfer model. *Proc*. *Natl*. *Acad*. *Sci*. *USA 105*, 13403–13408.
50. Ziv, G., and Haran, G. (2009) Protein folding, protein, collapse, and Tanford's transfer model: lessons from single-molecule FRET. *J*. *Am*. *Chem*. *Soc*. *131*, 2942–2947.
51. Wu, J-W., and Wang, Z-X. (1999) New evidence for the denaturant binding

model. *Protein Sci*. *9*, 2090−2097.

52. Pace, C. N., and Grimsley, G. R. (1988) Ribonuclease T1 is stabilized by cation and anion binding. *Biochemistry 27*, 3242−3246.
53. Bhuyan, A. K. (2002) Protein stabilization by urea and guanidine hydrochloride. *Biochemistry 41*, 13386–13394.
54. Kelly, L., and Holladay, L. A. (1990) A comparative study of the unfolding thermodynamics of vertebrate metmyoglobins. *Biochemistry 29*, 5062–5069.
55. Stumpe, M. C., and Grubmuller, H. (2007) Interaction of urea with amino acids: implications for urea-induced protein denaturation. *J*. *Am*. *Chem*. *Soc*. *129*, 16126−16131.
56. Hua, L., Zhou, R., Thirumalai, D., and Berne, B. J. (2008) Urea denaturation by stronger dispersion interactions with proteins than water implies a 2-stage unfolding. *Proc*. *Natl*. *Acad*. *Sci*. *USA 105*, 16928−16933.
57. Zangi, R., Zhou, R., and Berne, B. J. (2009) Urea's action on hydrophobic interaction. *J*. *Am*. *Chem*. *Soc*. *131*, 1535−1541.
58. Lee, S., Shek, Y. L., and Chalikian, T. V. (2010) Urea interactions with protein groups: a volumetric study. *Biopolymers 93*, 866−879.
59. Robinson, D. R., and Jencks, W. P. (1965) The effects of compounds of the urea-guanidinium class on the activity coefficient of acetyltetraglycyl ethyl ester and related compounds. *J*. *Am*. *Chem*. *Soc*. *87*, 2462–2470.
60. Pike, A. C. W., and Acharya, R. (1994) A structural basis for the interaction of urea with lysozyme. *Protein Sci*. *3*, 706–710.
61. Dunbar, J., Yennawar, H. P., Banerjee, S., Luo, J., and Farber, G. K. (1997) The effect of denaturants on protein structure. *Protein Sci*. *6*, 706–710.
62. Kumar, R., Prabhu, N. P., Yadaiah, M., and Bhuyan, A. K. (2004) Protein stiffening and entropic stabilization in the subdenaturing limit of guanidine hydrochloride. *Biophys*. *J*. *87*, 2656–2662.
63. Sturtevant, J. M. (1977) Heat capacity and entropy changes in processes involving proteins. *Proc*. *Natl*. Acad. *Sci*. *USA 74*, 2236–2240.
64. Timasheff, S. N. (1993) The control of protein stability and association by weak interactions with water: How do solvents affect these processes? *Annu*. *Rev*.

Biophys. *Biomol*. *Struct*. *22*, 67–97.

65. Modig, K., Kurian, E., Prendergast, F. G., and Halle, B. (2003) Water and urea interactions with native and unfolded forms of a β-barrel protein. *Protein Sci*. *12*, 2768−2781.
66. Rao, M. T., Bhuyan, A. K., Venu, K., and Sastry, V. S. S. (2009) Nonlinear effect of GdnHCl on hydration dynamics of proteins. *J*. *Phys*. *Chem*. *B*. *113*, 6994−7002.
67. Yang, A-S., and Honig, B. (1993) On the pH dependence of protein folding. *J*. *Mol*. *Biol*. *231*, 459-474.
68. Neri, D., Billeter, M., Wider, G., and Wuthrich, K. (1992) NMR determination of residual structure in a urea-denatured protein, the 434-repressor. *Science 257*, 1559–1563.
69. Pan, H., Barber, E., Barany, G., and Woodward, C. (1995) Extensive nonrandom structure in reduced and unfolded bovine pancreatic trypsin inhibitor. *Biochemistry 34*, 13974–13981.
70. Ptitsyn, O. B. (1995) Molten globule and protein folding. *Adv*. *Protein Chem*. *47*, 83−229.
71. Bowler, B. E. (2012) Residual structure in unfolded proteins. *Curr*. *Opin*. *Struct*. *Biol*. *22*, 4–13.
72. Singh, R., Hassan, M. I., Islam, A., and Ahmad, F. (2015) Cooperative unfolding of residual structure in heat denatured proteins by urea and guanidinium chloride. *PLoS ONE 10*(6): e0128740.
73. Cooper, A. (1976) Thermodynamic fluctuations in protein molecules. *Proc*. *Natl*. Acad. *Sci*. *USA 73*, 2740–2741.
74. Cooper, A. (1984) Protein fluctuations and the thermodynamic uncertainty principle. *Prog*. *Biophys*. *Mol*. *Biol*. *44*, 181–214.
75. Prabhu, N. V., and Sharp, K. A. (2005) Heat capacity in proteins. *Annu*. *Rev*. *Phys*. *Chem*. *56*, 521−548.
76. Frauenfelder, H., Young, R. D., and Fenimore, P. W. (2013) Dynamics and the free-energy landscape of proteins, explored with the Mössbauer effect and quasi-elastic neutron scattering. *J*. *Phys*. *Chem*. *B 117*, 13301–13307.
77. Frauenfelder, H., Sligar, S. G., and Wolynes, P. G. (1991) The energy landscapes

and motions of proteins. *Science 254*, 1598–1603.

78. Kresheck, G. C., and Benjamin, L. (1964) Calorimetric studies of the hydrophobic nature of several protein constituents and ovalbumin in water and in aqueous urea. *J. Phys. Chem. 68*, 2476–2486.
79. Liu, Y., and Sturtevant, J. M. (1996) The observed change in heat capacity accompanying the thermal unfolding of proteins depends on the composition of the solution and on the method employed to change the temperature of unfolding. *Biochemistry 35*, 3059–3062.

CHAPTER 3

Burst Reaction and Chevron Curvature in the Folding of Cytochrome *c*, Myoglobin, BSA, and Lysozyme Studied by Stopped-Flow

3.1 ABSTRACT

Two general observations in experimental protein folding kinetics are nonlinear dependence of observed rates as a function of the denaturant called - chevron rollover, and the burst phase reaction that entails the initial stages of folding. The origin of different degrees of chevron curvatures irrespective of size and folding-unfolding speed of proteins, and the role of the burst collapse in native structure acquisition are unclear. Folding kinetics of cytochrome *c*, myoglobin, bovine serum albumin (BSA), and lysozyme studied here at millisecond resolution show no connection between the burst reaction product and chevron rollover. Kinetics recorded by concomitant use of guanidinium hydrochloride (GdnHCl) and urea appear to indicate that the burst species is only marginally structured at best, and hence cannot be called a folding intermediate. Curvatures for both folding and unfolding limbs of chevron are essentially due to breakdown of the linear free energy model (LFEM) as elucidated by equilibrium experiments in the accompanying article. Continuous change of both structure and energy of the protein along the reaction coordinate, which in most cases can be verified by measuring the hydrodynamic radius (R_H) or some other properties, implies nonlinearity of energy change with the denaturant that results in curvature. Protein landscapes are generally rugged, and a high degree of ruggedness causes accumulation of specific intermediates whose delayed folding is reflected in chevron curvature. Results for BSA also reveal kinetic unfolding intermediates that are likely due to multidomain and subdomain structure of the protein.

3.2 INTRODUCTION

Protein folding literature of the past thirty years or so reveals steady progress toward understanding the mechanism of structure acquisition by unfolded polypeptides,

even though unifying all information appears difficult at this stage. Also hard is the citation of all of the influential studies that have appeared. Some of the general ideas that have emerged in classical description of folding include the reality of folding intermediates and sequential pathway[1,2] that have been demonstrated abundantly at sufficient details,[3-12] the molten globule state,[13-20] whose productive role appears controversial,[14,21-23] the curvature in folding chevron due to accumulation of kinetic folding intermediate[24-27] or other non-intermediate factors,[27-29] and fast contraction/collapse of the initial unfolded chain at the onset of folding.[30-38] Of these, variable degree of chevron curvature and polypeptide collapse are of particular interest for at least three reasons. First, proteins irrespective of size, structure type, and folding speed may or may not display rollover in the rate vs denaturant curve; chevrons of only some fast-folding proteins approach linearity. Second, even if the curvature of the folding limb is identified with accumulation of folding intermediate(s) at low denaturant, how to interpret the curvature of the unfolding limb observed in as many cases where unfolding kinetic intermediates are seldom described. Third, chevron rollover for fast-folding 'two-state' proteins can be explained if a 'structured' burst collapse product accumulates the folding speed of which limits the observed rate. This hypothesis can be tested by accurate measurement of burst amplitude in refolding (unfolding) experiments,[39-42] but unambiguous assignment of structure, dimension, and hydration to the collapsed product requires direct measurement of polypeptide collapse, which in most cases is completed in the microsecond regime.

An important development essentially based on the earlier idea of Regenfuss et al[43] was the construction of microsecond mixers to study stopped-flow unobserved submillisecond kinetics of protein folding.[33,38,44-51] Submillisecond kinetics have detected the earliest and often multiple phases of condensation of unfolded chain at the onset of folding. Concomitantly, the sensitivity of single-molecule fluorescence resonance energy transfer (SMFRET) has been exploited to study collapse and diffusivity of unfolded protein chains.[52-65] SMFRET experiments have particularly enabled application of

polymer principles in the interpretation of polypeptide response to the level of denaturant. These experiments also allow a detailed analysis of the connection between free energies of folding and polypeptide collapse.[61,66] Unfortunately, results for different proteins often provide divergent pictures concerning the order, specificity, and continuity of collapse.[63] A pesky problem is disparate degree of compaction reported by small-angle x-ray scattering[67] and FRET,[53,57] although the disparity also surfaces in equilibrium measurement of hydrodynamic radii.[68,69] The collapsed product may have highly non-native structure,[70] in contrast with specific helical interactions[71] or increasingly native-like contacts observed under low denaturant.[63] Another basic problem is the very comparison of polymer transitions with protein collapse. At least in one instance documented of late, the equivalent of coil-globule transition of polymers does not seem to occur in the polypeptide.[72]

This study examines burst folding (unfolding) kinetics and chevron curvature for ferricytochrome *c*, myoglobin, BSA, and lysozyme at millisecond resolution by using GdnHCl and urea, often both in conjunction. The basic principle of burial of protein surface in going from the collapsed to the transition state has been used to gauge structure in the former so as to tell qualitatively if the polypeptide condenses specifically to an intermediate structure. The inapplicability of the linear free energy model (LEM) discussed in the accompanying article appears to be the major source of chevron nonlinearity. Folding kinetics is more complex for multidomain BSA than for the other three proteins. Occurrence of kinetic unfolding intermediates for BSA presumably before the transition state is described.

3.3 MATERIALS AND METHODS

All experiments used commercial preparations of horse myoglobin, horse heart cytochrome *c*, and BSA purchased from Sigma, and hen egg white lysozyme obtained from Calbiochem or HiMedia. BSA was chromatographed on a Sephadex G75 column to isolate the monomeric form. Urea solutions were freshly prepared, and were used up within 24 hours. Buffers used were 0.2 M sodium acetate, pH 4.5, 20 mM sodium

phosphate, pH 7, 50 mM sodium phosphate, pH 7, and 20 mM sodium acetate, pH 5 for experiments with cytochrome c, myoglobin, BSA, and lysozyme, respectively. All experiments were done at 24.5(±0.5)ºC.

Measurements of folding-unfolding kinetics that engaged only one denaturant were done by the usual procedure of diluting one-part the initial solution of the native or denaturant-unfolded protein into seven-parts of the buffer containing desired denaturant concentrations. In experiments involving concurrent use of two denaturants, concentration of one of the denaturants was held constant while varying the other. The actual level of denaturants that were determined from refractive index data of final mixed solutions collected as stopped-flow waste are reported in the description of experimental results below. Folding and unfolding reactions were initiated by two-syringe mixing of protein and buffer solutions in volume ratio of 1:7 in a BioLogic SFM400 instrument, and time-domain signal was recorded using a single channel. Measured dead-time of the instrument was 1.6(±0.2) ms. Typically 7-9 traces were averaged for each concentration of the varying denaturant. Reported pH values refer to actual pH of mixed solutions measured after experiments.

Hydrodynamic radius (R_H) of proteins was determined using the sLED-PFG NMR pulse sequence.[73] Spectra were recorded at 25°C in a 500 MHz Bruker Avance III spectrometer with the z-gradient (diffusion gradient) strength fixed in the range of 3–50 Gauss cm^{-1}. Protein samples (2 mM) were prepared in D_2O buffer containing deuterated denaturants in the 0–8.3 M range. Deuteration was carried out by lyophilization or repeated drying of the denaturant from D_2O solutions under pure nitrogen gas. Each sample also contained 0.5 mM 1,4-dioxane as internal R_H standard.[74] Values of R_H are calculated by

$$I(g) = A\exp(-\mathrm{k}\, g^2)$$

$$R_{\mathrm{H}}^{\mathrm{protein}} = R_{\mathrm{H}}^{\mathrm{dioxane}}\left(\frac{\mathrm{k}_{\mathrm{dioxane}}}{\mathrm{k}_{\mathrm{protein}}}\right)$$

where, I and g are NMR signal intensity and gradient strength, respectively.

3.4 RESULTS

3.4.1 The Framework for Interpretation of Kinetic Results. Because the unfolded protein chain resembles homopolymers in terms of solvent quality-dependent hydrodynamic dimensions,[69,75-77] homopolymer principles are often used to model the initial stage of protein folding.[78] When driven to fold by diluting the denaturant, the unfolded protein chain responds initially by contraction and collapse to a disordered globule, which folds to the native state in a later stage involving occasionally detectable kinetic intermediates (Figure 1). These two stages, details of which are affected by denaturant concentration in the folding milieu, form a useful framework for interpretation of kinetic results obtained under variably perturbed reaction conditions created by using one or more denaturants.

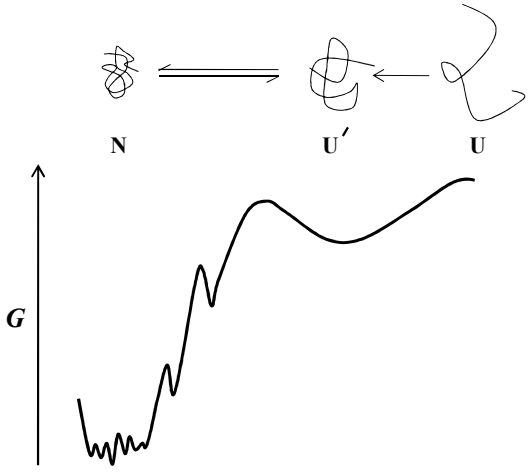

Figure 1. Highly simplified one-dimensional energy surface under refolding conditions depicting the assumed framework for interpretation of kinetic results. U, U′, and N are unfolded, collapsed, and native states, respectively.

3.4.2 Cytochrome *c*. Revisiting the folding kinetics of ferricytochrome *c* was necessary due of controversial results now and then coupled with inconsistent interpretations from different laboratories;[30,31,80-87] the major disagreements being the interference of the heme in correct chain folding, and whether the chain collapse is a barrier-limited event. Briefly, the heme in the unfolded protein makes transient contact with both native and non-native methionine and histidine side chains, and the population of non-native heme ligands can collapse and fold without the correct M80 ligand if dissociation times of the non-native intrapolypeptide ligands, H26 and H33 in particular, are longer than the chain collapse time. Apparent misfolding of ferricytochrome *c*, which incidentally does not occur in the case of ferrocytochrome *c*,[84] can be prevented by eliminating heme-histidine misligation

at acid pH where histidine side chains are protonated.[80] Experiments were hence performed at pH 4.5.

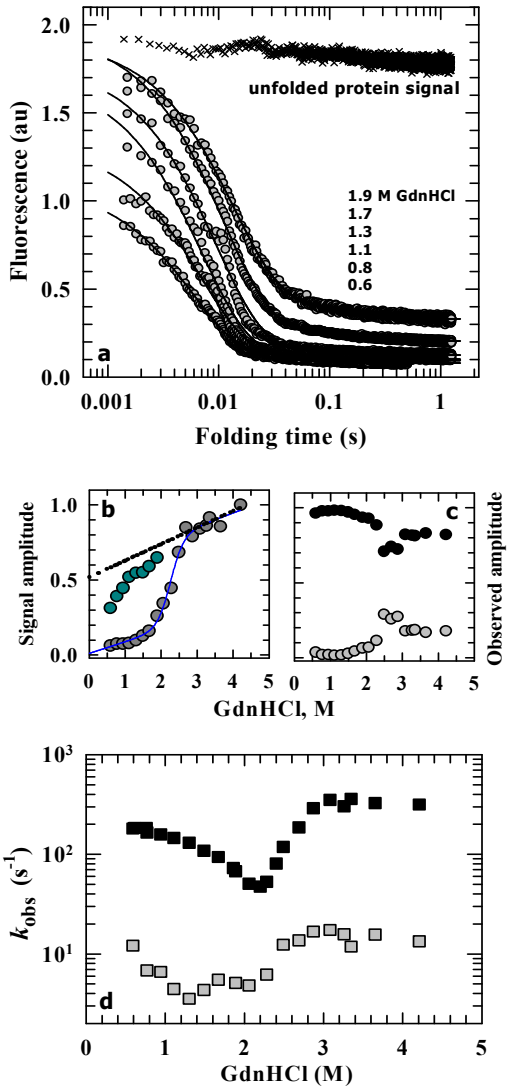

Figure 2. Refolding of cytochrome *c* in the presence of GdnHCl alone, 0.2 M acetate buffer, pH 4.5, 24.5(±0.5)ºC. (a) Some traces for refolding from 4.8 M GdnHCl to the final denaturant concentrations indicated. Observable kinetics are fitted best by two exponentials, of which the slower phase accounts for only 0-20% of the total amplitude. (b) Denaturant dependence of normalized burst phase signals determined by extrapolating the exponential fits to time t=0 along with equilibrium signals (t=∞). Two-state fit of the latter yields ΔG~8 kcal mol^{-1} and m_g~3.5 kcal mol^{-1} M^{-1}, consistent with values obtained from equilibrium melts under these experimental conditions. The dotted line represents a linear extrapolation of the unfolded baseline. (c) Denaturant dependence of normalized amplitudes corresponding to the fast and slow observed phases. (d) Folding chevron plots for the two observed rates showing curvatures in both folding and unfolding limbs. The lower chevron corresponding to the slow minor phase is not considered for description (see text).

Folding kinetics studied by diluting the unfolded protein solution (4.8 M GdnHCl) to different final concentration of the denaturant are described by a stopped-flow unobservable submillisecond burst phase followed by two observable exponentials (Figure 2a). These three phases completely describe the time course, because GdnHCl dependence of the fluorescence signals read at $t \rightarrow \infty$ of the traces produce an unfolding transition ($\Delta G^{o} \approx 8$ kcal mol^{-1} and $m_g \approx 3.5$ kcal mol^{-1} M^{-1}) that closely simulates the one measured independently (Figure 2b).

The availability of the initial unfolded-state fluorescence signal provides for quantifying the denaturant dependence of the missing fraction of the amplitude by $(S_U-S_o)/(S_U-S_N)$, where S_o is fluorescence signal at time t=0 determined by extrapolating the fitted exponential function to zero-time, and S_U and S_N are unfolded- and native-state signals estimated by linear extrapolation of respective baselines to the ordinate (Figure 2b). Regarding the two observed exponential phases, the apparent rate coefficient of the slower one (k_2) is at least 15-fold smaller than that of the faster phase and accounts for only 0.1-20% of the observed amplitude across the denaturant scale (Figure 2c). This phase most probably arises from a small population of aggregated species, and may be excluded from further consideration. The results lead to the following scheme for ferricytochrome *c* folding

$$\mathbf{N} \rightleftharpoons \mathbf{U}' \leftarrow \mathbf{U} \qquad \text{Scheme I}$$

where the collapse of the unfolded chain U to the U′ state (Figure 1) is not observed in our time window, and hence the observable major phase with the eigenvalue k_1 can be associated with the U′⇋N reaction.

Folding of cytochrome *c* in a single observable phase suggests a two-state reaction with no accumulation of temporally resolved kinetic intermediates. The two-state implication is, however, inconsistent with the denaturant dependence of k_1 (Figure 2d), parameterized by the kinetic *m*-value ($m^{\ddagger}=RT\ \partial lnk/\partial$[denaturant]), which is a measure of the surface area buried in the transition state. The value of $m^{\ddagger}$ for the folding or unfolding limb of the chevron is expected to be a constant for two-state folding.[88] Except for the transition region, deviation of k_1 vs GdnHCl from linearity is substantial under both strongly folding and unfolding conditions (Figure 2d), apparently indicating that the interpretation of two-state kinetics may not be correct. In fact, the nonlinearity of the folding limb under subdenaturing conditions is widely believed to originate from transient accumulation of a burst intermediate whose conversion to the native state is slow, because the intermediate is increasingly stabilized as stronger native-like conditions are approached. It is this slow folding of the intermediate which is suggested to limit the overall observable rate.[42,89] Thus, it might appear that the burst collapse species U′ is an

intermediate whose slow conversion to N rate-limits the observed folding, and hence the nonlinearity in the chevron folding limb (Figure 2d).

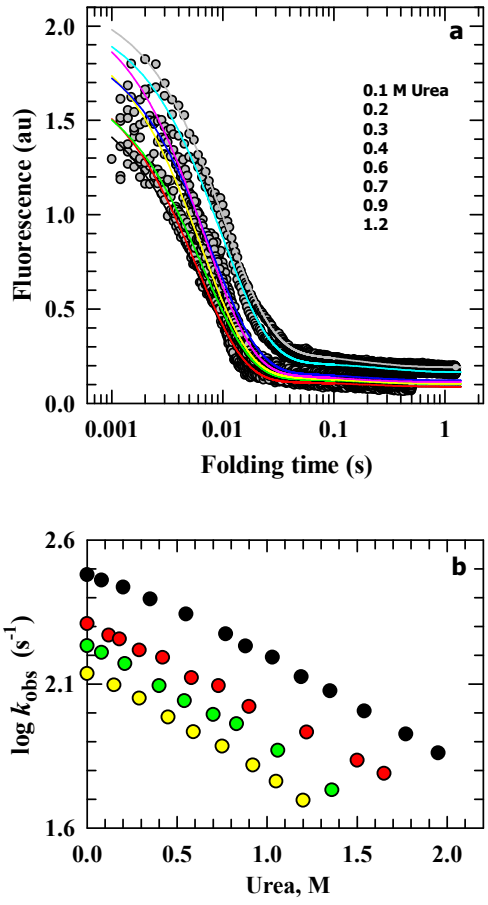

Figure 3. Refolding of cytochrome *c* by the use of both GdnHCl and urea. (a) Some traces for refolding of 5 M GdnHCl-unfolded protein, pH 2.5, to 1 M final GdnHCl, pH 4.5, in the presence of indicated urea. Two exponentials are needed to fit each trace, although the amplitude of the slower one is <10%. (b) Urea dependence of the observed rate of the major (fast) phase in the presence of 0.6 (●), 1.0 (●), 1.3 (●), and 1.5 (●) M GdnHCl.

To check if the collapsed chain U′ is a kinetic intermediate, refolding experiments were performed using both GdnHCl and urea. The protein unfolded in 5 M GdnHCl, pH 2.5, was refolded to 0.6, 1, 1.3, and 1.5 M GdnHCl, each in the presence of variable urea in the 0-2 M range (Figure 3a). Interestingly, the slope of the urea dependence of k varies little within error irrespective of the content of the primary denaturant GdnHCl in the folding milieu (Figure 3b). The constant value of $m^{\ddagger}$ (0.7±0.06) for all four sets of folding kinetics shows that the surface area buried in going from U′ to the transition state is virtually the same, and hence U′ is not a kinetic intermediate. If it were, the value of $m^{\ddagger}$ would vary with GdnHCl content, rather strongly because 0.6 M of this denaturant is expected to support an intermediate structure significantly compared to 1.5 M where an intermediate is unlikely to accumulate. These results suggest that U′ is not a kinetic intermediate, but a collapsed state of the unfolded chain that responds to denaturants by expansion and contraction in the same way the

unfolded chain does. It is concluded that the U→U′⇋N mechanism appropriately describes the folding of cytochrome *c*.

3.4.3 Myoglobin. Kinetic study of holomyoglobin folding has been scanty[90-92] due to heme dissociation from the protein chain under strongly unfolding conditions. But experiments can still be performed under moderate denaturant concentrations where the protein chain is fully unfolded, the heme-H93 ligation is retained, and a water molecule serves for the other axial ligand of the heme (aquomet-myoglobin or metmyoglobin). Within the limit of 2.3 M GdnHCl, pH 7, the protein is found to undergo complete and reversible unfolding without the loss of the heme. Hence, refolding experiments were performed with the protein unfolded initially at 3 M GdnHCl, pH 7, 24(±0.5)ºC.

Kinetics of myoglobin refolding is characterized by an initial burst loss of signal followed by a phase of fluorescence increase, and at least one slower phase where the fluorescence decreases (Figure 4a). Because the slow phase is incomplete within the 16 ms of kinetic traces shown here, the two-exponential fits of traces often required a constrained baseline. The rate of this slow phase is also measured reproducibly in manual mixing experiments. Unfolding kinetics do not show any substantial burst loss of signal, and two phases of fluorescence increase are observed (Figure 4b). Here as well, two-exponential fits required baseline constraint when concentrations of GdnHCl were large. Chevron plots of the two observed macroscopic rate constant (k_1 and k_2) are dissimilar − they are horizontally shifted, and have different values of $m^{\ddagger}$ for the folding limb (Figure 4c). The minimum of both chevrons is contained within the unfolding transition region, and the faster and slower phases correspond to ~40 and 60% of the observable fluorescence amplitude (Figure 4d,e). The horizontal shift of chevrons appears consistent with an earlier report under similar conditions,[92] but that study provides no other information.

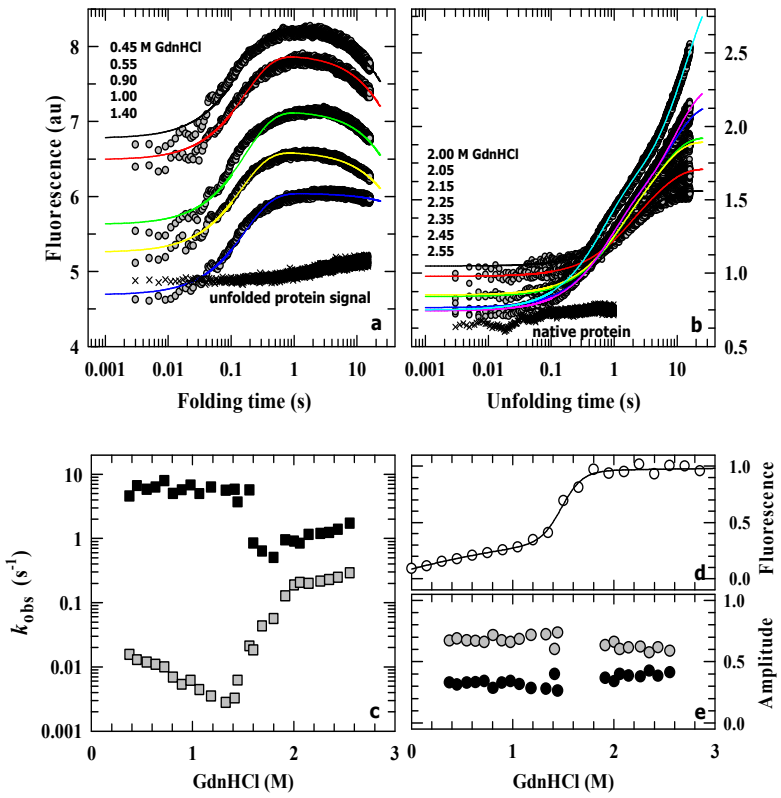

Figure 4. Kinetics of myoglobin in GdnHCl. (a) Traces for refolding of the protein initially unfolded in 3 M GdnHCl, pH 7, 24(±0.5)ºC show a burst signal change followed by observable phases of fast fluorescence rise and slow decay to the equilibrium value. (b) Unfolding traces do not indicate considerable burst signal change, and the fluorescence rises in two exponential phases. (c) Folding chevrons of the two observed rates are horizontally shifted, but the folding limb of the lower chevron shows little curvature. (d) Equilibrium unfolding transition of myoglobin under the same experimental conditions (ΔG~11.3 kcal mol^{-1} and m_g~2 kcal mol^{-1} M^{-1}) to show that the chevron minima are contained within the transition region. (e) Denaturant dependence of relative amplitudes of the fast (●) and slow (●) phases.

Because a folding burst phase is clearly observable (Figure 4a), and the fast observable phase is associated with increased emission contrary to the expected decrease, a refolding intermediate appears to occur which can be depicted by one of the following three schemes compatible with the two eigenvalues k_1 and k_2

$$\mathrm{N} \rightleftharpoons \mathrm{I} \rightleftharpoons \mathrm{U}' \leftarrow \mathrm{U} \qquad \text{Scheme 2a}$$

$$\mathrm{N} \rightleftharpoons \mathrm{U}' \leftarrow \mathrm{U} \qquad \text{2b}$$
$$\Downarrow$$
$$\mathrm{I}$$

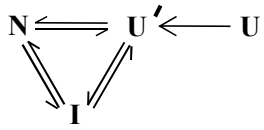

2c

The first of these (Scheme 2a) can be ruled out because the amplitudes associated with k_1 and k_2 do not change across the denaturant range (Figure 4e). The second (Scheme 2b) refers to an off-pathway or dead-end intermediate that must unfold to U′ for correct folding to N. The presence of dead-end intermediate generally produces sharp rollover or inversion in the folding limb of the chevron under low denaturant conditions,[84,93] which is not detected here (Figure 4c), and hence the second mechanism can also be excluded. The third scheme (Scheme 2c) features two parallel pathways, U′⇋N and U′⇋I⇋N, of which the latter assumes significance only when the intermediate is stabilized under strongly native-like conditions. Further, the intermediate is not obligated to a dead end, suggesting appropriateness of the cyclic mechanism (Scheme 2c) for description of myoglobin refolding.

The chevron behavior is however far from simple. For example, the denaturant dependence of k_1 is markedly flat across the subdenaturing region, which may appear to suggest the existence of a rate-limiting step. Since the chain collapse is the only event faster than k_1, the nature of the U′ state was examined by refolding experiments in which the initial unfolded state prepared in 3 M GdnHCl was allowed to refold to 0.25, 0.45, 0.6, and 0.75 M GdnHCl, each in the presence of different urea in the 0-2.4 M range. Figure 5a shows a few representative refolding traces that reproduce the features shown in Figure 4a. Curiously, the urea dependence of both k_1 and k_2 at all four concentrations of GdnHCl ($m^{\ddagger}$) are nearly identically flat, even as k_2 starts to decrease at >1 M urea due to onset of denaturation (Figure 5b). Identical urea dependence of k at all concentrations of GdnHCl implies, as it did for cytochrome *c* discussed earlier, that U′ is not an intermediate. The $m^{\ddagger}$ value of ~0.05 for both k_1 and k_2 suggest little difference in solvent accessible surfaces of U′ and the transition state, which means the latter resembles the

unfolded state.

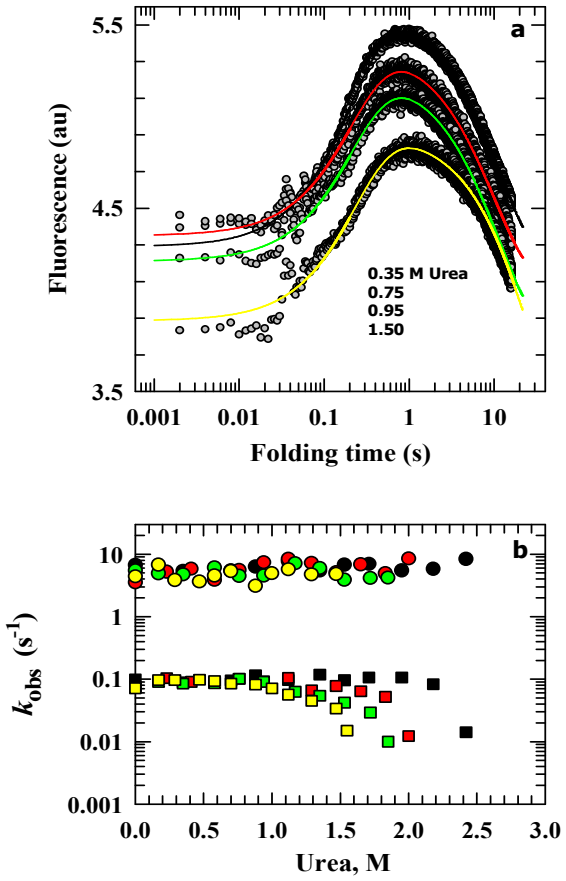

Figure 5. Double perturbant kinetics for myoglobin. (a) Representative traces for refolding of the protein from 3 M GdnHCl, pH 7, 24(±0.5)ºC to a final GdnHCl of 0.6 M in the presence of indicated level of urea. Kinetics are described by an initial (unfolding-like) rise in fluorescence followed by a decay to the equilibrium value. (b) Urea dependence of the rates for the fast (circles) and the slow (squares) phases in the presence of 0.25 (●,■), 0.45 (●,■), 0.6 (●,■), and 0.75 (●,■) M GdnHCl.

Confusion still remains concerning the rate-limiting process that produces the rollover in the folding limb of the k_1 chevron (Figures 4c, 5b). If the collapsed state is heterogeneous (U_1', U_2', U_3', … U_n') such that they interconvert within themselves rapidly compared to the conversion of each of them to I and N states, and the population distribution is modulated by the denaturant level in the folding milieu, then k may possibly roll over. This idea has been used in the past to explain chevron curvature for some proteins.[94] Assuming so, Scheme 2c is modified to the following to describe the folding kinetics of myoglobin.

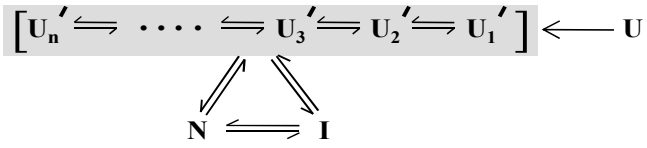

Scheme 3

3.4.4 Bovine Serum Albumin. Although BSA has been rarely used to study protein

folding kinetics due to its large size, three-domain structure, and binding affinity to a host of ligands − the availability of detailed information about its equilibrium unfolding justifies exploring kinetics. In the first set of experiments, we determined the GdnHCl dependence of folding and unfolding rates in 50 mM phosphate, pH 7, 24(±0.5)ºC. As shown by sample traces, refolding from 6 M GdnHCl is very slow in the stopped-flow window, but the dominating feature is a huge burst loss of signal in the submillisecond regime (Figure 6a). Unfolding also proceeds by a very large burst change in fluorescence (Figure 6b), but the millisecond unfolding kinetics is relatively faster than folding kinetics. Both folding and unfolding traces are best described by two exponentials, and k_1 and k_2 chevron minima correspond to the midpoint of the unfolding transition (Figure 6c). The GdnHCl dependence of burst signals for both folding and unfolding were quantified and are plotted along with the baseline fluorescence (t=∞) in Figure 6d. The overwhelming burst phase fluorescence (S_o) might tempt one to invoke submillisecond structural intermediates for both folding and unfolding, but results obtained further do not permit so (see below).

Since there is no evidence for two unfolded populations of BSA that refold at different rates, and because observed amplitudes of fast and slow folding phases appear to cross at a denaturant value a little lower than the midpoint of the unfolding transition(Figure 6e), the occurrence of two phases is indicative of a millisecond folding intermediate (I). No intermediate in the slower regime of unfolding needs to be invoked, because the amplitude of the slow unfolding phase that accounts for less than 10% of the observable amplitude in the region of 2.5−3.5 M denaturant is not substantial (Figure 6e). The interpretations at this stage are compatible with the minimal mechanism,

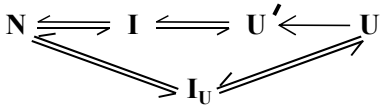

Scheme 4

where I_U is a high-energy unfolding intermediate (~5 kcal mol^{-1}) that forms in submillisecond regime.

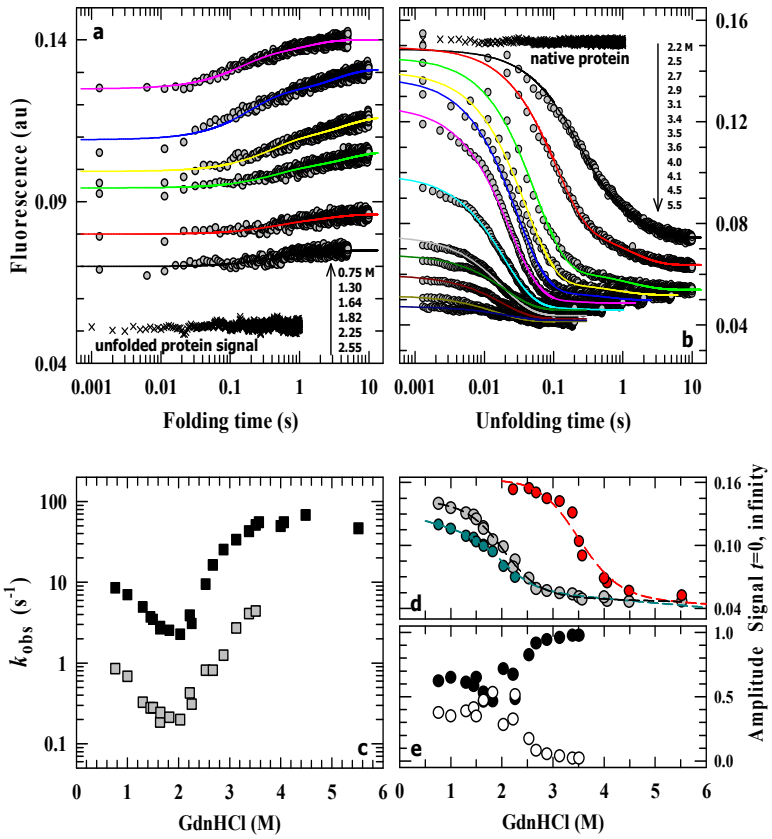

Figure 6. Folding kinetics for BSA. (a) Sample traces for refolding from 6 M GdnHCl, 50 mM phosphate, pH 7, 24(±0.5)ºC to the indicated level of GdnHCl. The observed kinetics are rather slow and biphasic, but a very large burst process dominates the refolding reaction. (b) Unfolding kinetics also shows a very large burst signal change. Observed kinetics are biphasic within the transition region, but is monophasic at higher denature-ant level. (c) Chevron plots for the two observed rates show no or marginal rollover in the folding limb, but accentuated curvature in the unfolding limb at higher denaturant concentration. (d) GdnHCl dependence of large burst phase signals for both folding and unfolding, and the baseline fluorescence (t=∞). The broken lines through burst phase unfolding (●) and refolding (●) signals are drawn with ΔG values of 5.2 and 3.7 kcal mol^{-1}, and m_g values of 1.5 and 1.8 kcal mol^{-1} M^{-1}, respectively. The broken line through the baseline signals (●) is drawn with ΔG and m_g values of 3.5 kcal mol^{-1} and 1.7 kcal mol^{-1} M^{-1}, respectively, both of which are about 2-fold smaller than those obtained from equilibrium melts. (e) Relative amplitudes of fast and slow phases observed.

The collapsed state (U′) in the BSA folding at neutral pH need not simply be the contracted unfolded chain because of the large size and three-domain structure of the protein.[95] It might as well be that all domains are not completely unfolded even though the refolding experiments were conducted with the protein unfolded in 6 M GdnHCl (Figure 6). On the other hand, equilibrium unfolding curves show only minor changes in fluorescence and CD signals beyond 3 M GdnHCl. Nevertheless, to obtain some clue on

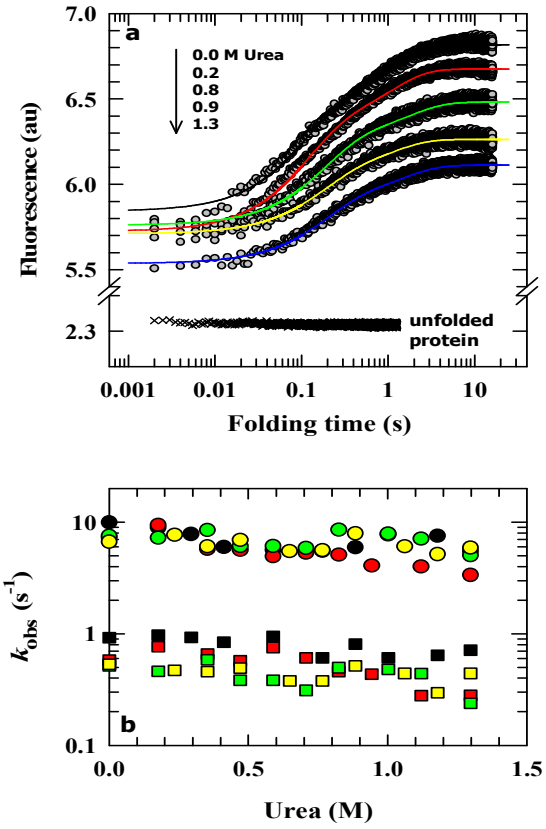

the structural content of U′ experiments were extended where the protein unfolded in 3 M GdnHCl, 50 mM phosphate, pH 7, was refolded as a function of urea at 0.3, 0.4, 0.5, and 0.6 M GdnHCl in the refolding milieu. As already discussed, refolding kinetics entails a large initial burst loss of fluorescence followed by two observable phases (Figure 7a), but the variation of $m_f^{\ddagger}$ values obtained from urea dependence of k_1 and k_2 plots are irregular with GdnHCl concentration (Figure 7b). These results do not permit drawing any inference regarding the nature of U′.

Figure 7. Refolding of BSA in the presence of both GdnHCl and urea, 50 mM phosphate, pH 7. (a) Sample traces for refolding of the initially unfolded protein in 3 M GdnHCl to a final concentration of 0.3 M and in the presence of indicated concentrations of urea. Observed kinetics are described by two-exponential phases. (b) Urea dependence of the fast (circles) and slow (squares) rate constants for refolding to 0.3 (●,■), 0.4 (●,■), 0.5 (●,■), and 1.5 (●,■) M GdnHCl.

Since finding the attribute of U′ − whether a structural intermediate or a contracted unfolded chain – is the major objective of this work, and results obtained with BSA thus far is inconclusive likely due to incomplete unfolding, we sought to find conditions where the protein can be maximally unfolded. Figure 8a,b show three-state pH denaturation of BSA, often called N⇋F⇋U transition,[96-98] where F that populates in the pH region 3-4 is an electrophoretically faster-moving and moderately expanded intermediate due to some structure loss in domain III, and U is the faster-moving acid-denatured form. The acid-denatured state appears to contain ~60% of the native-state

secondary structure, and ~20% still persists when the protein at pH 1 is heated up to 90ºC(Figure 8c). The denatured protein at pH 2 shows maximal unfolding at >4 M GdnHCl (Figure 8d,e).

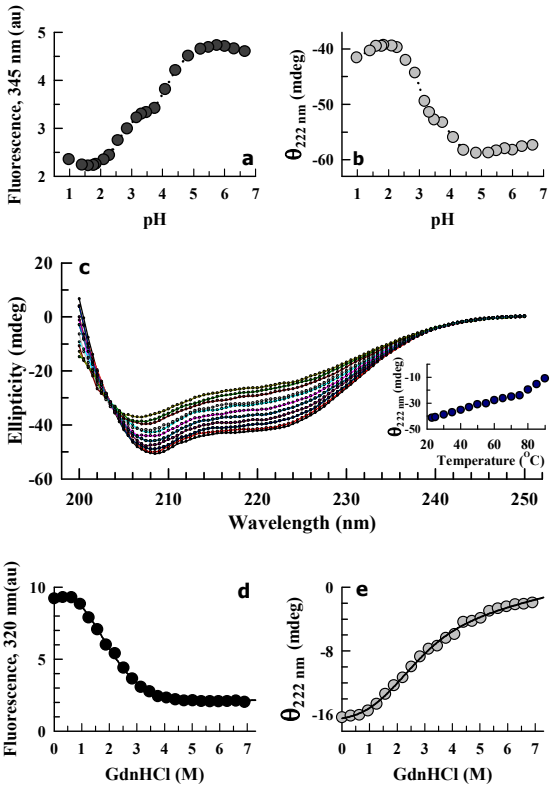

Figure 8. Equilibrium experiments with BSA. The effect of pH lowering monitored by fluorescence (a) and far-UV CD (b). The biphasic conformational transitions is often referred to as N⇋F⇋U transition, even though BSA is not completely unfolded at pH 2 (see text). (c) Temperature dependent CD spectra at pH 1 shows prevalence of residual structure even at 90ºC. GdnHCl-induced unfolding transition at pH 2 monitored by fluorescence (d) and 222-nm CD (e). The two equilibrium transitions are fitted with ΔG and m_g values of 1.1(±0.1) kcal mol^{-1} and 0.7(±0.1) kcal mol^{-1} M^{-1}, respectively.

Experiments were then extended in which BSA unfolded in ~4.5 M GdnHCl, pH 2, 24ºC was allowed to refold to different final concentrations of the denaturant at the same pH. Kinetics are described by a single exponential for both folding and unfolding, and very large burst loss of signal is recorded even under these conditions (Figure 9a,b). The observed rate (k) rolls downward under strongly native-like conditions (Figure 9c), suggesting some reconfigurations in the collapsed state(s) which rate-limit the observed kinetics. Again, urea dependence of the logarithm of the folding rate at two mildly perturbing GdnHCl concentrations produces comparable slope within the error limit(Figure 9c, *inset*), suggesting that the collapsed state(s) is not a folding intermediate. More importantly, the result that denaturant dependence of fluorescence values at $t\rightarrow 0$ and $t\rightarrow\infty$ are only marginally different (Figure 9d) strongly suggests that the typtophan reporters in the U′

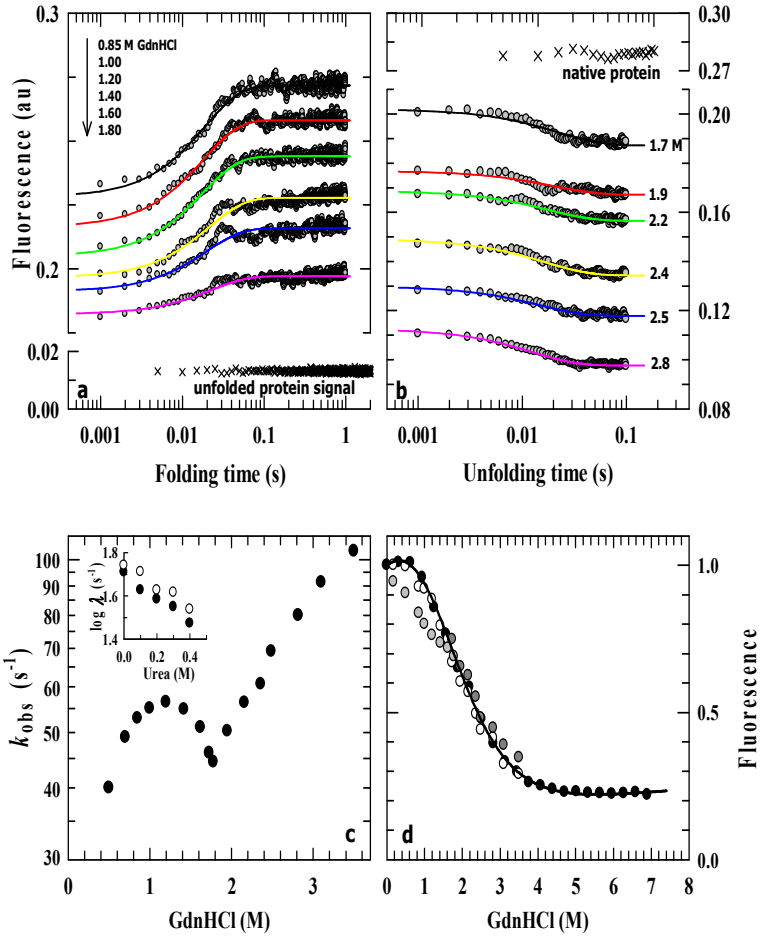

state vis a vis the U state are in very similar environment, meaning U and U′ chains are compareable both structurally and energetically. Hence, the collapse state is far from a compact intermediate.

Figure 9. Kinetics of refolding of BSA at pH 2, 24(±0.5)ºC. (a) Sample traces for refolding of the initially unfolded protein in 4.5 M GdnHCl to the indicated levels of the denaturant. Kinetics are marked by burst refolding followed by a single exponential phase. (b) Unfolding also proceeds by a large burst phase and a single observable phase. (c) The chevron of the lone observable phase shows a downwardly curved folding limb. The unfolding limb is only marginally curved, although data plotted are still within the transition region. Shown in the *inset* is urea dependence of the refolding rate constant for GdnHCl concentrations fixed at 0.7 (●) and 1 (○) M GdnHCl. (d) Normalized fluorescence signals at time t=0 of refolding (●) and unfolding (●) along with equilibrium signal at time t=∞ (○) are plotted with denaturant. The equilibrium transition observed under these conditions (see Figure 8d) is reproduced here for comparison.

Figure 9d also shows the denaturant dependence of fluorescence signals at t→0 and t→∞ obtained from the unfolding kinetic traces (Figure 9b) are very similar, suggesting that the unfolding burst product is structurally similar to the initial native state. By comparing this unfolding burst case developed at pH 2 (Figure 9d) with that at

pH 7(Figure 6d) one finds that unfolding under the latter condition involves a high-energy kinetic intermediate. This difference in both structure and energy of the two unfolding intermediates is not surprising because, notwithstanding the difference in proton inventory at different pH conditions, unfolding at pH 7 begins with all three domains of BSA folded, whereas domain III at pH 2 is already unfolded. The available results for the pH 2 condition are consistent with the mechanism

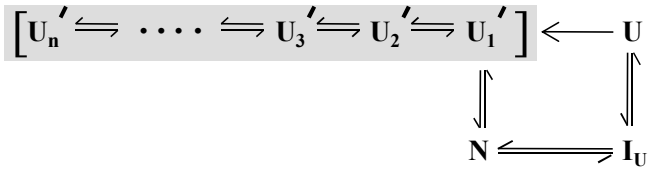

Scheme 5

where the collapsed ensemble undergoes rapid interconversion, the rates of which are not resolved by their conversion rate to the native state. The submillisecond unfolding intermediate I_U discussed above appears similar to the native state both structurally and energetically.

3.4.5 Lysozyme. In the light of ample scholarly studies of this protein in the past[93,99-106] experiments here are limited to examine folding kinetics primarily under subdenaturing conditions. The objective emanates from the results of previous equilibrium folding experiments that point to a rollover in the urea dependence of conformational stability indicating ruggedness toward the bottom of the folding funnel.[107]

Refolding kinetics of lysozyme at pH 5 under low denaturant conditions consist of a fast phase of fluorescence emission decay followed by a slow phase of fluorescence increase, and a slower phase of further increase (Figure 10a), consistent with earlier report.[106] As conditions turn from strongly native to denaturing due to increase in denaturant in the refolding medium the fluorescence increase associated with the slow phase gradually changes to a decrease (Figure 10a, *inset*). With increasing denaturant the amplitude of the fast phase continue to decrease at the expense of the slow (Figure 10b), and under unfolding conditions the fast phase reappears with increase in fluorescence (Figure 10b, *inset*). Earlier studies have assigned the fast refolding phase to the formation

of an intermediate (I) where the α-helical domain is structured substantially, but the chain segment corresponding to the β-sheet domain remains unstructured.[102,103] However, some molecules of unfolded lysozyme refold fast without involving the intermediate,[106] which has been rationalized by the minimal mechanism[93]

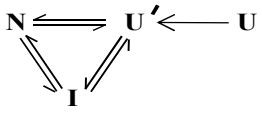

Scheme 6

that describes the denaturant dependence of the two observed rates corresponding to fast and slow phases (Figure 10c). The collapse process (U→ U′) has been added here for consistency in data interpretation. The rollover region of the folding chevron clearly indicates population of I at < 2 M GdnHCl.

To study the accumulation and stability of the intermediate further, refolding of lysozyme initially unfolded in a solution containing 2.4 M GdnHCl and 5 M urea was allowed in the presence of final 0.6, 1.1, 1.5, and 1.9 M urea while varying GdnHCl at each urea. The GdnHCl dependence of the two *k* values (Figure 10d-g), show features of a folding chevron most prominent at 1.1 and 1.5 M urea (Figure 10e,f). To note, this 'sub-chevron' feature is reproduced in another set of dependence of hydrodynamic experiments, where kinetics of refolding of 5.5 M GdnHCl-unfolded lysozyme to subdenaturing amounts of GdnHCl was studied by varying urea (Figure 11). As shown below, the 'sub-chevron' indicates the folding-unfolding of the intermediate (I) between N and a relatively less structured intermediate or even a group of partially folded structures before it disappears at higher GdnHCl, say 1.9 M (Figure 10g), where intermediate(s) do not accumulate.

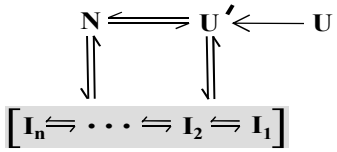

Scheme 7

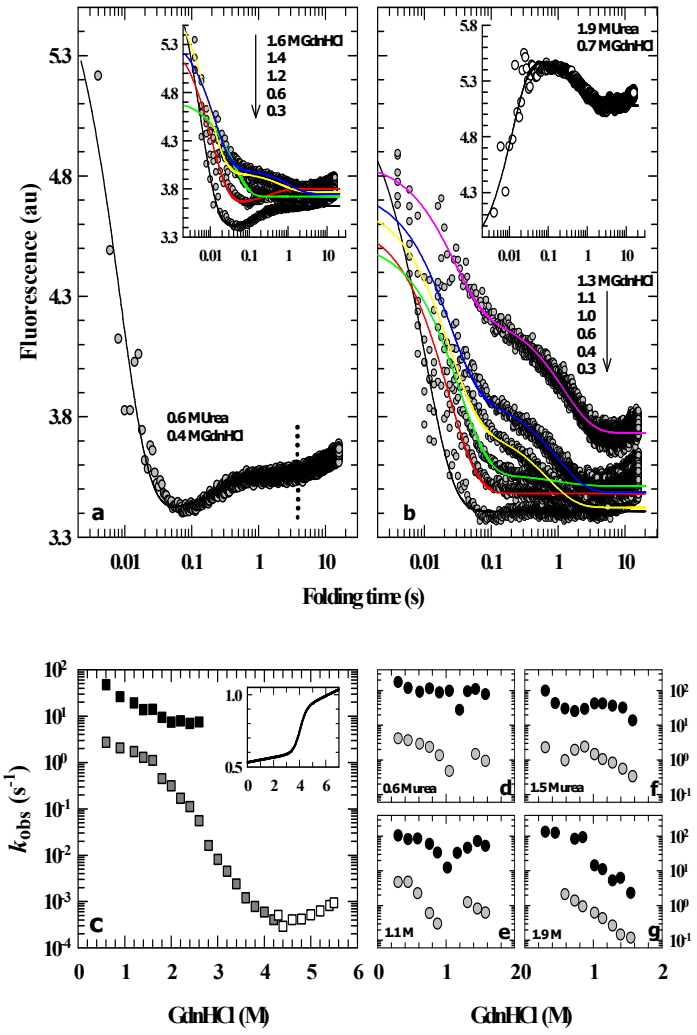

While the observation of sub-chevron is a rare result, the ensemble of differently struct - ured intermediates, I_1 through I_n, has been introduced for consistency with the earlier finding of rollover in the ΔG^o vs denaturant curve for lysozyme folding that has been interpreted to arise from multiple intermediates, and hence ruggedness toward the bottom of the folding funnel.

Figure 10. Refolding kinetics of lysozyme in 20 mM sodium acetate, pH 5, 24(±0.5)ºC. (a) Typical refolding kinetics shown here for refolding in the concomitant presence of 0.6 M urea and 0.45 M GdnHCl from the initial condition of 2.4 M GdnHCl and 5 M Urea. The trace shown is fitted to two exponentials after truncating the very slow phase (shown by the dotted vertical line). The *inset* plots some traces for refolding to 0.6 M urea in the presence of indicated concentrations of GdnHCl to show the changing sign of the amplitude for the slow phase. (b) Refolding traces to show that the slow phase amplitude continues to increases at the expanse of the fast one as the conditions turn increasingly denaturing. Under highly denaturing conditions the amplitude of the fast phase changes sign (*inset*). (c) The rate-GdnHCl plot under identical conditions of pH and temperature, but without the inclusion of urea, shows rollover in the folding arm of the slow-rate chevron. The inset shows the equilibrium transition under these experimental conditions. (d-e) The GdnHCl dependence of observed refolding rates (●, fast, and ○, slow) in the presence of urea fixed at 0.6, 1.1, 1.5, and 1.9 M.

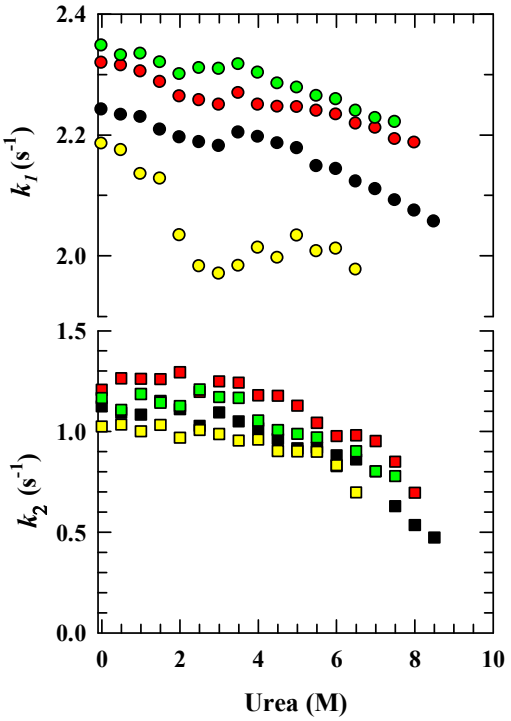

Figure 11. Urea dependence of the fast (circles) and slow (squares) rate constants for refolding of lysozyme to 0.6 (●,■), 1.0 (●,■), 1.4 (●,■), and 1.9 (●,■) M GdnHCl, 20 mM sodium acetate, pH 5, 24(±0.5)ºC.

3.5 DISCUSSION

3.5.1 The Collapse Model of Folding Kinetics. Two ideas of polymer principles are widely used to model the initial event in the folding of an unfolded protein. One, dimensions of a homopolymer with N monomers follow the scaling law by which the radius of gyration R_g of the polymer in good and poor solvents are given by $\sim N^{3/5}$ and $\sim N^{1/3}$, respectively,[36] which is in reasonable agreement with studies of hydrodynamic radii ($R_H \sim 0.64 R_g$) of native and denaturant-unfolded proteins. For a chain behaving as a self-avoiding walk, $R_H \sim N^{3/5}$.[108] Two, the transition between homopolymer phases in good and bad solvents is second order and continuous,[77,109] which is also the case at least for the unfolded state of some proteins that undergoes continuous expansion with increments of the denaturant.[34,53,54,56,57,69,110,111] There are reports however that some unfolded protein chains do not exhibit expansion with higher levels of the denaturant.[68,112] This point is illustrated in Figure 12 that maps denaturant dependence of NMR-determined $\langle R_H \rangle$ of ferricytochrome *c* and lysozyme – the former appears to expand continuously with GdnHCl, but the unfolded state of the latter does not, although it initially contracts and then expands when subdenaturing concentrations of urea is used.[107] Hydrodynamic data for BSA and myoglobin could not be obtained due to extremely poor NMR spectrum of the former and dimerization of the letter under unfolding conditions. Further, denaturant dependence of $\langle R_H \rangle$ of unfolded cytochrome *c* are different when determined by NMR (Figure 12) vis a vis observed by SAXS.[68] Similar inconsistency in single molecule

FRET- and SAXS- measured chain dimension of protein L in the 1.4−5 M range of GdnHCl has been reported.[67] Such results put a constraint as to what extent the solvent-dependent polymer transition ideas are applicable to protein folding, because the coil-globule transition event associated with transferring a homopolymer from a good to a poor solvent is widely used to model the submillisecond collapse of the unfolded protein chain when driven to fold by diluting the denaturant. It is also not clear if the expansion of a protein unfolded not by denaturant, but otherwise, is similar to polymer expansion with solvent quality. It has in fact been pointed out that the notion of collapse transition of the unfolded protein chain as the initial event of protein folding remains inconclusive.[67,72] Nevertheless, earlier reports of submillisecond chain collapse in the folding of several proteins,[33,38,51,63,113-115] and observations of overwhelming submillisecond signal change in kinetics of all four proteins examined here leads to assume the occurrence of some ultrafast event(s), which at this stage is operationally taken as a chain collapse or contraction transition.

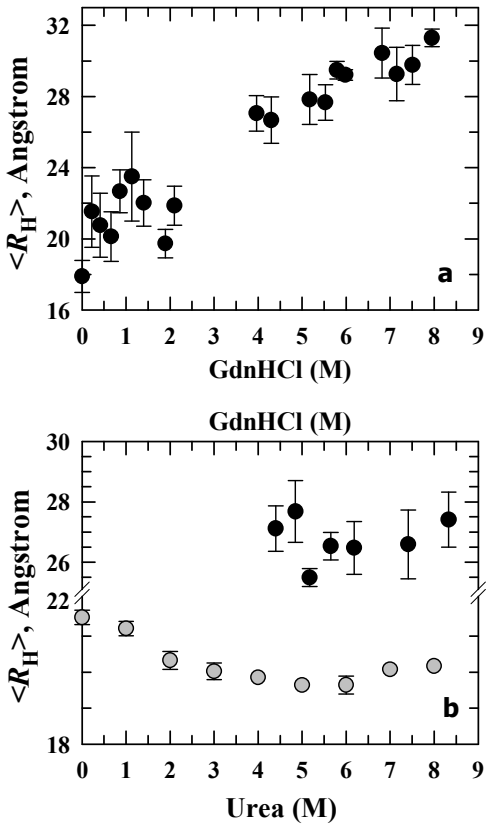

Figure 12. Denaturant dependence of hydrodynamic radius for (a) ferricytochrome *c*, and (b) lysozyme determined by pulsed filed gradient NMR at 24(±0.5)ºC.

3.5.2 Specificity of Burst Phase Kinetics Examined by the *m*-value Test. The folding problem could be considerably narrowed if polypeptide collapse is universally the earliest step in folding kinetics and the collapse process is deterministic. Desolvation and

redistributed backbone $\phi-\psi$ angles in such an overly ideal collapse product would reduce the conformational search problem dramatically. The idea pronounces that the initial polypeptide chain undergoes a barrier-limited collapse transition[46,116,117] specifically to a distinct thermodynamic state – an intermediate or a molten globule-like species – that makes a transition to the native state later,[38,46,118-123] thus simplifying the folding reaction to the minimal U⇋I⇋N model, where I is the collapse product given as U′ in this study. Similar argument appears to emerge from the work of Lapidus et al,[33] who used microfluidics to study submillisecond kinetics of cytochrome *c*, apomyoglobin, and lysozyme. The double perturbation millisecond kinetic experiments presented here and in an earlier study with ferrocytochrome *c*[87] provide a low-resolution basic test for the folding intermediate attribute of U′. The test relies on comparing the kinetic *m*-values ($m_f^{\ddagger}=RT\ \partial lnk/\partial$[denaturant]) for folding of a set of U′ states, distinguished from each other by the content of the primary denaturant, to different final concentration of the secondary denaturant, the transition state for folding being invariable. If it is an intermediate, the U′ state would be increasingly stabilized with lowering denaturant, and hence its folding as a function of another denaturant would produce increasingly larger value of $m_f^{\ddagger}$, because $m_f^{\ddagger}$ measures the surface area buried in the transition state relative to that in the U′ state.[124]

The recorded $m_f^{\ddagger}$ values in the presence of the secondary perturbant for different concentration of the primary perturbant are more or less uniform for all four proteins. For cytochrome *c* where the chain collapse to the U′ state occurs in ~17-500 μs,[33,38,46,49,125] and which is the burst phase of our stopped-flow kinetics, the uniformity of $m_f^{\ddagger}$ values (Figure 3b) is consistent with the earlier report on ferrocytochrome *c* that addressed the same issue of intermediate nature of U′.[87] In the myoglobin case, collapse data for the holoprotein is not available, but apomyoglobin is known to collapse in <300 μs,[33,126] and the kinetic *m*-value test shows that the collapsed state of holomyoglobin is not a folding intermediate (Figure 5b). Regarding BSA whose submillisecond kinetics accounts for a startling change in amplitude at both neutral and acidic pH, the variations of t=0 and t=∞

signals with the denaturant are quite similar (Figures 6,9), providing firm evidence that the collapse product at the lowered denaturant and the unfolded chain at the initial higher denaturant are similar in energy. We use this as an evidence to suggest that the U′ state corresponds to a contracted unfolded chain rather than being an intermediate. The limited millisecond data at acid pH obtained for the folding of the U′ state at two different GdnHCl concentrations and variable urea (Figure 9c, *inset*) also lends little support to the notion of intermediate nature of the collapsed state. For lysozyme, the collapse to U′ at pH 7 occurs in the 20-300 μs range,[33] and the *m*-value test for folding to different concentrations of a denaturant, each as a function of another denaturant (Figures 10d-g,11) does not indicate structure content in the collapse product.

That the U′ state may not represent a folding intermediate has also been argued by considering less substantiation of real-time collapse kinetics and interpretational ambiguities.[30,82,85,127] In earlier claims, the U′ state of some proteins have been compared with contracted unfolded chains that are unlikely to harbor structural contacts,[30,87,127] and can often exist in rapid equilibrium between differently contracted forms,[128-130] similar to the equilibria thought for myoglobin, BSA, and lysozyme (Schemes 3,5,7). Non-specific chain collapse has been documented for the SH3 domain of P13 kinase.[131] A study also appears to indicate that collapse specificity may be defined only in a restricted manner along part(s) of the polypeptide sequence,[63] although documentation of this result for additional proteins is desirable. More is yet to learn, including universality of polypeptide collapse, for understanding the role of submillisecond kinetics.

3.5.3 Chevron Rollover. Since the early suggestion that the curvature in the folding limb of the barnase chevron could originate from the presence of structural intermediate(s) whose folding rate-limits the overall rate observed,[24] it has been generally thought that rollover is a reflection of transient accumulation of folding intermediate,[42,132-135] depicted by the minimal U⇋I⇋N mechanism. Rollover observed for highly cooperative two-state (U⇋N) folders has been interpreted in the past by invoking landscape roughness,[26] and

movement of the rate-limiting transition state ensemble in a denaturant dependent manner.[28,136,137] Theory and simulations have also endeavored to explain the widely observed chevron curvatures.[27,138-140] In the context of burst kinetics, interpretation of curvature in the folding limb would be quite simple if the polypeptide collapses specifically over a barrier to an intermediate structure, I (U⇋I⇋N), which rate-limits folding. This argument was, in fact, used in the past to correlate burst kinetics and rollover,[42,121,141] but as it appears now the initial contraction/collapse response of the unfolded chain is more complex than a specific barrier-limited process.

A particularly simple interpretation of chevron curvature in the folding limb emerges from the finding noted in the accompanying article that the linear free energy model (LFEM) used for the description of thermodynamics is invalid for the folding of myoglobin, BSA, and lysozyme, and very likely for many other proteins whose ΔG vs denaturant behavior has not been investigated at very low denaturants. Curvatures in ΔG vs denaturant curves of these three proteins shown in the accompanying article provide a clear indication that structural and energetic properties are gradually changing under subdenaturing conditions. This must be true also for cytochrome *c* whose hydrodynamic radius is seen to change gradually across the denaturant scale (Figure 12), even though the set of experiments employed in the accompanying article did not detect curvature in the ΔG vs denaturant plot. The chain dimension result for cytochrome *c* (Figure 12), consistent with denaturant dependence of gyration radius of several other proteins reported,[53,56,57,61,66,69,110,142,143] provide evidence that the gradual change of structural and energetic properties occurs also at post-denaturing high denaturant. Thus inapplicability of LFEM is rife, which might be the case even at the transition state level. Changing structure and energy across the denaturant scale means both limbs of the chevron should show curvature, the degree of which will be determined by the details of free-energy landscape and thermodynamic cooperativity of folding. The argument already embraces the effect of internal friction of the folding structure on chevron curvature,[69,144,145] the contribution of which is not expected to be as significant as that of ΔG-denaturant

nonlinearity.

3.5.4 Kinetic Unfolding Intermediates of BSA. The record of description of unfolding kinetic intermediates is sparse, partly due to rapidity of intermediate unfolding when placed under unfolding conditions.[146] Nevertheless, kinetic intermediates in the unfolding of a few proteins, including RNAse A,[147] DHFR,[148] lysozyme,[149] colicin E1 channel peptide,[150] apomyoglobin,[151] acyl-CoA binding protein,[152] the cataract-forming F9S mutant of γS crystalline,[153] a 139-residue fragment of ovine prion protein,[154] and single-chain monellin[155] have been documented. These are small single-domain proteins compared to the size and domain structure of BSA for which kinetic unfolding intermediates, one each at pH 7 and 2, have been detected (Figures 6,9). There could be even more unfolding intermediates for the multidomain BSA; human serum albumin, which shares 76% sequence identity with BSA has three structural domains, each of which in turn has two subdomains.[156-158] The pH 7 intermediate of BSA is a high-energy intermediate (ΔG~5 kcal mol^{-1}, Figure 6d), but the one detected at pH 2 is more native-like (ΔG~1 kcal mol^{-1}, Figure 9d); the difference arises from partial loss of structure of domain III at pH 2.[98] It should also be stated that the type of intrachain interactions and folding mechanisms for small single domain and large multidomain proteins could be very different. To cite, different domains of maltose binding protein fold at different times,[159] and N-terminal loops of adenylate kinase close up faster than the β-strands before the transition barrier occurs.[160] These observations underscore a detailed study of BSA domain folding.

The unfolding energy difference for the pH-specific intermediates is pictured by 1-D energy surfaces under unfolding conditions in Figure 13, according to which the intermediate occurs before the rate-limiting transition state. The occurrence of unfolding intermediate(s), whether before the rate-limiting step or after,[116] is still unknown. The placement before the transition state (highest energy) here is based on the unfolding limb curvature in the upper chevron at pH 7 (Figure 6c). Here the curvature is indeed accentuated, which outweighs the mild rollover effects that may arise from denaturant

dependent dimension of the unfolded state. The formation of the intermediate is complete in the submillisecond regime encoded in the burst phase, and the unfolding of the accumulated intermediate over the transition barrier is slower. At pH 2, the intermediate is native-like because the titration of the burst amplitude with the denaturant is very similar to that for the native state (Figure 9d). Intermediates that occur after the transition barrier will unfold too fast in order to be rate-limiting.

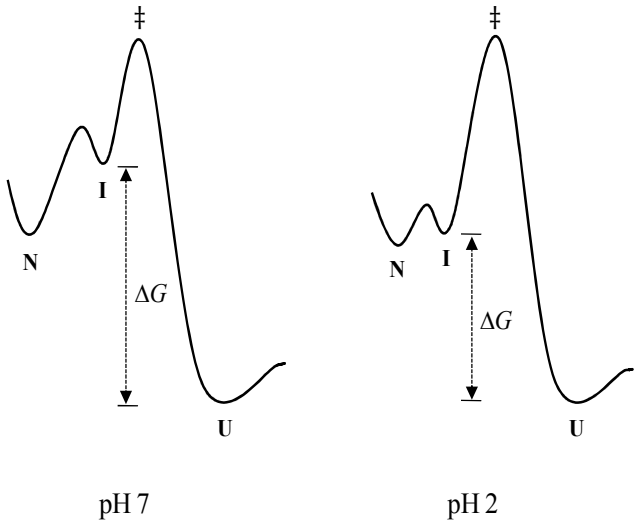

Figure 13. Schematic of one-dimensional free energy surface under unfolding conditions. The free energy difference between I and U corresponds to the value of ΔG measured by the titration of the burst amplitude with denaturant.

3.6 CONCLUSIONS

Whether the earliest event of protein folding can be modeled by polymer chain collapse transition is not clear at present, because all protein chains do not follow the tenet of expansion with increasing denaturant. By corollary, the response of the unfolded chain when placed under native-like conditions may not be consistent for all proteins. Inapplicability of the linear free energy model (LFEM) is a major factor for curvatures in chevron limbs, although the contribution of rate-limiting conversion of intermediates is not undermined. Validity of LFEM is best checked by equilibrium unfolding experiments that employ multiple perturbants, both GdnHCl and urea, for example. Kinetic version of double perturbation experiments performed here show that the earliest protein state formed during folding, say the collapsed/contracted state (U′), is little structured. Hence, U′ is not the prototype of a rate-limiting structural intermediate, and therefore cannot be implicated in chevron curvature.

3.7 REFERENCES

1. Kim, R. F., and Baldwin, R. L. (1982) Specific intermediates in the folding reactions of small proteins and the mechanism of protein folding. *Annu*. *Rev*. *Biochem*. *51*, 459–489.
2. Kim, R. F., and Baldwin, R. L. (1989) Intermediates in the folding reactions of small proteins. *Annu*. *Rev*. *Biochem*. *59*, 631–660.
3. Udgaonkar, J. B., and Baldwin, R. L. (1988) NMR evidence for an earlt framework intermediate on the folding pathway of ribonuclease A. *Nature 335*, 694–699.
4. Rode, H., Elove, G. A., and Englander, S. W. (1988) Structural characterization of folding intermediates in cytochrome *c* by H-exchange labeling and proton NMR. *Nature 335*, 700–704.
5. Baldwin, R. L., and Roder, H. (1991) Characterizing protein folding intermediates. *Curr*. *Biol*. *1*, 218–220.
6. Duan, Y., and Kollman P. A. (2000) Pathways to a protein folding intermediate observed in a 1-microsecond simulation in aqueous solution. *Science 282*, 740–744.
7. Krishna, M. M. G., Lin, Y., Mayle, L., and Englander, S. W. (2003) Intimate view of a kinetic protein folding intermediate: residue-resolved structure, interactions, stability, folding and unfolding rates, homogeneity. *J*. *Mol*. *Biol*. *334*, 501–513.
8. Religa, T. L., Markson, J. S., Mayor, U,m Freunds, A. M. V., and Fersht, A. R. (2005) Solution structure of a protein denatured state and folding intermediate. Nature 437, 1053–1056.
9. Zhou, Z., Feng, H., Ghirlando, R., and Bai, Y. (200*) The high-resolution NMR structure of the early folding intermediate of the *Thermus thermophilus* ribonuclease H. *J*. *Mol*. *Biol*. *384*, 531−539.
10. Neudecker, P., Robustelli, P., Cavalli, A., Walsh, P., Lundström, P., Zarine-Afsar, A., Sharpe, S., Vendruscolo, M., and Lay, L. E. (2012) Structure of an intermediate state in protein folding and aggregation. *Science 336*, 362–366.

11. Yamada, S., Ford, N. D. B., Keller, G. E., Ford, W. C., Gray, H. B., and Winkler, J. R. (2013) Snapshots of a protein folding intermediate. *Proc. Natl. Acad. Sci. USA 110*, 1606−1610.
12. Englander, S. W., and Mayne, L. (2014) The nature of protein folding pathways. *Proc. Natl. Acad. Sci. USA 111*, 15873−15880.
13. Ohgushi, M., and Wada, A. (1983) 'Molten globule state': a compact form of globular proteins with mobile side-chains. *FEBS Lett. 164*, 21–24.
14. Kuwajima, K. (1989) The molten globule state as a clue for understanding the folding and coopertivity of globular-protein structure. *Proteins 6*, 87–103.
15. Jeng, M-F., and Englander, S. W. (1991) Stable submolecular folding units in a non-compact form of cytochrome *c*. *J. Mol. Biol. 221*, 1045–1061.
16. Kataoka, M., Hagihara, Y., Mihara, K., and Goto, Y. (1993) Molten globule of cytochrome c studied by small angle X-ray scattering. *J. Mol. Biol. 229*, 591–596.
17. Ptitsyn, O. B. (1995) Molten globule and protein folding. *Adv. Protein Chem. 47*, 83–229.
18. Arai, M., and Kuwajima, K. (2000) Role of the molten globule state in protein folding. *Adv. Protein Chem. 53*, 209–271.
19. Bhattacharya, S., and Varadarajan, R. (2013) Packing in molten globules and native states. *Curr. Opin. Struct. Biol. 23*, 11–21.
20. Zaidi, S., Hassan, M. I., Islam, A., and Ahmad, F. (2015) Structural characteristics of stable folding intermediates of yeast iso-1 cytochrome *c*. *Biomacromol. J. 1*, 19–45.
21. Bhuyan, A. K. (2010) Off-pathways status for the alkali molten globule of horse ferricytochrome *c*. *Biochemistry 49*, 7764-7773.
22. Baldwin, R. L., and Rose, G. D. (2013) Molten globules, entropy-driven conformational change and protein folding. *Curr. Opin. Struct. Biol. 23*, 4–10.
23. Lindhoud, S., Pirchi, M., Westphal, A. H., Haran, G., and van Mierlo, C. P. M. (2015) Gradual folding of an off-pathway molten globule detected at the single-molecule level. *J. Mol. Biol. 427*, 3148–3157.

24. Matouschek, A., Kellis, J. T., Serrano, L., Bycroft, M., Fersht, A. R. (1990) Transient folding intermediates characterized by protein engineering. *Nature 346*, 440–445.
25. Khorasanizadeh, S., Peters, I. D., and Roder, H. (1996) Evidence for a three-state model of protein folding from kinetic analysis of ubiquitin variants with altered core residues. *Nat. Struct. Biol. 3*, 193–205.
26. Chan, H. S., and Dill, K. A. (1998) Protein folding in the landscape perspective: chevron plots and non-Arrhenius kinetics. *PROTEINS: Struct. Funct. Genet. 30*, 2–33.
27. Chen, T., and Chan H. S. (2014) Effects of desolvation barriers and sidechains on local-nonlocal coupling and chevron behaviors in coarse-grained models of protein folding. *Phys. Chem. Chem. Phys. 16*, 6460–6479.
28. Otzen, D. E., Kirstensen, O., Proctor, M., and Oliveberg, M. (1999) Structural changes in the transition state of protein folding: alternative interpretations of curved chevron plots. *Biochemistry 38*, 6499–6511.
29. Myers, J. K., and Oas, T. G. (2002) Mechanism of fast protein folding. *Annu. Rev. Biochem. 71*, 783–815.
30. Sosnick, T. R., Shtilerman, M. D., Mayne, L., and Englander, S. W. (1997) Ultrafast signals in protein folding and the polypeptide contracted state. *Proc. Natl. Acad. Sci. USA 94*, 8545–8550.
31. Shastry, M. C. R., Sauder, J. M., and Roder, H. (1998) Kinetic and structural analysis of submillisecond folding events in cytochrome *c*. *Acc. Chem. Res. 31*, 717–725.
32. Kimura, T., Uzawa, T., Ishimori, K., Morishima, I., Takahashi, S., Konno, T., Akiyama, S., and Fujisawa, T. (2005) Specific collapse followed by slow hydrogen-bond formation of β-sheet in the folding of single-chain monellin. *Proc. Natl. Acad. Sci. USA 102*, 2748–2753.
33. Lapidus, L. J., Yao, S., McGarrity, K. S., Hertzog, D. E., Tubman, E., and Bakajin, O. (2007) Protein Hydrophobic collapse and early folding steps observed in a microfluidic mixer. *Biophys. J. 93*, 218–224.
34. Jha, S. K., and Udgaonkar, J. B. (2009) Direct evidence for a dry molten globule

intermediate during the unfolding of a small protein. *Proc*. *Natl*. *Acad*. *Sci*. *USA 106*, 12289−12294.

35. Sosnick, T. R., and Barrick, D. (2011) The folding of single domain proteins − have we reached a consensus? *Curr*. *Opin*. *Struct*. *Biol*. *21*, 12−24.
36. Haran, G. (2012) How, when and why proteins collapse: the relation to folding. *Curr*. *Opin*. *Struct*. *Biol*. *22*, 14−20.
37. Hofmann, H., Soranno, A., Borgia, A., Gast, K., Nettels, D., and Schuler, B. (2012) Polymer scaling laws of unfolded and intrinsically disordered proteins quantified with single-molecule spectroscopy. *Proc*. *Natl*. *Acad*. *Sci*. *USA 109*, 16155−16160.
38. Kathuria, S. V., Kayatekin, C., Barrea, R., Kondrashkina, E., Graceffa, R., Guo, L., Nobrega, R. P., Vhakravarthy, S., Matthews, C. R., Irving, T. C., and Bilsel, O. (2014) Microsecond barrier-limited chain collapse observed by time-resolved FRET and SAXS. *J*. *Mol*. *Biol*. *426*, 1980−1994.
39. Kuwajima, K., Yamaya, H., Miwa, S., Sugai, S., Nagamura, T. (1987) Rapid formation of secondary structure framework in protein folding studied by stopped-flow circular dichroism. *FEBS Lett*. *221*, 115−118.
40. Elöve, G. A., Chaffotte, A. F., Roder, H., and Goldberg, M. E. (1992) Early steps in cytochrome c folding probed by time-resolved circulasr dichroism and fluorescence spectroscopy. *Biochemistry 31*, 6876-6883.
41. Matthews, C. R. (1993) Pathways of protein folding. *Annu*. *Rev*. *Biochem*. *62*, 653-683.
42. Roder, H., and Colón, W. (1997) Kinetic role of early intermediates in protein folding. *Curr*. *Opin*. *Struct*. *Biol*. *7*, 15−28.
43. Regenfuss, P., Clegg, R. M., Fulwyler, M. J., Barrantes, F. J., and Jovin, T. M. (1985) Mixing liquids in microseconds. *Rev*. *Sci*. *Instrum*. *56*, 283−290.
44. Chan, C.-K., Hu, Y., Takahashi, S., Rousseau, D. L., Eaton, W. A., and Hofrichter, J. (1997) Submillisecond protein folding kinetics studied by ultrarapid mixing. *Proc*. *Natl*. *Acad*. *Sci*. *USA 94*, 1779−1784.

Chapter 3

45. Takahashi, S., Yeh, S.-R., Das, T. K., Chan C.-K., Gottfried, D. S., and Rousseau, D. L. (1997) Folding of cytochrome *c* initiated by submillisecond mixing. *Nat*. *Struct*. Biol. *4*, 44–50.
46. Shastry, M. C. R., and Roder, H. (1998) Evidence for barrier-limited protein folding kinetics on the microsecond time scale. *Nat*. *Struct*. *Biol*. *5*, 385–392.
47. Shastry, M. C. R., Luck, S. D., and Roder, H. (1998) Continuous-flow capillary mixer to monitor reactions on the microsecond time scale. *Biophys*. *J*. *74*, 2714–2721.
48. Akiyama, S., Takahashi, S., Ishimori, K., and Morishima, I. (2000) Stepwise formation of α-helices during cytochrome *c* folding. *Nat*. *Struct*. *Biol*. *7*, 514–520.
49. Akiyama, S., Takahashi, S., Kimura, T., Ishimori, K., Morishima, I., Nishikawa, Y., and Fujisawa, T. (2002) Conformational landscape of cytochrome *c* folding studied by microsecond-resolved small-angle x-ray scattering. *Proc*. *Natl*. *Acad*. *Sci*. *USA* 99, 1329–1334.
50. Bilsel, O., Kayatekin, C., Wallace, L. A., and Matthews, C. R. (2005) A microchannel solution mixer for studying microsecond protein folding reactions. *Rev*. *Sci*. *Instrum*. *76*, 014302.
51. Sinha, K. K., and Udgaonkar, J. B. (2008) Barrierless evolution of structure during the submillisecond refolding reaction of a small protein. *Proc*. *Natl*. *Acad*. *Sci*. *USA* 105, 7998–8003.
52. Laurence, T. A., Kong, X., Jager, M., and Weiss, S. (2005) Probing structural heterogeneities and fluctuations of nucleic acids and denatured proteins. *Proc*. *Natl*. *Acad*. *Sci*. *USA* 102, 17348–17353.
53. Sherman, E. and Haran, G. (2006) Coil-globule transition in the denatured state of a small protein. *Proc*. *Natl*. *Acad*. *Sci*. *USA 103*, 11539–11543.
54. Kuzmenkina, E. V., Heyes, C. D>, and Nienhaus, G. U. (2006) Single-molecule FRET study of denaturant induced unfolding of RNAse H. *J*. *Mol*. *Biol*. *357*, 313–324.
55. Tezuka-Kawakami, T., Gell, C., Brockwell, D. J., Radford, S. E., and Smith, D. A. (2006) Urea-induced unfolding of the immunity protein Im9 monitored by spFRET.

Biophys. *J*. *91*, L42–L44.

56. Hoffmann, A., Kane, A., Nettels, D., Hertzog, D. E., Baumgartel, P., Lengefeld, J., Reichardt, G., Horsley, D. A., Seckler, R., Bakajin, O., and Schuler, B. (2007) Mapping protein collapse with single-molecule fluorescence and kinetic synchrotron radiation circular dichroism spectroscopy. *Proc*. *Natl*. *Acad*. *Sci*. *USA 104*, 105–110.
57. Merchant, K. A., Best, R. B., Louis, J. M., Gopich, I. V., and Eaton, W. A. (2007) Characterizing the unfolded states of proteins using single-molecule FRET spectroscopy and molecular simulations. *Proc*. *Natl*. *Acad*. *Sci*. *USA 104*, 1528–1533.
58. Hofmann, H., Golbik, R. P., Ott, M., Hubner, C. G., Ulbrich-Hofmann, R. (2008) Coulomb forces control the density of the collapsed unfolded state of barstar. *J*. *Mol*. *Biol*. *376*, 597–605.
59. Liu, P., Meng, X., Qu, P., Zhao, X. S., and Wang, C. C. (2009) Subdomain-specific collapse of denatured staphylococcal nuclease revealed by single molecule fluorescence resonance energy transfer measurement. *J*. *Phys*. *Chem*. *113*, 12030–12036.
60. Nettels, D., Muller-Spath, S., Kuster, F., Hofmann, H., Haenni, D., Ruegger, S., Reymond, L., Hoffmann, A., Kubelka, J., Heinz, B., Gast, K., Best, R. B., and Schuler, B. (2009) Single-molecule spectroscopy of the temperature-induced collapse of unfolded proteins. *Proc*. *Natl*. *Acad*. *Sci*. *USA 106*, 20740–20745.
61. Ziv, G., and Haran, G. (2009) Protein folding, protein collapse, and Tanford's transfer model: lessons from single molecule FRET. *J*. *Am*. *Chem*. *Soc*. *131*, 2942–2947.
62. Rieger, R., Kobitski, A., Sielaff, H., and Nienhaus, G. U. (2011) Evidence of a folding intermediate in RNAse H from single-molecule FRET experiments. *Chemphyschem 12*, 627–633.
63. Udgaonkar, J. B. (2013) Polypeptide chain collapse and protein folding. *Arch*. *Biochem*. *Biophys*. *531*, 24–33.
64. Chung, H. S., Cellmer, T., Louis, J. M., and Eaton, W. A. (2013) Measuring ultrafast protein folding rates from photon-by-photon analysis of single-molecule fluorescence trajectories. *Chem*. *Phys*. *422*, 229–237.

Chapter 3

65. Chung, H. S., Piana-Agostinetti, S., Shaw, D. E., and Eaton, W. A. (2015) Structural origin of slow diffusion in protein folding. *Science 349*, 1504–1510.
66. England, J. L., and Haran, G. (2011) Role of salvation effects in protein denaturation: from thermodynamics to single molecules and back. *Annu. Rev. Phys. Chem. 62*, 257-277.
67. Yoo, T. Y., Meisburger, S. P., Hinshaw, J., Pollack, L., Haran, G., Sosnick, T. R., and Plaxco, K. (2012) *J. Mol. Biol. 418*, 226–236.
68. Segel, D. J., Fink, A. L., Hodgson, K. O., and Doniach, S. (1998) Protein Denaturation: a Small Angle X-ray Scattering Study of the Ensemble of Unfolded States of Cytochrome *c*. *Biochemistry 37*, 12443–12451.
69. Yasin, U. M., Sashi, P., and Bhuyan, A. K. (2013) Expansion and internal friction in unfolded protein chain. *J. Phys. Chem. B. 117*, 12059–12064.
70. Konuma, T., Sahurai, K., Yagi, M., Goto, Y., Fujisawa, T., and Takahashi, S. (2015) Highly collapsed conformation of the initial folding intermediates of β-lactoglobulin with non-native α-helix. *J. Mol. Biol. 427*, 3158–3165.
71. Fazelinia, H., Xu, M., Cheng, H., and Roder, H. (2014) Ultrafast hydrogen exchange reveals specific structural events during the initial stages of folding of cytochrome *c*. *J. Am. Chem. Soc. 136*, 733–740.
72. Maity, H., and Reddy, G. (2016) Folding of protein L with implications for collapse in the denatured state ensemble. *J. Am. Chem. Soc*. DOI: 10.1021/jacs.5b11300.
73. Altieri, A. S., Hinton, D. P., and Byrd, R. A. (1995) Association of biomolecular systems via pulsed field gradient NMR self-diffusion measurements, *J. Am. Chem. Soc. 117*, 7566–7567.
74. Jones, J. A., Wilkins, D. K., Smith, L. J., and Dobson, C. M. (1997) Characterization of Protein Unfolding by NMR Diffusion Measurements. *J. Biomol. NMR 10*, 199–203.
75. Dill, K. A. (1985) Theory for the Folding and Stability of Globular Proteins. *Biochemistry 24*, 1501–1509.
76. Dill, K. A., and Shortle, D. (1991) Denatured States of Proteins. *Annu. Rev. Biochem.*

60, 795–825.

77. Grosberg, A. Y., and Kokhlov, A. R. (1994) *Statistical Physics of Macromolecules*. New York: AIP.
78. Qiu, L., Zachariah, C., and Hagen, S. J. (2003) Fast chain contraction during protein folding: "foldability" and collapse dynamics. *Phys*. *Rev*. *Lett*. 168103.
79. Fitzkee, N. C., and Rose, G. D. (2004) Reassessing random-coil statistics in unfolded proteins. *Proc*. *Natl*. *Acad*. *Sci*. *USA 101*, 12497–12502.
80. Sosnick, T. R., Mayne, L., Hiller, R., and Englander, S. W. (1994) The barriers in protein folding, *Nat*. *Struct*. *Biol*. *1*, 149–156.
81. Elöve , G. A., Bhuyan, A. K., and Roder, H. (1994) Kinetic mechanism of cytochrome *c* folding: involvement of the heme and its ligands. *Biochemistry 33*, 6925-6935.
82. Sosnick, T. R., Mayne, L., and Englander, S. W. (1996) Molecular collapse: the rate-limiting step in twostate cytochrome *c* folding. *Proteins*: *Struct*. *Funct*. *Genet*. *24*, 413–426.
83. Colón, W., Wakem, L. P., Sherman, F., and Roder, H. (1997) Identification of the predominant non-native histidine ligands in unfolded cytochrome *c*. *Biochemistry 36*, 12535–12541.
84. Bhuyan, A. K., and Udgaonkar, J. B. (2001) Folding of horse cytochrome *c* in the reduced state. *J*. *Mol*. *Biol*. *312*, 1135–1160.
85. Krantz, B. A., Mayne, L., Rumbley, J., Englander, S. W., and Sosnick, T. R. (2002) Fast and slow intermediate accumulation and the initial barrier mechanism in protein folding. *J*. *Mol*. *Biol*. *324*, 359–371.
86. Bhuyan, A. K., and Kumar, R. (2002) Kinetic barriers to the folding of horse cytochrome *c* in the reuced state. *Biochemistry 41*, 12821–12834.
87. Kumar, R., and Bhuyan, A. K. (2005) Two-state folding of horse ferrcytochrome *c*: analyses of linear free energy relationship, chevron curvature, and stopped-flow burst relaxation kinetics. *Biochemistry 44*, 3024–3033.
88. Jackson, S. E., and Fersht, A. R. (1991) Folding of chymotrypsin inhibitor 2. 1.

Evidence for a two-state transition. *Biochemistry 30*, 10428–10435.

89. Morris, E. R., and Searle, M. S. (2012) Overview of protein folding mechanism: experimental and theoretical approaches to protein energy landscapes. *Curr*. *Protoc*. *Protein Sci*. *68*, 28.2.1–28.2.22.
90. Chiba, K., Ikai, A., Kawamura-Konishi, Y., and Kihara, H. (1994) Kinetic study on myoglobin refolding monitored by five optical probe stopped-flow methods. *Proteins 19*, 110–119.
91. Wittung-Stafshede, P., Malmstrom, B. G., Winkler, J. R., and Gray, H. B. (1998) Folding of deoxymyoglobin triggered by electron transfer. *J*. *Phys*. *Chem*. *102*, 5599–5601.
92. Moczygemba, C, Guidry, J., and Wittung-Stafshede, P. (2000) Heme orientation affects holomyoglobin folding and unfolding kinetics. *FEBS Lett*. *470*, 203–206.
93. Wildegger, G., and Kiefhaber, T.(1997) Three-state model for lysozyme folding: triangular folding mechanism with an energetically trapped intermediate. *J*. *Mol*. *Biol*. *270*, 294–304.
94. Parker, M. J., and Marqusee, S. (1999) The cooperativity of burst phase reactions explored. *J*. *Mol*. *Biol*. *293*, 1195–1210.
95. Brown, J. R. (1976) Structural origins of mammalian albumin. *Fed*. *Proc*. *35*, 2141–2144.
96. Aoki, K., and Foster, J. F. (1957) Electrophoretic behavior of bovine plasma albumin at low pH. *Org*. *Biol*. *Chem*. *79*, 3385–3393.
97. Aoki, K., and Foster, J. F. (1957) Electrophoretic and hydrogen ion binding behavior of bovine plasma albumin in the presence of 0.02 M tiocyanate ion. *Org*. *Biol*. *Chem*. *79*, 3393–3396.
98. Khan, M. Y., and Salahuddin, A. (1984) Lack of N–F transition in the N-terminal fragment (domain I+II) of bovine serum albumin. *Eur*. *J*. *Biochem*. *141*, 473–475.
99. Tanford, C., Aune, K. C., and Ikai, A. (1973) Kinetics of unfolding and refolding of proteins. III. Results for lysozyme. *J*. *Mol*. *Biol*. *73*, 185–197.

100. Kuwajima, K., Hiraoka, Y., Ikeguchi, M., and Sugai, S. (1985) Comparison of transient folding intermediates in lysozyme and α-lactalbumin. *Biochemistry 24*, 874–881.

101. Chaffotte, A. F., Guillou, Y., and Goldberg, M. E. (1992) Kinetic resolution of peptide bond and side-chain far-UV CD during folding of HEWL. *Biochemistry 31*, 9694–9702.

102. Radford, S. E., Dobson, C. M., and Evans, P. A. (1992) The folding of hen lysozyme involves partially structured intermediates and multiple pathways. *Nature 358*, 302–307.

103. Miranker, A. D., Robinson, C. V., Radford, S. E., Aplin, R. T., and Dobson, C. M. (1993) Detection of transient protein folding populations by MS. *Science 262*, 896–900.

104. Itzhaki, L. S., Evans, P. A., Dobson, C. M., and Radford, S. E. (1994) Tertiary interactions in the folding pathway of hen lysozyme: kinetic study using fluorescent probes. *Biochemistry 33*, 5212–5220.

105. Parker, M. J., Spencer, J., and Clarke, A. R. (1995) An integrated kinetic analysis of intermediates and transition states in protein folding reactions. *J. Mol. Biol. 253*, 771–786.

106. Kiefhaber, T. (1995) Kinetic traps in lysozyme folding. *Proc. Natl. Acad. Sci. USA 92*, 9029–9033.

107. Yasin, U. M., Sashi, P., and Bhuyan, A. K. (2014) Free energy landscape of lysozyme: multiple near-native conformational states and rollover in the urea dependence of folding energy. *J. Phys. Chem. B 118*, 6662–6669.

108. Ziv, G., Thirumalai, D., and Haran, G. (2009) Collapse transition in proteins. *Phys. Chem. Chem. Phys. 11*, 83–93.

109. Williams, C., Brochard, F., and Frisch, H. L. (1981) Polymer collapse. *Annu. Rev. Phys. Chem. 32*, 433–451.

110. Schuler, B., Lipman, E. A., and Eaton, W. A. (2002) Probing the free energy surface

for protein folding with single-molecule fluorescence spectroscopy. *Nature 419*, 743–747.

111. Huang, F., Ying, L., and Fersht, A. R. (2009) Direct observation of barrier-limited folding of BBL by single molecule fluorescence resonance energy transfer. *Proc. Natl. Acad. Sci. USA 106*, 12289–12294.

112. Jacob, J., Dothager, R. S., Thiyagarajan, P., and Sosnick, T. R. (2007) Early collapse is not an obligate step in protein folding. *J. Mol. Biol. 338*, 369–382.

113. Arai, M., Ito, K., Inobe, T., Nakao, M., Maki, K., Kamagata, K., Kihara, H., Amenmiya, Y., and Kuwajima, K. (2002) Fast compaction of α-lactalbumin during folding studied by stopped-flow x-ray scattering *J. Mol. Biol. 321*, 121–132.

114. Arai, M., Kondrashkina, E., Kayatekin, C., Matthews, C. R., Iwakura, M., and Bilsel, O. (2007) Microsecond hydrophobic collapse in the folding of *Escherichia coli* dihydrofolate reductase, an α/β-type protein. *J. Mol. Biol. 368*, 219–229.

115. Chattopadhyay, K., Elson, E. L., and Frieden, C. (2005) The kinetics of conformational fluctuations in an unfolded protein measured by fluorescence methods. *Proc. Natl. Acad. Sci. USA 102*, 2385–2389.

116. Baldwin, R. L. (1996) On-pathway versus off-pathway folding intermediates. *Fold. Design 1*, R1–R8.

117. Hagen S. J., and Eaton, W. A. (2000) Two-state expansion and collapse of a polypeptide. *J. Mol. Biol. 297*, 781–789.

118. Jennings, P. A., and Wright, P. E. (1993) Formation of a molten globule intermediate early in the kinetic folding pathway of apomyoglobin. *Science 262*, 892–896.

119. Luo, Y., Kay, M. S., and Baldwin, R. L. (1997) Cooperativity of folding of the apomyoglobin pH 4 intermediate studied by glycine and proline mutations. *Nat. Struct. Biol. 4*, 925–930.

120. Bachmann, A., Segel, D., and Kiefhaber, T. (2002) Test for cooperativity in the early kinetic intermediate in lysoZyme folding. *Biophys. Chem. 96*, 141–151.

121. Maki, K., Cheng, H., Dolgikh, D. A., Shastry, M. C., and Roder, H. (2004) Early

events during folding of wild-type staphylococcal nuclease and a single-tryptophan variant studied by ultrarapid mixing. *J. Mol. Biol. 338*, 383–400.

122. Welker, E., Maki, K., Shastry, M. C., Juminaga, D., Bhat, R., Scheraga, H. A., and Roder, H. (2004) Ultrarapid mixing experiments shed new light on the characterization of the initial conformational ensemble during the folding of ribonuclease A. *Proc. Natl. Acad. Sci. USA 101*, 17681–17686.
123. Wu, Y., Vadrevu, R., Yang, X., and Matthews, C. R. (2005) Specific structure appears at the N-terminus in the submillisecond folding intermediate of the alpha subunit of tryptophan synthase, a TIM barrel protein. *J. Mol. Biol. 351*, 445–452.
124. Baldwin, R. L., and Rose, G. D. (1999) Is protein folding hierarchic? II. Folding intermediates and transition states. *Trends Biochem. Sci. 24*, 77–83.
125. Pollack, L., Tate, M. W., Darnton, N. C., Knight, J. B., Gruner, S. M., Eaton, W. A., and Austin, R. H. (1999) Compactness of the denatured state of a fast-folding protein measured by submillisecond small-angle x-ray scattering. *Proc. Natl. Acad. Sci. USA 96*, 10115–10117.
126. Uzawa, T, Akiyama, S., Kimura, T., Takahashi, S., Ishimori, K., Morishima, I., and Fujisawa, T. (2004) Collapse and search dynamics of apomyoglobin folding revealed by submillisecond observations of α-helical content and compactness. *Proc. Natl. Acad. Sci. USA 101*, 1171–1176.
127. Qi, P. Q., Sosnick, T. R., and Englander, S. W. (1998) The burst phase in ribonuclease A folding: solvent dependence of the unfolded state, *Nat. Struct. Biol. 5*, 882-884.
128. Segel, D. J., Eliezer, D., Uversky, V., Fink, A. L., Hodgson, K. O., and Doniach, S. (1999) Transient dimer in the refolding kinetics of cytochrome *c* characterized by small-angle x-ray scattering. *Biochemistry 38*, 15352–15359.
129. Tezcan, F. A., Findley, W. M., Crane, B. R., Ross, S. A., Lyubovitsky, J. G., Gray, H. B., and Winkler, J. R. (2002) Using deeply trapped intermediates to map the cytochrome *c* folding landscape. *Proc. Natl. Acad. Sci. USA 99*, 8626–8630.

Chapter 3

130. Lyubovitsky, J. G., Gray, H. B., and Winkler, J. R. (2002) Mapping the cytochrome *c* folding landscape. *J. Am. Chem. Soc. 124*, 5481–5485.

131. Dasgupta, A., and Udgaonkar, J. B. (2010) Evidence for initial non-specific polypeptide chain collapse during the refolding of the SH3 domain of PI3 kinase. *J. Mol. Biol. 403*, 430–445.

132. Sánchez, I. E., and Kiefhaber, T. (2003) Evidence for sequential barriers and obligatory intermediates in apparent two-state protein folding. *J. Mol. Biol. 325*, 367–376.

133. Scott, K. A., and Clarke, J. (2005) Spectrin R16: broad energy barrier or sequential transition states? *Protein Sci. 14*, 1617–1629.

134. Brockwell, D. J., and Radford, S. E. (2007) Intermediates: ubiquitous species on folding energy landscapes? *Curr. Opin. Struct. Biol. 17*, 30–37.

135. Tsytlonok, M., and Itzhaki, L. S. (2013) The how's and why's of protein folding intermediates. *Arch. Biochem. Biophys. 531*, 14–23.

136. Matouschek, A., and Fersht, A. R. (1993) application of physical organic chemistry to engineered mutant proteins: Hammond postulate behavior in the transition state of protein folding. *Proc. Natl. Acad. Sci. USA 90*, 7814–7818.

137. Matthews, J. M., and Fersht, A. R. (1995) Exploring the energy surface of protein folding by structure-reactivity relationships and engineered proteins: observation of Hammond behavior for the gross structure of the transition state and anti-Hammond behavior for structural elements for unfolding/folding of barnase. *Biochemistry 34*, 6805–6810.

138. Kaya, H., and Chan, H. S. (2003) Simple two-state protein folding kinetics requires non-Levinthal thermodynamic cooperativity. *Proteins*: *Struct. Funct. Genet. 52*, 510–523.

139. Kaya, H., and Chan, H. S. (2003) Origins of chevron rollovers in non-two-state protein folding kinetics. *Phys. Rev. Lett. 90*, 258104.

140. Kaya, H., and Chan, H. S. (2005) Explicit-chain model of native-state hydrogen

exchange: implications for event ordering and cooperativity in protein folding. *Proteins*: *Struct*. *Funct*. *Bioinf*. *58*, 31–44.

141. Park, H. S., Shastry, M. C., and Roder, H. (1999) Folding dynamics of the B1 domain of protein G explored by ultrarapid mixing. *Nat*. *Struct*. *Biol*. *6*, 943–947.
142. Huang, F., Sato, S., Sharpe, T. D., Ying, L., and Fersht, A. R. (2007) Distinguishing between cooperative and unimodal downhill protein folding. *Proc*. *Natl*. *Acad*. *Sci*. *USA 104*, 123–127.
143. Mukhopadhyay, S., Krishnan, R., Lemke, E. A., Lindquist, S., and Deniz, A. A. (2007) A natively unfolded yeast prion monomer adopts an ensemble of collapsed and rapidly fluctuating structures. *Proc*. *Natl*. *Acad*. *Sci*. *USA 104*, 2649-2654.
144. Plaxco, K. W., and Baker, D. (1998)Limited internal friction in the rate-limiting step of a two-state protein folding reaction. *Proc*. *Natl*. *Acad*. *Sci*. *USA 95*, 13591–13596.
145. Chung, H. S., and Eaton, W. A. (2013) Single-molecule fluorescence probes dynamics of barrier crossing. *Nature 502*, 695–688.
146. Schmid, F. X. (1992) in *Protein Folding*. (Creighton, T. E., Ed.) pp 197–241, Freeman, New York.
147. Kiefhaber, T., Labhardt, A. M., and Baldwin, R. L. (1995) Direct NMR evidence for an intermediate preceding the rate-limiting step in the unfolding of ribonuclease A. *Nature 375*, 513–515.
148. Hoeltzli, S. D., and Frieden, C. (1995) Stopped-flow NMR spectroscopy: real time unfolding studies of 6-^{19}F-tryptophan-labeled *Escherichia coli* dihydrofolate reductase. *Proc*. *Natl*. *Acad*. *Sci*. *USA 92*, 9318–9322.
149. Laurents, D. V., and Baldwin, R. L. (1997) Characterization of the unfolding pathway of hen egg white lysozyme. *Biochemistry 36*, 1496–1504.
150. Steer, B. A., and Merrill, A. R. (1997) Characterization of an unfolding intermediate and kinetic analysis of guanidine hydrochloride-induced denaturation of the colicin E1 channel peptide. *Biochemistry 36*, 3037–3046.
151. Jamin, M., Yeh, S-R., Rousseau, D. L., and Baldwin, R. L. (1999) Submillisecond

unfolding kinetics of apomyoglobin and its pH 4 intermediate. *J. Mol. Biol. 292*, 731-740.

152. Teilum, K., Poulsen, F. M., and Akke, M. (2006) The inverted chevron plot measured by NMR relaxation reveals a native-like intermediate in acyl-CoA binding protein. *Proc. Natl. Acad. Sci. USA 103*, 6877−6882.

153. Mahler, B., Doddapaneni, K., Kleckner, I., Yuan, C., Wistow, G., and Wu, Z. (2011) Characterization of a transient unfolding intermediate in a core mutant of γS-crystallin. *J. Mol. Biol. 405*, 840-850.

154. Chen, K-C., Xu, M., Wedemeyer, W. J., and Roder, H. (2011) Microsecond unfolding kinetics of sheep prion protein reveals an intermediate that correlates with susceptibility to classical scrapie. *Biophys. J. 101*, 1221−1230.

155. Malhotra, P., and Udgaonkar, J. B. (2014) High-energy intermediates in protein unfolding characterized by thiol labeling under nativellike conditions. *Biochemistry 53*, 3608−3620.

156. He, X. M., and Carter, D. C. (1992) Atomic structure and chemistry of human serum albumin. *Nature 358*, 209−215.

157. Carter, D. C., and Ho, J. X. (1994) Structure of serum albumin. Adv. *Protein Chem. 45*, 153−203.

158. Curry, S., Mandelkow, H., Brick, P., and Franks, N. (1998) Crystal structure of human serum albumin complexed with fatty acid reveals an asymmetric distribution of binding sites. *Nat. Struct. Biol. 5*, 827−835.

159. Walters, B. T., Mayne, L., Hinshaw, J. R., Sosnick, T. R., and Englander, S. W. (2013) Folding of a large protein at high structural resolution. *Proc. Natl. Acad. Sci. USA 110*, 18898−18903.

160. Orevi, T., Ben Ishay, E., Gershanov, S. L., Dalak, M. B., Amir, D., and Haas, E. (2014) Fast closure of N-terminal long loops but slow formation of β strands precedes the folding transition state of *Escherichia coli* adenylate kinase. *Biochemistry 53*, 3169−3178.

List of Publications

1. **Ramakrishna, D.,** and Bhuyan, A. K. Protein Folding Energy is Not Universally Linear with Denaturant: A Revisit to the Linear Free Energy Model. (Submitted to Biochemistry).

2. **Ramakrishna, D.,** and Bhuyan, A. K. Burst Reaction and Chevron Curvature in the Folding of Cytochrome *c*, Myoglobin, BSA, and Lysozyme Studied by Stopped-Flow. (Submitted to Biochemistry).

3. **Ramakrishna, D.,** Sashi, P., and Bhuyan, A. K. Interaction of Micellar Levels of Sodium Dodecyl Sulfate with Holo- and Apocytochrome c: Binding Characteristics and Chain Expansion. (being communicated).

4. Sashi, P., **Ramakrishna, D.,** and Bhuyan, A. K. Dispersion Forces and the Molecular Origin of Internal Friction in Protein. (being communicated).

5. Sashi, P., Yasinu, UM., Balasubramanian, H., Sree, MU., **Ramakrishna, D**. and Bhuyan, A. K. Preferencial Water Exclusion in Protein Unfolding. J. Phys. Chem. B. **2014,**118, 717-23.

6. Sudhamalla, B., Kumar, M., Kumar, SR., Sashi, P., Yasin, UM., **Ramakrishna, D.,** Rao, PN., and Bhuyan, A. K. Enzyme Dimention of the Ribosomal Protein S4 across Plant and Animal Kingdoms. Biochem. Biophys. Acta (General Subjects). **2013,** 1830, 5335-41.

7. Yadaiah, M., Sudhamalla, B., Rao, PN., Roy, KR., **Ramakrishna, D.,** Hussain Syed, G., Ramaiah, KV., and Bhuyan, A. K. Arrested cell proliferation through cysteine protease activity of eukaryotic ribosomal protein S4. FASEB J. **2013,** 27, 803-10.

8. **Ramakrishna, D.,** Prasad, MD., and Bhuyan, A. K. Hydrophobic collapse overrides Coulombic repulsion in ferricytochrome c fibrillation under extremely alkaline condition. Arch. Biochem. Biophys. **2012,**528, 67-71.

9. Sudhamalla, B., Yadaiah, M., **Ramakrishna, D**., and Bhuyan, A. K. Cysteine protease attribute of eukaryotic ribosomal protein S4. Biochim. Biophys. Acta (General Subjects). **2012,** 1820, 1535-42.

10. Yadaiah, M., Rao, PN., Sudhamalla, B., **Ramakrishna, D.,** Yasin, UM., and Bhuyan, A. K. Cloning, Escherichia coli expression, purification, characterization, and enzyme assay of the ribosomal protein S4 from wheat seedlings (Triticum vulgare). Protein Expr. Purif. **2012,** 81, 55-62.

Studies on Thermodynamics and Kinetics of Protein Folding for Interpretation of Some Basic Assumptions

ORIGINALITY REPORT

4%	1%	4%	0%
SIMILARITY INDEX	INTERNET SOURCES	PUBLICATIONS	STUDENT PAPERS

PRIMARY SOURCES

1. Jain, Rishu, Deepak Sharma, Sandeep Kumar, and Rajesh Kumar. "Factor Defining the Effects of Glycine Betaine on the Thermodynamic Stability and Internal Dynamics of Horse Cytochrome c", Biochemistry, 2014.

   Publication 1%

2. G. Bhanuprakash Reddy. "Linear free-energy model description of the conformational stability of uracil-DNA glycosylase inhibitor. A thermodynamic characterization of interaction with denaturant and cold denaturation", European Journal of Biochemistry, 5/1999.

   Publication 1%

3. Yasin, U. Mahammad, Pulikallu Sashi, and Abani K. Bhuyan. "Free Energy Landscape of Lysozyme: Multiple Near-Native Conformational States and Rollover in the Urea Dependence of Folding Energy", The Journal of Physical Chemistry B, 2014.

   Publication <1%

4. Kumar, Rajesh, and Abani K. Bhuyan. "Two-State Folding of Horse Ferrocytochrome *c*: Analyses of Linear Free Energy Relationship, Chevron Curvature, and Stopped-Flow Burst Relaxation Kinetics, Biochemistry, 2005.

Publication <1%

5. Rajesh Kumar."Entropic stabilization of myoglobin by subdenaturing concentrations of guanidine hydrochloride", JBIC Journal of Biological Inorganic Chemistry, 01/2009.

Publication <1%

6. Ibarra-Molero, Beatriz, and Jose M. Sanchez-Ruiz. "A Model-Independent, Nonlinear Extrapolation Procedure for the Characterization of Protein Folding Energetics from Solvent-Denaturation Data", Biochemistry, 1996.

Publication <1%

7. Bhuyan, Abani K., and Rajesh Kumar. "Kinetic Barriers to the Folding of Horse Cytochrome *c* in the Reduced State", Biochemistry, 2002.

Publication <1%

8. Liang, X.. "Partially Unfolded Forms and Non-two-state Folding of a beta-Sandwich: FHA Domain from Arabidopsis Receptor Kinase-associated Protein Phosphatase", Journal of Molecular Biology, 20061124.

Publication <1%

9. intl-glycob.oxfordjournals.org

Internet Source <1%

10. Jyothi, T.C. "Napin from Brassica juncea: Thermodynamic and structural analysis of stability", BBA - Proteins and Proteomics, 200707.

Publication <1%

---

11. Rao, D. Krishna, N. Prakash Prabhu, and Abani K. Bhuyan. "Extensive Misfolding in the Refolding Reaction of Alkaline Ferrocytochrome *c*", Biochemistry, 2006.

Publication <1%

---

12. Ouellette, T.. "Production and purification of refolded recombinant human IL-7 frominclusion bodies", Protein Expression and Purification, 200308.

Publication <1%

---

13. "Research Reports from University of Pisa Provide New Insights into Hemeproteins. (Report)", Life Science Weekly, Dec 25, 2012 Issue

Publication <1%

---

14. Patra, Ashish K., and Jayant B. Udgaonkar."Characterization of the Folding and Unfolding Reactions of Single-Chain Monellin: Evidence for Multiple Intermediates and Competing Pathways", Biochemistry, 2007.

Publication <1%

---

15. Kumar, Rajesh, and Abani K. Bhuyan."Viscosity Scaling for the Glassy Phase of Protein Folding", The Journal of Physical Chemistry B, 2008.

Publication <1%

---

16. Milam, S.L.. "Rapid Folding and Unfolding of Apaf-1 CARD", Journal of Molecular Biology, 20070525.

Publication <1%

17. Yadaiah, M., Rajesh Kumar, and Abani K. Bhuyan. "Glassy Dynamics in the Folding Landscape of Cytochrome *c* Detected by Laser Photolysis", Biochemistry, 2007.

Publication <1%

18. García-Cuesta, M. C., A. M. Lozano, J. J. Meléndez-Martínez, F. Luna-Giles, A. L. Ortiz, L. M. González-Méndez, and F. L. Cumbrera. "Structure determination of nitrato-κO-bis[2-(2-pyridyl-κN)amino-5,6-dihydro-4H-1,3-thiazine-κN]copper(II) nitrate via molecular modeling coupled with X-ray powder diffractometry", Journal of Applied Crystallography, 2004.

Publication <1%

19. Bhuyan, Abani K.. "Protein Stabilization by Urea and Guanidine Hydrochloride", Biochemistry, 2002.

Publication <1%

20. Li, Y.. "The Cold Denatured State Is Compact but Expands at Low Temperatures: Hydrodynamic Properties of the Cold Denatured State of the C-terminal Domain of L9", Journal of Molecular Biology, 20070420.

Publication <1%

21. phys.strath.ac.uk

Internet Source <1%

22. drseo.snu.ac.kr

Internet Source <1%

23. Katayama, Derrick S., Mark Cornell Manning, and Paul Jarosz. "Solution Behavior of a Novel Biopharmaceutical Drug Candidate: A Gonadotropin-Toxin Conjugate", Drug Development and Industrial Pharmacy, 2006.

Publication <1%

24. Rao, D. Krishna, Rajesh Kumar, M. Yadaiah, and Abani K. Bhuyan. "The Alkali Molten Globule State of Ferrocytochrome *c*: Extraordinary Stability, Persistent Structure, and Constrained Overall Dynamics", Biochemistry, 2006.

Publication <1%

25. Bhuyan, Abani K.. "Off-Pathway Status for the Alkali Molten Globule of Horse Ferricytochrome *c*", Biochemistry, 2010.

Publication <1%